

Introduction to

**Mobile Robot Control**

by  
*Spyros G. Tzafestas*

National Technical University of Athens  
Athens, Greece

Spyros G. Tzafestas  
School of Electrical and Computer Engineering  
National Technical University of Athens  
Zographou, Athens  
Greece  
[tzafesta@cs.ntua.gr](mailto:tzafesta@cs.ntua.gr)  
<http://users.softlab.ece.ntua.gr/~sgt/>

## **To the Robotics Teacher and Learner**

*For the things we have to learn before  
we can do them, we learn by doing them.*

**Aristotle**

*The second most important job in the world,  
second only to being a parent, is being a good teacher.*

**S.G. Ellis**

*In learning you will teach,  
and in teaching you will learn.*

**Phil Collins**



## Preface

*Robotics* has been a dominant contributor to the development of the human society over the years. It is a field that needs the synergy of a variety of scientific areas such as mechanical engineering, electrical-electronic engineering, control engineering, computer engineering, sensor engineering, and others. Robots and other automated machines have to live together with people. In this symbiosis human needs and preferences should be predominantly respected, incorporated, and implemented. To this end, modern robots, especially wheeled or legged mobile robots, incorporate and realize in a purposeful and profitable way the ‘*perception-action cycle*’ principle borrowed from biological systems and human cognitive and adaptation capabilities.

The objective of this book is to present in a cohesive way a set of fundamental conceptual and methodological elements, developed over the years for nonholonomic and omnidirectional wheeled mobile robots. The core of the book (chapters 5 through 10) is devoted to the analysis and design of several mobile robot controllers that include basic Lyapunov-based controllers, invariant manifold –based controllers, affine model-based controllers, model reference adaptive controllers, sliding –mode and Lyapunov –based robust controllers, neural controllers, fuzzy-logic controllers, vision- based controllers, and mobile manipulator controllers. The topics of mobile robot drives, kinematics, dynamics, and sensing are covered in the first four chapters. The topics of path planning, motion planning, task planning, localization, and mapping are covered in chapters 11 and 12, including most fundamental concepts and techniques at a detail compatible with the purpose and size of the book. Chapter 13 provides a selection of experimental results obtained by many of the methods studied in the book. These results were drawn from the research literature and include some of the author’s results. Chapter 14 provides a conceptual overview of some generic systemic and software architectures developed for implementing integrated intelligent control of mobile robots. Finally, chapter 15 provides a tour to the applications of mobile robots in the factory and society at an encyclopedic level. For the convenience of the reader, the first section of each chapter involves the required mathematical, mechanics, control, and fixed-robot background concepts that are used in the chapter. The book is actually complementary to most books in the field, in the sense that it provides a solid model-based analysis and design of a large repertory of mobile robot control schemes, not covered in other books.

The book is suitable for senior undergraduate, and graduate instructional courses on general and mobile robotics. It can also be used as an introductory reference book by researchers and practitioners in the field that need a consolidated methodological source for their work.

I am grateful to all publishers and authors for granting their permission to include in the book the requested illustrations and experimental plots.

Spyros. G. Tzafestas

Athens, April 2013

## Contents

### 1. Mobile Robots: General Concepts

- 1.1 Introduction
- 1.2 Definition and History
  - 1.2.1 What is a Robot?
  - 1.2.2 Robot History
- 1.3 Ground Robot Locomotion
  - 1.3.1 Legged Locomotion
  - 1.3.2 Wheeled Locomotion
    - 1.3.2.1 Wheel Types
    - 1.3.2.2 Drive Types
    - 1.3.2.3 WMR Maneuverability

References

### 2. Mobile Robot Kinematics

- 2.1 Introduction
- 2.2 Background Concepts
  - 2.2.1 Direct and Inverse Kinematics
  - 2.2.2 Homogeneous Transformations
  - 2.2.3 Nonholonomic Constraints
- 2.3 Nonholonomic Mobile Robots
  - 2.3.1 Unicycle
  - 2.3.2 Differential Drive WMR
  - 2.3.3 Tricycle
  - 2.3.4 Car-Like WMR
  - 2.3.5 Chain and Brockett Integrator Models
    - 2.3.5.1 Unicycle WMR
    - 2.3.5.2 Rear-Wheel Driving Car
  - 2.3.6 Car-Pulling Trailer WMR
- 2.4 Omnidirectional WMR Kinematic Modeling
  - 2.4.1 Universal Multi-Wheel WMR
  - 2.4.2 Four-Wheel Omnidirectional WMR with mecanum wheels

References

### 3. Mobile Robot Dynamics

- 3.1 Introduction

- 3.2 General Robot Dynamic Modeling
  - 3.2.1 Newton-Euler Dynamic Model
  - 3.2.2 Lagrange Dynamic Model
  - 3.2.3 Lagrange Model of a Multi-Link Robot
  - 3.2.4 Dynamic Modeling of Nonholonomic Robots
- 3.3 Differential Drive WMR
  - 3.3.1 Newton –Euler Dynamic Model
  - 3.3.2 Lagrange Dynamic Model
  - 3.3.3 Dynamics of WMR with Slip
- 3.4 Car-Like WMR Dynamic Model
- 3.5 Three-Wheel Omnidirectional Mobile Robot
- 3.6 Four Mecanum-Wheel Omnidirectional Robot
- References

#### **4. Mobile Robot Sensors**

- 4.1 Introduction
- 4.2 Sensor Classification and Characteristics
  - 4.2.1 Sensor Classification
  - 4.2.2 Sensor Characteristics
- 4.3 Position and Velocity Sensors
  - 4.3.1 Position Sensors
  - 4.3.2 Velocity Sensors
- 4.4 Distance Sensors
  - 4.4.1 Sonar Sensors
  - 4.4.2 Laser Sensors
  - 4.4.3 Infrared Sensors
- 4.5 Robot Vision
  - 4.5.1 General Issues
  - 4.5.2 Sensing
    - 4.5.2.1 Camera Calibration
    - 4.5.2.2 Image Acquisition
    - 4.5.2.3 Illumination
    - 4.5.2.4 Imaging Geometry
  - 4.5.3 Preprocessing
  - 4.5.4 Image Segmentation
  - 4.5.5 Image Description
  - 4.5.6 Image Recognition
  - 4.5.7 Image Interpretation
  - 4.5.8 Omnidirectional Vision
- 4.6 Some Other Robotic Sensors
  - 4.6.1 Gyroscope
  - 4.6.2 Compass
  - 4.6.3 Force and Tactile Sensors
    - 4.6.3.1 Force Sensors
    - 4.6.3.2 Tactile Sensors
- 4.7 Global Positioning System
- 4.8 Appendix : Lens and Camera Optics
- References

#### **5. Mobile Robot Control I: The Lyapunov-Based Method**

- 5.1 Introduction



- 5.2 Background Concepts
  - 5.2.1 State Space Model
  - 5.2.2 Lyapunov Stability
  - 5.2.3 State Feedback Control
  - 5.2.4 Second-Order Systems
- 5.3 General Robot Controllers
  - 5.3.1 Proportional plus Derivative Position Control
  - 5.3.2 Lyapunov Stability- Based Control Design
  - 5.3.3 Computed Torque Control
  - 5.3.4 Robot Control in Cartesian Space
- 5.4 Control of Differential Drive Mobile Robot
  - 5.4.1 Nonlinear Kinematic Tracking Control
  - 5.4.2 Dynamic Tracking Control
- 5.5 Computed-Torque Control of Differential Drive Mobile Robot
  - 5.5.1 Kinematic Tracking Control
  - 5.5.2 Dynamic Tracking Control
- 5.6 Car-Like Mobile Robot Control
  - 5.6.1 Parking Control
  - 5.6.2 Leader-Follower Control
    - 5.6.2.1 Kinematic Controller
    - 5.6.2.2 Dynamic Controller
- 5.7 Omnidirectional Mobile Robot Control

References

## **6. Mobile Robot Control II: Affine Systems and Invariant Manifold**

### **Methods**

- 6.1 Introduction
- 6.2 Background Concepts
  - 6.2.1 Affine Dynamic Systems
  - 6.2.2 Manifolds
  - 6.2.3 Lyapunov Stability Using Invariant Sets
- 6.3 Feedback Linearization of Mobile Robots
  - 6.3.1 General Issues
  - 6.3.2 Differential Drive Robot Input-Output Feedback Linearization
    - 6.3.2.1 Kinematic Constraints Revisited
    - 6.3.2.2 Input-Output Feedback Linearization
    - 6.3.2.3 Trajectory Tracking Control
- 6.4 Mobile Robot Feedback Stabilizing Control Using Invariant Manifolds
  - 6.4.1 Stabilizing Control of Unicycle in Chained Model Form
  - 6.4.2 Dynamic Control of Differential Drive Robots Modelled by the Double Brockett Integrator
  - 6.4.3 Stabilizing Control of Car-Like Robot in Chained Model Form

References

## **7. Mobile Robot Control III: Adaptive and Robust Methods**

- 7.1 Introduction
- 7.2 Background Concepts
  - 7.2.1 Model Reference Adaptive Control
  - 7.2.2 Robust Nonlinear Sliding –Mode Control
  - 7.2.3 Robust Control Using the Lyapunov Stabilization Method
- 7.3 Model Reference Adaptive Control of Mobile Robots
  - 7.3.1 Differential –Drive WMR

- 7.3.2 Adaptive Control Via Input-Output Linearization
    - 7.3.2.1 Tracking Control for Known Parameters
    - 7.3.2.2 Adaptive Tracking Controller
  - 7.3.3 Omnidirectional Robot Model Reference Adaptive Control
  - 7.4 Sliding-Mode Control of Mobile Robots
  - 7.5 Sliding-Mode Control in Polar Coordinates
    - 7.5.1 Modeling
    - 7.5.2 Sliding –Mode Control
  - 7.6 Robust Control of Differential –Drive Robot Using the Lyapunov Method
- References

## **8. Mobile Robot Control IV: Fuzzy and Neural Methods**

- 8.1 Introduction
- 8.2 Background Concepts
  - 8.2.1 Fuzzy Systems
    - 8.2.1.1 Fuzzy Sets
    - 8.2.1.2 Fuzzy Systems Structure
  - 8.2.2 Neural Networks
    - 8.2.2.1 The Basic Artificial Neuron Model
    - 8.2.2.2 The Multilayer Perceptron
    - 8.2.2.3 The Backpropagation Algorithm
    - 8.2.2.4 The Radial Basis Function Network
    - 8.2.2.5 The Universal Approximation Property
- 8.3 Fuzzy and Neural Robot Control: General Issues
  - 8.3.1 Fuzzy Robot Control
  - 8.3.2 Neural Robot Control
- 8.4 Fuzzy Control of Mobile Robots
  - 8.4.1 Adaptive Fuzzy Tracking Controller
  - 8.4.2 Fuzzy Local Path Tracker for Dubins Car
    - 8.4.2.1 The Problem
    - 8.4.2.2 Tracking
  - 8.4.3 Fuzzy Sliding-Mode Control
    - 8.4.3.1 The Mobile Robot Model
    - 8.4.3.2 Similarity of Fuzzy Logic Controller and Sliding-Mode Controller
    - 8.4.3.3 Analytical Representation of a Diagonal Type FLC
    - 8.4.3.4 Application to the Mobile Robot
- 8.5 Neural Control of Mobile Robots
  - 8.5.1 Adaptive Tracking Controller Using Multilayer Perceptron Network
  - 8.5.2 Adaptive Tracking Controller Using Radial Basis Function Network
  - 8.5.3 Appendix: Proof of Neurocontroller Stability

References

## **9. Mobile Robot Control V: Vision-Based Methods**

- 9.1 Introduction
- 9.2 Background Concepts
  - 9.2.1 Classification of Visual Robot Control
  - 9.2.2 Kinematic Transformations
  - 9.2.3 Camera Visual Transformations

- 9.2.4 Image Jacobian Matrix
- 9.3 Position-Based Visual Control: General Issues
  - 9.3.1 Point-to-Point Positioning
  - 9.3.2 Pose-Based Motion Control
- 9.4 Image –Based Visual Control: General Issues
  - 9.4.1 Use of the Inverse Jacobian
  - 9.4.2 Use of the Transpose Extended Jacobian
  - 9.4.3 Estimation of the Image Jacobian Matrix
- 9.5 Mobile Robot Visual Control
  - 9.5.1 Pose Stabilizing Control
  - 9.5.2 Wall Following Control
  - 9.5.3 Leader-Follower Control
- 9.6 Keeping a Landmark in the Field of View
- 9.7 Adaptive Straight-Path Following Visual Control
  - 9.7.1 Image Jacobian
  - 9.7.2 The Visual Controller
    - 9.7.2.1 Kinematic Controller
    - 9.7.2.2 Dynamic Controller
    - 9.7.2.3 Adaptive Controller
- 9.8 Image-Based Mobile Robot Visual Servoing
- 9.9 Mobile Robot Visual Servoing Using Omnidirectional Vision
  - 9.9.1 General Issues: Hyperbola, Parabola and Ellipse Equations
  - 9.9.2 Catadioptic Projection Geometry
  - 9.9.3 Omnidirectional Vision-Based Mobile Robot Visual Servoing

#### References

### **10. Mobile Manipulator Modeling and Control**

- 10.1 Introduction
- 10.2 Background Concepts
  - 10.2.1 The Denavit-Hartenberg Method
  - 10.2.2 Robot Inverse Kinematics
  - 10.2.3 Manipulability Measure
  - 10.2.4 The Two-Link Planar Robot
    - 10.2.4.1 Kinematics
    - 10.2.4.2 Dynamics
    - 10.2.4.3 Manipulability Measure
- 10.3 Mobile Manipulator Modeling
  - 10.3.1 General Kinematic Model
  - 10.3.2 General Dynamic Model
  - 10.3.3 Modeling a Five DOF Nonholonomic Manipulator
    - 10.3.3.1 Kinematics
    - 10.3.3.2 Dynamics
  - 10.3.4 Modeling an Omnidirectional Mobile Manipulator
    - 10.3.4.1 Kinematics
    - 10.3.4.2 Dynamics
- 10.4 Control of Mobile Manipulators
  - 10.4.1 Computed-Torque Control of a Differential Drive Mobile Manipulator
  - 10.4.2 Sliding- Mode Control of Omnidirectional Mobile Manipulator
- 10.5 Vision-Based Control of Mobile Manipulators
  - 10.5.1 General Issues

10.5.2 Full-State MM Visual Control

References

**11. Mobile Robot Path, Motion, and Task Planning**

11.1 Introduction

11.2 General Concepts

11.3 Path Planning of Mobile Robots

11.3.1 Basic Operations of Robot Navigation

11.3.2 Classification of Path Planning Methods

11.4 Model-Based Robot Path Planning

11.4.1 Configuration Space

11.4.2 Road Map Path Planning Methods

11.4.2.1 Road Maps

11.4.2.2 Cell Decomposition

11.4.2.3 Potential Fields

11.4.2.4 Vector Field Histograms

11.4.3 Integration of Global and Local Path Planning

11.4.4 Complete Coverage Path Planning

11.5 Mobile Robot Motion Planning

11.5.1 General On-Line Method

11.5.2 Motion Planning Using Vector Fields

11.5.3 Analytic Motion Planning

11.6 Mobile Robot Task Planning

11.6.1 General Issues

11.6.2 Plan Representation and Generation

11.6.2.1 Plan Representation

11.6.2.2 Plan Generation

11.6.3 World Modeling, Task Specification, and Robot Program

Synthesis

11.6.3.1 World Modeling

11.6.3.2 Task Specification

11.6.3.3 Robot Program Synthesis

References

**12. Mobile Robot Localization and Mapping**

12.1 Introduction

12.2 Background Concepts

12.2.1 Stochastic Processes

12.2.2 Stochastic Dynamic Models

12.2.3 Discrete-Time Kalman Filter and Predictor

12.2.4 Bayesian Learning

12.3 Sensor Imperfections

12.4 Relative Localization

12.5 Kinematic Analysis of Dead Reckoning

12.6 Absolute Localization

12.6.1 General Issues

12.6.2 Localization by Trilateration

12.6.3 Localization by Triangulation

12.6.4 Localization by Map Matching

12.7 Kalman Filter –Based Localization, and Sensor Calibration and Fusion

12.7.1 Robot Localization

- 12.7.2 Sensor Calibration
- 12.7.3 Sensor Fusion
- 12.8 Simultaneous Localization and Mapping (SLAM)
  - 12.8.1 General Issues
  - 12.8.2 Extended Kalman Filter SLAM
  - 12.8.3 Bayesian Estimator SLAM
  - 12.8.4 Particle Filter SLAM

References

### **13. Experimental Studies**

- 13.1 Introduction
  - 13.2 Model Reference Adaptive Control
  - 13.3 Lyapunov –Based Robust Control
  - 13.4 Parking-Stabilizing Control by a Polar –Based Controller
  - 13.5 Stabilization Using Invariant Manifold –Based Controllers
  - 13.6 Sliding –Mode Fuzzy Logic Control
  - 13.7 Vision –Based Control
    - 13.7.1 Leader –Follower Control
    - 13.7.2 Coordinated Open/Closed –Loop Control
    - 13.7.3 Omnidirectional Vision-Based Control
  - 13.8 Sliding –Mode Control of Omnidirectional Robot
  - 13.9 Control of Differential Drive Mobile Manipulator
    - 13.9.1 Computed Torque Control
    - 13.9.2 Control with Maximum Manipulability
  - 13.10 Integrated Global and Local Fuzzy Logic-Based Path Planner
  - 13.11 Hybrid Fuzzy-Neural Path Planning in Uncertain Environments
  - 13.12 Extended Kalman Filter –Based Mobile Robot SLAM
  - 13.13 Particle Filter-Based SLAM for the cooperation of Two Robots
  - 13.14 Neural Network Mobile Robot Control and Navigation
    - 13.14.1 Trajectory Tracking Control
    - 13.14.2 Navigation for Obstacle Avoidance
      - 13.14.2.1 Local Model Networks
      - 13.14.2.2 The Fuzzy C- Means Algorithm
      - 13.14.2.3 Experimental Results
  - 13.15 Fuzzy Tracking Control of Differential Drive Robot
  - 13.16 Vision-Based Adaptive Robust Tracking Control of Differential Drive Robot
  - 13.17 Mobile Manipulator Spherical Catadioptric Visual Control
- References

### **14. Generic Systemic and Software Architectures for Mobile Robot**

#### **Intelligent Control**

- 14.1 Introduction
- 14.2 Systemic Intelligent Control Architectures
  - 14.2.1 General Issues
  - 14.2.2 Hierarchical Intelligent Control Architecture
  - 14.2.3 Multiresolutional Intelligent Control Architecture
  - 14.2.4 Reference Model Intelligent Control Architecture
  - 14.2.5 Behavior-Based Intelligent Control Architectures
- 14.3 Characteristics of Mobile Robot Control Software Architectures

- 14.4 Brief Description of Two Mobile Robot Control Software Architectures
  - 14.4.1 The Jde Component Oriented Architecture
  - 14.4.2 Layered Mobile Robot Control Software Architecture
- 14.5 Comparative Evaluation of Two Mobile Robot Control Software Architectures
  - 14.5.1 Preliminary Issues
  - 14.5.2 The Comparative Evaluation
    - 14.5.2.1 Operating System and Language Support
    - 14.5.2.2 Communication Facilities
    - 14.5.2.3 Hardware Abstraction
    - 14.5.2.4 Porting and Application Building
    - 14.5.2.5 Run-Time Consideration
    - 14.5.2.6 Documentation
- 14.6 Intelligent Human-Robot Interfaces
  - 14.6.1 Structure of an Intelligent HRI
  - 14.6.2 Principal Functions of HRIs
  - 14.6.3 Natural Language HRIs
  - 14.6.4 Graphical HRIs
- 14.7 Two Intelligent Mobile Robot Research Prototypes
  - 14.7.1 The SENARIO Intelligent Wheelchair
  - 14.7.2 The ROMAN Intelligent Service Mobile Manipulator
- 14.8 Discussion of Some Further Issues
  - 14.8.1 Design for Heterogeneity
  - 14.8.2 Modular Design

#### References

### **15. Mobile Robots at Work**

- 15.1 Introduction
- 15.2 Mobile Robots in the Factory and Industry
- 15.3 Mobile Robots in the Society
  - 15.3.1 Mobile Manipulators for Rescue
  - 15.3.2 Robotic Canes, Guiding Assistants, and Hospital Mobile Robots
  - 15.3.3 Mobile Robots for Home Services
- 15.4 Assistive Mobile Robots
- 15.5 Mobile Telerobots and Web-Robots
- 15.6 Other Mobile Robot Applications
  - 15.6.1 War Robots
  - 15.6.2 Entertainment Robots
  - 15.6.3 Research Robots
- 15.7 Mobile Robot Safety

#### References

### **Problems**

- A. Kinematics
- B. Dynamics
- C. Sensors
- D. Control
- E. Visual Servoing
- F. Fuzzy and Neural Methods

G. Planning	
H. Affine Systems and Invariant Manifolds	
<b>Robotics Web Sites</b>	
1. General Robotics	
2. Mobile Robotics	
<b>Thirty Mobile Robot Companies</b>	
<b>A Sample of Commercial Mobile Robots</b>	
<b>List of Acknowledged Authors and Collaborators</b>	

## Principal Symbols and Acronyms

$t, k$	Continuous, discrete time
$l, s, D, d$	Linear distance (length)
$\mathbf{p}, \mathbf{d}, \mathbf{x}$	Position vector
$\mathbf{R}$	Rotation matrix
$\mathbf{R}_x, \mathbf{R}_y, \mathbf{R}_z$	Rotation matrix w.r.t. axis $x, y, z$
$\mathbf{n}, \mathbf{o}, \mathbf{a}$	normal, orientation and approach unit vectors
$\mathbf{A}, \mathbf{T}$	Homogeneous $(4 \times 4)$ matrix
$\mathbf{q}$	Generalized variable (linear, angular)
$\mathbf{v}, \mathbf{v}$	Linear velocity vector
$\boldsymbol{\omega}, \dot{\boldsymbol{\theta}}$	Angular velocity vector
$\mathbf{J}(\mathbf{q})$	Jacobian matrix
$\mathbf{J}^{-1}(\mathbf{q})$	Inverse of $\mathbf{J}(\mathbf{q})$
$\mathbf{J}^{\dagger}(\mathbf{q})$	Generalized inverse (pseudoinverse) of $\mathbf{J}(\mathbf{q})$
$D-H$	Denavit-Hartenberg
$\det(\cdot)$	Determinant
$\mathbf{F}, \boldsymbol{\tau}, (\mathbf{N})$	Force, torque vector
$L$	Lagrangian function
$K, P$	Kinetic, potential energy
$\mathbf{D}(\mathbf{q})$	Inertial matrix
$\mathbf{g}(\mathbf{q})$	Gravity term
$HRI$	Human-robot interface
$GHRI$	Graphical human-robot interface
$IC$	Intelligent control
$ICA$	Intelligent control architecture
$NL$	Natural Language
$NL-HRI$	Natural language HRI
$UI$	User interface
$\mathbf{C}(\mathbf{q}, \dot{\mathbf{q}})\dot{\mathbf{q}}$	Centrifugal/Coriolis term
$O_{xyz}$	Coordinate frame
$WMR$	Wheeled mobile robot

$MM$	Mobile manipulator
$LS$	Least squares
$\phi, \psi$	WMR direction, steering angles
$DOF$	Degree of freedom
$c.o.g$	Center of gravity
$COM$	Center of mass
$\mathbf{M}(\mathbf{q})$	Nonholonomic constraint
$CS$	Configuration space
$GPS$	Global positioning system
$l_f$	Lens focal length
$\mathbf{K}_p, \mathbf{K}_v$	Position, velocity gain matrix
$KF, EKF$	Kalman filter, extended Kalman filter
$SLAM$	Simultaneous localization and mapping
$\hat{\mathbf{x}}, \hat{\boldsymbol{\theta}}$	Estimate of $\mathbf{x}, \boldsymbol{\theta}$
$\tilde{\mathbf{x}}, \tilde{\boldsymbol{\theta}}$	Error of the estimate $\hat{\mathbf{x}}, \hat{\boldsymbol{\theta}}$
$\boldsymbol{\Sigma}_x, \boldsymbol{\Sigma}_\theta$	Covariance matrix of $\tilde{\mathbf{x}}, \tilde{\boldsymbol{\theta}}$
$AI$	Artificial intelligence
$RF$	Radio frequency
$CAD$	Computer-aided design
$\bar{x}(s)$	Laplace transform of $x(t)$
$G(s), \bar{g}(s)$	Transfer function
$\omega_n$	Natural angular frequency
$\zeta$	Damping factor
$P, PD$	Proportional, proportional plus derivative
$PI, PID$	Proportional plus integral (plus derivative)
$MRAC$	Model reference adaptive control
$SMC$	Sliding mode control
$\mathbf{J}_{im}$	Image Jacobian
$VRS(VRC)$	Visual robot servoing (control)
$FL(FC)$	Fuzzy logic (fuzzy control)
$NN$	Neural network
$BP$	Back propagation
$RFN$	Radial basis function neural network (RBF-NN)
$MLP$	Multi-layer perceptron
$NF$	Neurofuzzy
$MB$	Model-based
$tg, \tan$	Trigonometric tangent of an angle
$tg^{-1}, \arctan$	Inverse of $tg, \tan$



## Quotations about Robotics

**Aristotle** *If every tool, when ordered, or even of its own accord, could do the work that benefits it, just as the creations of Daedalus move by themselves..., then there would be no need of apprentices for the master workers or of slaves for their lords.*

**Allen Newel** *From where I stand it is easy to see the science lurking in robotics. It lies in the welding of intelligence to energy. That is, it lies in intelligent perception and intelligent control of motion.*

**Rod Grupen** *At bottom, robotics is about us. It is the discipline of emulating our lives, of wondering how we work.*

**Rob Spencer** *Got a dirty, dangerous, dull job? Let a robot do it and keep your workers safe.*

**Marvin Minsky** *We wanted to solve robot problems and needed some vision, action, reasoning, planning, and so on.....Eventually, robots will make everything.*

**David Hanson** *Making realistic robots is going to polarize the market. You will have people who love it and some people who will really be disturbed.*

**John McCarthy** *Every aspect of learning or any other feature of intelligence can in principle be so precisely described that a machine can be made to simulate it. No robot has ever been designed that is ever aware of what is doing; but most of the time, we aren't either.*

**John McDermott** *To be useful, a system has to do more than just correctly perform some task.*

**Chuck Gosdzinski** *The top two awards don't even go to robots*

## Chapter 2

# Mobile Robot Kinematics

### 2.1 Introduction

*Robot kinematics* deals with the configuration of robots in their workspace, the relations between their geometric parameters, and the constraints imposed in their trajectories. The kinematic equations depend on the geometrical structure of the robot. For example, a fixed robot can have a Cartesian, cylindrical, spherical or articulated structure, and a mobile robot may have one two, three or more wheels with or without constraints in their motion. The study of kinematics is a fundamental prerequisite for the study of dynamics, the stability features, and the control of the robot. The development of new and specialized robotic kinematic structures is still a topic of ongoing research, towards the end of constructing robots that can perform more sophisticated and complex tasks in industrial and societal applications.

The objectives of this chapter are the following :

- To present the fundamental analytical concepts required for the study of mobile robot kinematics.
- To present the kinematic models of nonholonomic mobile robots (unicycle, differential drive, tricycle, car-like WMRs).
- To present the kinematic models of 3-wheel, 4-wheel, and multi-wheel omnidirectional WMRs.

### 2.2 Background Concepts

As a preparation for the study of mobile robot kinematics the following background concepts are presented :

- Direct and inverse robot kinematics
- Homogeneous transformations
- Nonholonomic constraints

#### 2.2.1 Direct and Inverse Robot Kinematics

Consider a fixed or mobile robot with generalized coordinates  $q_1, q_2, \dots, q_n$  in the joint (or actuation) space and  $x_1, x_2, \dots, x_m$  in the task space. Define the vectors :

$$\mathbf{q} = \begin{bmatrix} q_1 \\ q_2 \\ \vdots \\ q_n \end{bmatrix}, \mathbf{p} = \begin{bmatrix} x_1 \\ x_2 \\ \vdots \\ x_m \end{bmatrix} \quad (2.1)$$

The problem of determining  $\mathbf{p}$  knowing  $\mathbf{q}$  is called the *direct kinematics* problem. In general  $\mathbf{p} \in R^m$  and  $\mathbf{q} \in R^n$  ( $R^n$  denotes the n-dimensional Euclidean space) are related by a nonlinear function (model) as :

$$\mathbf{p} = \mathbf{f}(\mathbf{q}), \mathbf{f}(\mathbf{q}) = \begin{bmatrix} f_1(\mathbf{q}) \\ f_2(\mathbf{q}) \\ \vdots \\ f_m(\mathbf{q}) \end{bmatrix} \quad (2.2)$$

The problem of solving Eq.(2.2), i.e. of finding  $\mathbf{q}$  from  $\mathbf{p}$ , is called the *inverse kinematic* problem expressed by :

$$\mathbf{q} = \mathbf{f}^{-1}(\mathbf{p}) \quad (2.3)$$

The direct and inverse kinematic problems are pictorially shown in Fig. 2.1.

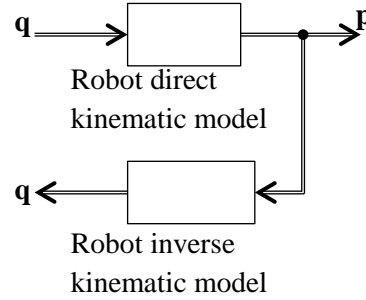


**Fig. 2.1 : Direct and inverse robot kinematic models.**

In general, kinematics is the branch of mechanics that investigates the motion of material bodies without referring to their masses / moments of inertia and the forces / torques that produce the motion. Clearly, the kinematic equations depend on the fixed geometry of the robot in the fixed world coordinate frame.

To get these motions we must tune appropriately the motions of the joint variables, expressed by the velocities  $\dot{\mathbf{q}} = [\dot{q}_1, \dot{q}_2, \dots, \dot{q}_n]^T$ . We therefore need to find the differential relation of  $\mathbf{q}$  and  $\mathbf{p}$ . This is called *direct differential kinematics* and is expressed by :

$$d\mathbf{p} = \mathbf{J}d\mathbf{q} \quad (2.4)$$

where :

$$d\mathbf{q} = \begin{bmatrix} dq_1 \\ \vdots \\ dq_n \end{bmatrix}, d\mathbf{p} = \begin{bmatrix} dx_1 \\ \vdots \\ dx_m \end{bmatrix}$$

and the  $m \times n$  matrix :

$$\mathbf{J} = \begin{bmatrix} \frac{\partial x_1}{\partial q_1} & \frac{\partial x_1}{\partial q_2} & \dots & \frac{\partial x_1}{\partial q_n} \\ \dots & \dots & \dots & \dots \\ \dots & \dots & \dots & \dots \\ \frac{\partial x_m}{\partial q_1} & \frac{\partial x_m}{\partial q_2} & \dots & \frac{\partial x_m}{\partial q_n} \end{bmatrix} = [\mathbf{J}_{ij}] \quad (2.5)$$

with  $(i, j)$  element  $J_{ij} = \partial x_i / \partial q_j$  is called the *Jacobian matrix* of the robot<sup>2</sup>.

<sup>2</sup> It is remarked that in many works the Jacobian matrix is defined as the transpose of that defined in Eq.(2.5).

For each configuration  $q_1, q_2, \dots, q_n$  of the robot, the Jacobian matrix represents the relation of the displacements of the joints with the displacement of the position of the robot in the task space.

Let  $\dot{\mathbf{q}} = [\dot{q}_1, \dots, \dot{q}_n]^T$  and  $\dot{\mathbf{p}} = [\dot{x}_1, \dot{x}_2, \dots, \dot{x}_m]^T$  be the velocities in the joint and task spaces.

Then, dividing Eq.(2.4) by  $dt$  we get formally :

$$\frac{d\mathbf{p}}{dt} = \mathbf{J} \frac{d\mathbf{q}}{dt} \text{ or } \dot{\mathbf{p}} = \mathbf{J}\dot{\mathbf{q}} \quad (2.6)$$

Under the assumption that  $m = n$  ( $\mathbf{J}$  square) and that the inverse Jacobian matrix  $\mathbf{J}^{-1}$  exists (i.e., its determinant is not zero :  $\det \mathbf{J} \neq 0$ ), from Eq.(2.6) we get :

$$\dot{\mathbf{q}} = \mathbf{J}^{-1}\dot{\mathbf{p}} \quad (2.7)$$

This is the inverse differential kinematics equation, and is illustrated in Fig. 2.2.

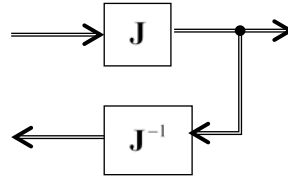


**Fig. 2.2 : Direct and inverse differential kinematics.**

If  $m \neq n$ , then we have two cases :

**Case 1** There are more equations than unknowns ( $m > n$ ), i.e.,  $\dot{\mathbf{q}}$  is *overspecified*. In this case  $\mathbf{J}^{-1}$  in Eq.(2.7) is replaced by the generalized inverse  $\mathbf{J}^{\dagger}$  given by :

$$\mathbf{J}^{\dagger} = (\mathbf{J}^T \mathbf{J})^{-1} \mathbf{J}^T \quad (2.8a)$$

under the condition that  $\mathbf{J}$  is full rank (i.e.  $\text{rank } \mathbf{J} = \min(m, n) = n$ ) so as  $\mathbf{J}^T \mathbf{J}$  is invertible. The expression (2.8a) of  $\mathbf{J}^{\dagger}$  follows by minimizing the squared norm of the difference  $\dot{\mathbf{p}} - \mathbf{J}\dot{\mathbf{q}}$ , i.e. of the function :

$$V = \|\dot{\mathbf{p}} - \mathbf{J}\dot{\mathbf{q}}\|^2 = (\dot{\mathbf{p}} - \mathbf{J}\dot{\mathbf{q}})^T (\dot{\mathbf{p}} - \mathbf{J}\dot{\mathbf{q}})$$

with respect to  $\dot{\mathbf{q}}$ . The optimality condition is :

$$\partial V / \partial \dot{\mathbf{q}} = -2(\dot{\mathbf{p}} - \mathbf{J}\dot{\mathbf{q}})^T \mathbf{J} = \mathbf{0}$$

which, if solved for  $\dot{\mathbf{q}}$ , gives :

$$\dot{\mathbf{q}} = (\mathbf{J}^T \mathbf{J})^{-1} \mathbf{J}^T \dot{\mathbf{p}} = \mathbf{J}^{\dagger} \dot{\mathbf{p}}$$

**Case 2** There are less equations than unknowns ( $m < n$ ), i.e.,  $\dot{\mathbf{q}}$  is *underspecified* and many choices of  $\dot{\mathbf{q}}$  lead to the same  $\dot{\mathbf{p}}$ . In this case we select  $\dot{\mathbf{q}}$  with the minimum norm, i.e., we solve the constrained minimization problem :

$$\min \|\dot{\mathbf{q}}\|^2 \text{ subject to } \dot{\mathbf{p}} - \mathbf{J}\dot{\mathbf{q}} = \mathbf{0}, \quad \dot{\mathbf{q}} \in R^n$$

Introducing the Lagrange multiplier vector  $\lambda$ , we get the augmented (unconstrained) Lagrangian minimization problem :

$$\min_{\dot{\mathbf{q}}, \lambda} L(\dot{\mathbf{q}}, \lambda), \quad L(\dot{\mathbf{q}}, \lambda) = \dot{\mathbf{q}}^T \dot{\mathbf{q}} + \lambda^T (\dot{\mathbf{p}} - \mathbf{J}\dot{\mathbf{q}})$$

The optimality conditions are :

$$\partial L / \partial \dot{\mathbf{q}} = 2\dot{\mathbf{q}} - \mathbf{J}^T \lambda = \mathbf{0}, \quad \partial L / \partial \lambda = \dot{\mathbf{p}} - \mathbf{J}\dot{\mathbf{q}} = \mathbf{0}$$

Solving the first for  $\dot{\mathbf{q}}$  we get  $\dot{\mathbf{q}} = (1/2)\mathbf{J}^T\lambda$ .

Introducing this result into  $\partial L / \partial \lambda = \mathbf{0}$  yields :

$$\lambda = 2(\mathbf{J}\mathbf{J}^T)^{-1}\dot{\mathbf{p}}$$

Therefore, finally we find :

$$\dot{\mathbf{q}} = \mathbf{J}^T (\mathbf{J}\mathbf{J}^T)^{-1} \dot{\mathbf{p}} = \mathbf{J}^\dagger \dot{\mathbf{p}}$$

where :

$$\mathbf{J}^\dagger = \mathbf{J}^T (\mathbf{J}\mathbf{J}^T)^{-1} \quad (2.8b)$$

under the condition that  $\text{rank } \mathbf{J} = m$  (i.e.,  $\mathbf{J}\mathbf{J}^T$  invertible). Therefore, when  $m < n$  the generalized inverse Eq.(2.8b) should be used.

Formally, the generalized inverse  $\mathbf{J}^\dagger$  of a  $m \times n$  real matrix  $\mathbf{J}$  is defined to be the unique  $n \times m$  real matrix that satisfies the following four conditions :

$$\begin{aligned} \mathbf{J}\mathbf{J}^\dagger\mathbf{J} &= \mathbf{J}, \quad \mathbf{J}^\dagger\mathbf{J}\mathbf{J}^\dagger = \mathbf{J}^\dagger \\ (\mathbf{J}\mathbf{J}^\dagger)^T &= \mathbf{J}\mathbf{J}^\dagger, \quad (\mathbf{J}^\dagger\mathbf{J})^T = \mathbf{J}^\dagger\mathbf{J} \end{aligned}$$

It follows that  $\mathbf{J}^\dagger$  has the properties :

$$(\mathbf{J}^\dagger)^\dagger = \mathbf{J}, \quad (\mathbf{J}^T)^\dagger = (\mathbf{J}^\dagger)^T, \quad (\mathbf{J}\mathbf{J}^T)^\dagger = (\mathbf{J}^\dagger)^T \mathbf{J}^\dagger$$

All the above relations are useful when dealing with overspecified or underspecified linear algebraic systems (encountered, for example, in underactuated or overactuated mechanical systems).

### 2.2.2 Homogeneous Transformations

The position and orientation of a solid body (e.g., a robotic link) with respect to the fixed world coordinate frame Oxyz (Fig. 2.3) are given by a  $4 \times 4$  transformation matrix  $\mathbf{A}$ , called *homogeneous transformation*, of the type :

$$\mathbf{A} = \begin{bmatrix} \mathbf{R} & \mathbf{p} \\ \mathbf{0} & 1 \end{bmatrix} \quad (2.9)$$

where  $\mathbf{p}$  is the position vector of the center of gravity  $O'$  (or some other fixed point of the link) with respect to Oxyz, and  $\mathbf{R}$  is a  $3 \times 3$  matrix defined as :

$$\mathbf{R} = [\mathbf{n} \mid \mathbf{o} \mid \mathbf{a}] \quad (2.10)$$

In Eq.(2.10),  $\mathbf{n}$ ,  $\mathbf{o}$  and  $\mathbf{a}$  are the unit vectors along the axes  $x_b$ ,  $y_b$ ,  $z_b$  of the local coordinate frame  $O'x_b y_b z_b$ . The matrix  $\mathbf{R}$  represents the rotation of  $O'x_b y_b z_b$  with respect to the reference (world) frame Oxyz. The columns  $\mathbf{n}$ ,  $\mathbf{o}$  and  $\mathbf{a}$  of  $\mathbf{R}$  are pairwise orthonormal, i.e.,  $\mathbf{n}^T \mathbf{o} = 0$ ,  $\mathbf{o}^T \mathbf{a} = 0$ ,  $\mathbf{a}^T \mathbf{n} = 0$ ,  $|\mathbf{n}| = 1$ ,  $|\mathbf{o}| = 1$ ,  $|\mathbf{a}| = 1$ , where  $\mathbf{b}^T$  denotes the transpose (row) vector of the column vector  $\mathbf{b}$ , and  $|\mathbf{b}|$  denotes the Euclidean norm of  $\mathbf{b}$  ( $|\mathbf{b}| = [b_x^2 + b_y^2 + b_z^2]^{1/2}$ ), with  $b_x$ ,  $b_y$  and  $b_z$  being the  $x, y, z$  components of  $\mathbf{b}$ , respectively.

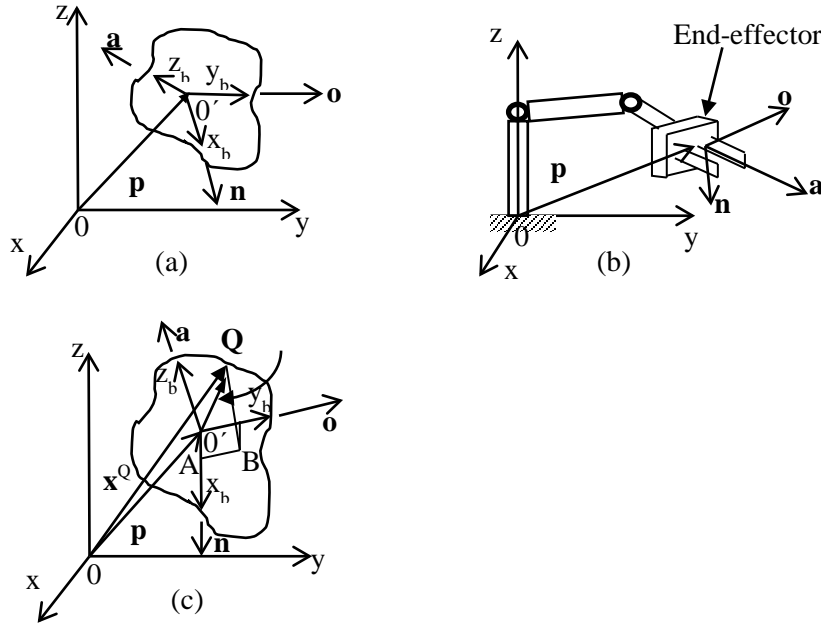


**Fig. 2.3 :** (a) Position and orientation of a solid body, (b) Position and orientation of a robotic end-effector ( $\mathbf{a}$  = approach vector,  $\mathbf{n}$  = normal vector,  $\mathbf{o}$  = orientation or sliding vector), (c) Position vectors of a point  $Q$  with respect to the frames  $Oxyz$  and  $O'x_h y_h z_h$ .

Thus the rotation matrix  $\mathbf{R}$  is orthonormal, i.e. :

$$\mathbf{R}^{-1} = \mathbf{R}^T \quad (2.11)$$

To work with homogeneous matrices we use 4-dimensional vectors (called *homogeneous vectors*) of the type :

$$\mathbf{X}^Q = \begin{bmatrix} x^Q \\ y^Q \\ z^Q \\ 1 \end{bmatrix} = \begin{bmatrix} \mathbf{x}^Q \\ 1 \end{bmatrix}, \quad \mathbf{X}_b^Q = \begin{bmatrix} x_b^Q \\ y_b^Q \\ z_b^Q \\ 1 \end{bmatrix} = \begin{bmatrix} \mathbf{x}_b^Q \\ 1 \end{bmatrix} \quad (2.12)$$

Suppose that  $\mathbf{X}_b^Q$  and  $\mathbf{X}^Q$  are the homogeneous position vectors of a point  $Q$  in the coordinate frames  $O'x_h y_h z_h$  and  $Oxyz$ , respectively. Then, from Fig. 2.3c we obtain the following vectorial equation :

$$\overrightarrow{OQ} = \overrightarrow{OO'} + \overrightarrow{O'A} + \overrightarrow{AB} + \overrightarrow{BQ}$$

where :

$$\overrightarrow{OQ} = \mathbf{x}^Q, \quad \overrightarrow{OO'} = \mathbf{p}, \quad \overrightarrow{O'A} = x_b^Q \mathbf{n}, \quad \overrightarrow{AB} = y_b^Q \mathbf{o}, \quad \overrightarrow{BQ} = z_b^Q \mathbf{a}$$

Thus :

$$\mathbf{x}^Q = \mathbf{p} + x_b^Q \mathbf{n} + y_b^Q \mathbf{o} + z_b^Q \mathbf{a} = \mathbf{p} + \begin{bmatrix} \mathbf{n} & \mathbf{o} & \mathbf{a} \end{bmatrix} \begin{bmatrix} x_b^Q \\ y_b^Q \\ z_b^Q \end{bmatrix} = \mathbf{p} + \mathbf{R} \mathbf{x}_b^Q \quad (2.13a)$$

or

$$\mathbf{X}^Q = \left[ \begin{array}{ccc|c} \mathbf{n} & \mathbf{o} & \mathbf{a} & \mathbf{p} \\ \hline 0 & 0 & 0 & 1 \end{array} \right] \mathbf{X}_b^Q = \mathbf{A} \mathbf{X}_b^Q \quad (2.13b)$$

where  $\mathbf{A}$  is given by Eqs.(2.9)-(2.10). Equation (2.13b) indicates that the homogeneous matrix  $\mathbf{A}$  contains both the position and orientation of the local coordinate frame  $O'x_by_bz_b$  with respect to the world coordinate frame  $Oxyz$ .

It is easy to verify that :

$$\mathbf{A}^{-1} = \begin{bmatrix} \mathbf{R}^T & -\mathbf{R}^T \mathbf{p} \\ 0 & 1 \end{bmatrix} \quad (2.14)$$

Indeed, from Eq.(2.13a) we have :  $\mathbf{x}_b^O = -\mathbf{R}^{-1}\mathbf{p} + \mathbf{R}^{-1}\mathbf{x}^O$ , which by Eq.(2.11) gives :

$$\begin{bmatrix} \mathbf{x}_b^O \\ 1 \end{bmatrix} = \begin{bmatrix} \mathbf{R}^T & -\mathbf{R}^T \mathbf{p} \\ 0 & 1 \end{bmatrix} \begin{bmatrix} \mathbf{x}^O \\ 1 \end{bmatrix} = \mathbf{A}^{-1} \begin{bmatrix} \mathbf{x}^O \\ 1 \end{bmatrix}$$

The columns  $\mathbf{n}$ ,  $\mathbf{o}$  and  $\mathbf{a}$  of  $\mathbf{R}$  consist of the direction cosines with respect to  $Oxyz$ . Thus the rotation matrices with respect to axes  $x, y, z$  which are represented as :

$$\mathbf{n}_x = \begin{bmatrix} 1 \\ 0 \\ 0 \end{bmatrix}, \mathbf{o}_y = \begin{bmatrix} 0 \\ 1 \\ 0 \end{bmatrix}, \mathbf{a}_z = \begin{bmatrix} 0 \\ 0 \\ 1 \end{bmatrix}$$

are given by :

$$\mathbf{R}_x(\phi_x) = \begin{bmatrix} 1 & 0 & 0 \\ 0 & \cos \phi_x & -\sin \phi_x \\ 0 & \sin \phi_x & \cos \phi_x \end{bmatrix} \quad (2.15a)$$

$$\mathbf{R}_y(\phi_y) = \begin{bmatrix} \cos \phi_y & 0 & -\sin \phi_y \\ 0 & 1 & 0 \\ \sin \phi_y & 0 & \cos \phi_y \end{bmatrix} \quad (2.15b)$$

$$\mathbf{R}_z(\phi_z) = \begin{bmatrix} \cos \phi_z & -\sin \phi_z & 0 \\ \sin \phi_z & \cos \phi_z & 0 \\ 0 & 0 & 1 \end{bmatrix} \quad (2.15c)$$

where  $\phi_x$ ,  $\phi_y$  and  $\phi_z$  are the rotation angles with respect to  $x$ ,  $y$  and  $z$ , respectively.

In mobile robots moving on an horizontal plane, the robot is rotating only with respect to the vertical axis  $z$ , and so Eq.(2.15c) is used. Thus, for convenience, we drop the index  $z$ .

For better understanding, the upper left block of Eq.(2.15c) is obtained directly using the  $Oxy$  plane geometry shown in Fig. 2.4.

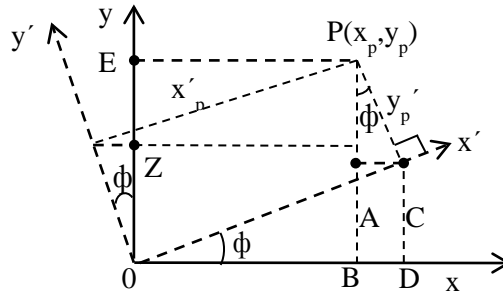


**Fig. 2.4 : Direct trigonometric derivation of the rotation matrix with respect to axis  $z$ .**

Let a point  $P(x_p, y_p)$  in the coordinate frame Oxy, which is rotated about the axis Oz by the angle  $\phi$ . The coordinates of  $P$  in the frame  $Ox'y'$  are  $x'_p$  and  $y'_p$  as shown in Fig. 2.4. From this figure we see that :

$$\begin{aligned} x_p &= (OB) = (OD) - (BD) = x'_p \cos \phi - y'_p \sin \phi \\ y_p &= (OE) = (EZ) + (ZO) = x'_p \sin \phi + y'_p \cos \phi \end{aligned} \quad (2.16)$$

i.e. :

$$\begin{bmatrix} x_p \\ y_p \end{bmatrix} = \begin{bmatrix} \cos \phi & -\sin \phi \\ \sin \phi & \cos \phi \end{bmatrix} \begin{bmatrix} x'_p \\ y'_p \end{bmatrix} \quad (2.17)$$

Similarly, one can derive the respective  $2 \times 2$  blocks  $\mathbf{R}_x(\phi_x)$  and  $\mathbf{R}_y(\phi_y)$  for the rotations about the  $x$  and  $y$  axis, respectively.

Given an open kinematic chain of  $n$  links, the homogeneous vector  $\mathbf{X}^n$  of the local coordinate frame  $O_n x_n y_n z_n$  of the  $n$ th link, expressed in the world coordinate frame Oxyz can be found by successive application of Eq.(2.13b), i.e., as :

$$\mathbf{X}^0 = \mathbf{A}_1^0 \mathbf{A}_2^1 \cdots \mathbf{A}_n^{n-1} \mathbf{X}^n \quad (2.18)$$

where  $\mathbf{A}_i^{i-1}$  is the  $4 \times 4$  homogeneous transformation matrix that leads from the coordinate frame of link  $i$  to that of link  $i-1$ . The matrices  $\mathbf{A}_i^{i-1}$  can be computed by the so-called *Denavit-Hartenberg (D-H)* method (see Sec.10.2.1). The general relation (2.18) is of the form (2.2), and provides the robot Jacobian as indicated in Eq.(2.5).

### 2.2.3 Nonholonomic Constraints

A nonholonomic constraint (relation) is defined to be a constraint that contains time derivatives of generalized coordinates (variables) of a system and is not integrable. To understand what this means we first define an *holonomic constraint* as any constraint which can be expressed in the form :

$$F(\mathbf{q}, t) = 0 \quad (2.19)$$

where  $\mathbf{q} = [q_1, q_2, \dots, q_n]^T$  is the vector of generalized coordinates.

Now, suppose we have a constraint of the form :

$$f(\mathbf{q}, \dot{\mathbf{q}}, t) = 0 \quad (2.20)$$

If this constraint can be converted to the form :

$$F(\mathbf{q}, t) = 0 \quad (2.21)$$

we say that it is *integrable*. Therefore, although  $f$  in Eq.(2.20) contains the time derivatives  $\dot{\mathbf{q}}$ , it can be expressed in the holonomic form Eq.(2.21), and so it is actually an holonomic constraint. More specifically we have the following definition.

**Definition 2.1** (*Nonholonomic constraint*)

A constraint of the form (2.20) is said to be *nonholonomic* if it cannot be rendered to the form (2.21) such that to involve only the generalized variables themselves ■

Typical systems that are subject to nonholonomic constraints (and hence are called *nonholonomic systems*) are underactuated robots, wheeled mobile robots (**WMR**), autonomous underwater vehicles (**AUV**), and unmanned aerial vehicles (**UAV**). It is emphasized that “holonomic” does not necessarily mean unconstrained. Surely, a



mobile robot with no constraint is holonomic. But a mobile robot capable of only translations is also holonomic.

*Nonholonomicity* occurs in several ways. For example a robot has only a few motors, say  $k < n$ , where  $n$  is the number of degrees of freedom, or the robot has redundant degrees of freedom. The robot can produce at most  $k$  independent motions. The difference  $n - k$  indicates the existence of nonholonomicity. For example, a differential drive WMR has two controls (the torques of the two wheel motors), i.e.,  $k = 2$ , and three degrees of freedom, i.e.,  $n = 3$ . Therefore it has one ( $n - k = 1$ ) nonholonomic constraint.

**Definition 2.2** (*Pfaffian constraints*)

A nonholonomic constraint is called a Pfaffian constraint if it is linear in  $\dot{\mathbf{q}}$ , i.e., if it can be expressed in the form :

$$\mu_i(\mathbf{q})\dot{\mathbf{q}} = 0, \quad i = 1, 2, \dots, r$$

where  $\mu_i$  are linearly independent row vectors and  $\mathbf{q} = [q_1, q_2, \dots, q_n]^T$  ■

In compact matrix form the above  $r$  Pfaffian constraints can be written as :

$$\mathbf{M}(\mathbf{q})\dot{\mathbf{q}} = \mathbf{0}, \quad \mathbf{M}(\mathbf{q}) = \begin{bmatrix} \mu_1(\mathbf{q}) \\ \mu_2(\mathbf{q}) \\ \vdots \\ \mu_r(\mathbf{q}) \end{bmatrix} \quad (2.22)$$

An example of integrable Pfaffian constraint is :

$$\mu(\mathbf{q})\dot{\mathbf{q}} = q_1\dot{q}_1 + q_2\dot{q}_2 + \dots + q_n\dot{q}_n, \quad \mathbf{q} \in R^n \quad (2.23)$$

This is integrable because it can be derived via differentiation, with respect to time, of the equation of a sphere :

$$s(\mathbf{q}) = q_1^2 + q_2^2 + \dots + q_n^2 - a^2 = 0$$

with constant radius  $a$ . The particular resulting sphere by integrating Eq.(2.23) depends on the initial state  $\mathbf{q}(t)_{t=0} = \mathbf{q}_0$ . The collection of all concentric spheres with center at the origin and radius “ $a$ ” is called a *foliation* with spherical leaves. For example, if  $n = 3$  the foliation produces a maximal integral manifold  $(0, 0, a)$  :

$$\mathcal{M} = \{\mathbf{q} \in R^3 : s(\mathbf{q}) = q_1^2 + q_2^2 + q_3^2 - a^2 = 0\}$$

The nonholonomic constraint encountered in mobile robotics is the motion constraint of a disk that rolls on a plane without slipping (Fig. 2.5). The no-slipping condition does not allow the generalized velocities  $\dot{x}$ ,  $\dot{y}$  and  $\dot{\phi}$  to take arbitrary values.

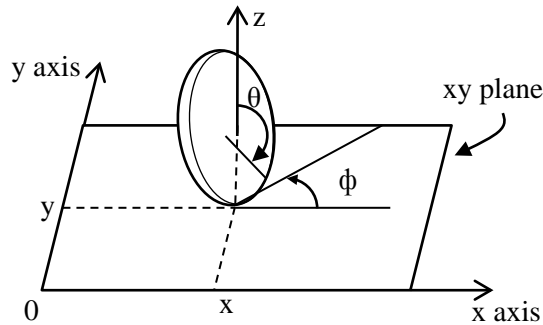


**Fig. 2.5 :** The generalized coordinates  $x$ ,  $y$  and  $\phi$ .

Let  $r$  be the disk radius. Due to the no-slipping condition the generalized coordinates are constrained by the following equations :

$$\dot{x} = r\dot{\theta} \cos \phi, \quad \dot{y} = r\dot{\theta} \sin \phi \quad (2.24)$$

which are not integrable. These constraints express the condition that the velocity vector of the disk center lies in the midplane of the disk. Eliminating the velocity  $v = r\dot{\theta}$  in Eq.(2.24) gives :

$$v = r\dot{\theta} = \frac{\dot{x}}{\cos \phi} = \frac{\dot{y}}{\sin \phi}$$

or

$$\dot{x} \sin \phi - \dot{y} \cos \phi = 0 \quad (2.25)$$

This is the non holonomic constraint of the motion of the disk. Because of the kinematic constraints (2.24), the disk can attain any final configuration  $(x_2, y_2, \phi_2, \theta_2)$  starting from any initial configuration  $(x_1, y_1, \phi_1, \theta_1)$ . This can be done in two steps as follows :

**Step 1 :** Move the contact point  $(x_1, y_1)$  to  $(x_2, y_2)$  by rolling the disk along a line of length  $(2k\pi + \theta_2 - \theta_1)r$ ,  $k = 0, 1, 2, \dots$

**Step 2 :** Rotate the disk about the vertical axis from  $\phi_1$  to  $\phi_2$ .

Given a kinematic constraint one has to determine whether it is integrable or not. This can be done via the *Frobenius theorem* which uses the differential geometry concepts of *distributions* and *Lie Brackets*. We will come to this later (See Sec.6.2.1).

Two other systems that are subject to nonholonomic constraints are the *rolling ball* on a plane without spinning on place, and the *flying airplane* that cannot instantaneously stop in the air or move backwards.

## 2.3 Nonholonomic Mobile Robots

The kinematic models of the following nonholonomic WMRs will be derived :

- Unicycle
- Differential drive WMR
- Tricycle WMR
- Car-like WMR

### 2.3.1 Unicycle

Unicycle has a kinematic model which is used as a basis for many types of nonholonomic WMRs. For this reason this model has attracted much theoretical attention by WMR controlists and nonlinear systems workers.

Unicycle is a conventional wheel rolling on an horizontal plane, while keeping its body vertical (see Fig. 2.5). The unicycle configuration (as seen from the bottom via a glass floor) is shown in Fig. 2.6.

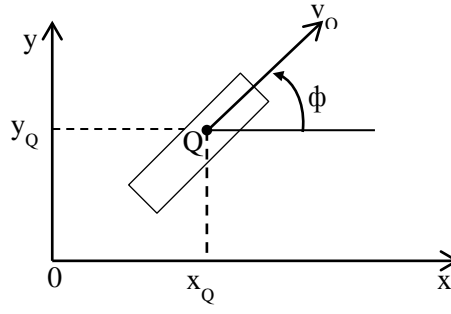


**Fig. 2.6 : Kinematic structure of a unicycle.**

Its configuration is described by a vector of generalized coordinates :  $\mathbf{p} = [x_Q, y_Q, \phi]^T$ , i.e., the position coordinates of the point of contact  $Q$  with the ground in the fixed coordinate frame  $Oxy$ , and its orientation angle  $\phi$  with respect to the  $x$  axis. The linear velocity of the wheel is  $v_Q$  and its angular velocity about its instantaneous rotational axis is  $v_\phi = \dot{\phi}$ . From Fig. 2.6 we find :

$$\dot{x}_Q = v_Q \cos \phi, \quad \dot{y}_Q = v_Q \sin \phi, \quad \dot{\phi} = v_\phi \quad (2.26)$$

Eliminating  $v_Q$  from the first two equations (2.26) we find the holonomic constraint (2.25) :

$$-\dot{x}_Q \sin \phi + \dot{y}_Q \cos \phi = 0 \quad (2.27)$$

Using the notation  $v_1 = v_Q$  and  $v_2 = v_\phi$ , for simplicity, the kinematic model (2.26) of the unicycle can be written as :

$$\dot{\mathbf{p}} = \begin{bmatrix} \cos \phi \\ \sin \phi \\ 0 \end{bmatrix} v_1 + \begin{bmatrix} 0 \\ 0 \\ 1 \end{bmatrix} v_2, \quad \dot{\mathbf{p}} = \begin{bmatrix} \dot{x}_Q \\ \dot{y}_Q \\ \dot{\phi} \end{bmatrix} \quad (2.28a)$$

or

$$\dot{\mathbf{p}} = \mathbf{J}\dot{\mathbf{q}}, \quad \dot{\mathbf{q}} = [v_1, v_2]^T \quad (2.28b)$$

where  $\mathbf{J}$  is the system Jacobian matrix :

$$\mathbf{J} = \begin{bmatrix} \cos \phi & 0 \\ \sin \phi & 0 \\ 0 & 1 \end{bmatrix} \quad (2.28c)$$

The linear velocity  $v_1 = v_Q$  and the angular velocity  $v_\phi = v_2$  are assumed to be the action (joint) variables of the system.

The model (2.28a) belongs to the special class of nonlinear systems, called *affine systems*, and described by a dynamic equation of the form (see Chapter 6) :

$$\dot{\mathbf{x}} = \mathbf{g}_0(\mathbf{x}) + \sum_{i=1}^m \mathbf{g}_i(\mathbf{x}) u_i \quad (2.29a)$$

$$= \mathbf{g}_0(\mathbf{x}) + \mathbf{G}(\mathbf{x}) \mathbf{u} \quad (2.29b)$$

where  $u_i$  ( $i = 1, 2, \dots, m$ ) appear linearly, and :

$$\mathbf{x} = [x_1, x_2, \dots, x_n]^T \in \mathcal{X}, \mathbf{u} = [u_1, u_2, \dots, u_m]^T \in \mathcal{U}$$

$$\mathbf{G}(\mathbf{x}) = [\mathbf{g}_1(\mathbf{x}) : \mathbf{g}_2(\mathbf{x}) : \dots : \mathbf{g}_m(\mathbf{x})] \quad (2.30)$$

If  $m < n$  the system has a less number of actuation variables (controls) than the degrees of freedom under control and is known as *underactuated* system. If  $m > n$  we have an *overactuated* system. In practice, usually  $m < n$ . The vector  $\mathbf{x}$  is actually the state vector of the system and  $\mathbf{u}$  the control vector. The term  $\mathbf{g}_0(\mathbf{x})$  is called “drift”, and the system with  $\mathbf{g}_0(\mathbf{x}) = \mathbf{0}$  is called a “driftless” system. The column vector set :

$$\mathbf{g}_1(\mathbf{x}) = \begin{bmatrix} g_{11}(\mathbf{x}) \\ g_{12}(\mathbf{x}) \\ \vdots \\ g_{1n}(\mathbf{x}) \end{bmatrix}, \mathbf{g}_2(\mathbf{x}) = \begin{bmatrix} g_{21}(\mathbf{x}) \\ g_{22}(\mathbf{x}) \\ \vdots \\ g_{2n}(\mathbf{x}) \end{bmatrix}, \dots, \mathbf{g}_m(\mathbf{x}) = \begin{bmatrix} g_{m1}(\mathbf{x}) \\ g_{m2}(\mathbf{x}) \\ \vdots \\ g_{mn}(\mathbf{x}) \end{bmatrix} \quad (2.31)$$

is referred to as the system’s *vector field*. It is assumed that the set  $\mathcal{U}$  contains at least an open set that involves the origin of  $R^m$ . If  $\mathcal{U}$  does not contain the origin, then the system is not “driftless”.

The unicycle model (2.28a) is a 2-input driftless affine system with two vector fields :

$$\mathbf{g}_1 = \begin{bmatrix} \cos \phi \\ \sin \phi \\ 0 \end{bmatrix}, \mathbf{g}_2 = \begin{bmatrix} 0 \\ 0 \\ 1 \end{bmatrix} \quad (2.32)$$

The Jacobian formulation (2.28c) organizes the two column vector fields into a matrix  $\mathbf{J} = \mathbf{G}$ . Each action variable  $u_i \in R$  in Eq.(2.29a) is actually a coefficient that determines how much of  $\mathbf{g}_i(\mathbf{x})$  is contributing into the result  $\dot{\mathbf{x}}$ . The vector field  $\mathbf{g}_1(\phi)$  of the unicycle allows *pure translation*, and the field  $\mathbf{g}_2$  allows *pure rotation*.

### 2.3.2 Differential Drive WMR

Indoor and other mobile robots use the differential drive locomotion type (see Fig. 1.20). The *Pioneer* WMR shown in Fig. 1.11 is an example of differential drive WMR. The geometry and kinematic parameters of this robot are shown in Fig. 2.7. The pose (position / orientation) vector of the WMR and its speed are respectively :

$$\mathbf{p} = \begin{bmatrix} x_Q \\ y_Q \\ \phi \end{bmatrix}, \dot{\mathbf{p}} = \begin{bmatrix} \dot{x}_Q \\ \dot{y}_Q \\ \dot{\phi} \end{bmatrix} \quad (2.33)$$

The angular positions and speeds of the left and right wheel are  $\{\theta_l, \dot{\theta}_l\}$ ,  $\{\theta_r, \dot{\theta}_r\}$ , respectively.

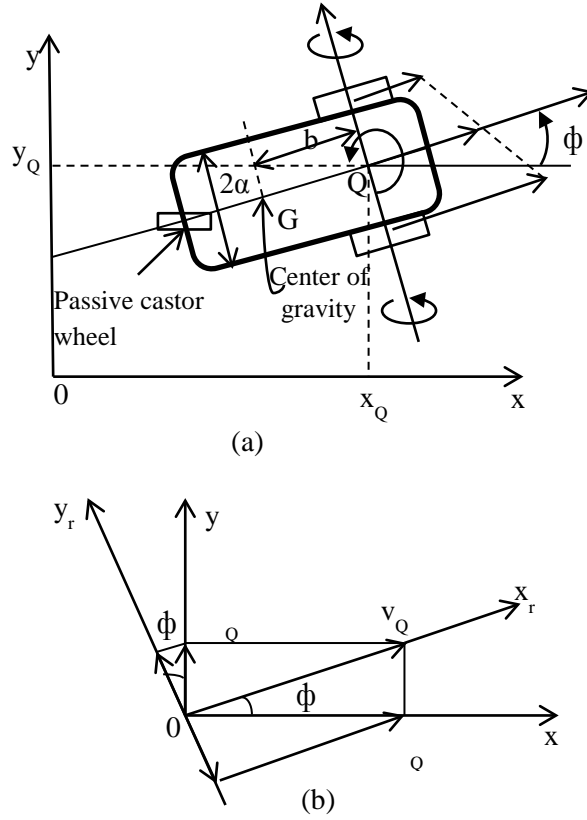


**Fig. 2.7 : (a) Geometry of differential drive WMR, (b) Diagram illustrating the nonholonomic constraint.**

The following assumptions are made :

- Wheels are rolling without slippage
- The guidance (steering) axis is perpendicular to the plane  $Oxy$
- The point  $Q$  coincides with the center of gravity  $G$ , i.e.,  $\|\overline{GQ}\| = 0$ <sup>3</sup>.

Let  $v_l$  and  $v_r$  be the linear velocity of the left and right wheel respectively, and  $v_Q$  the velocity of the wheel mid-point  $Q$  of the WMR. Then, from Fig. 2.7a we get :

$$v_r = v_Q + a\dot{\phi}, \quad v_l = v_Q - a\dot{\phi} \quad (2.34a)$$

Adding and subtracting  $v_r$  and  $v_l$  we get

$$v_Q = \frac{1}{2}(v_r + v_l), \quad 2a\dot{\phi} = v_r - v_l \quad (2.34b)$$

where, due to the non slippage assumption, we have  $v_r = r\dot{\theta}_r$  and  $v_l = r\dot{\theta}_l$ . As in the unicycle case  $\dot{x}_Q$  and  $\dot{y}_Q$  are given by :

$$\dot{x}_Q = v_Q \cos \phi, \quad \dot{y}_Q = v_Q \sin \phi \quad (2.35)$$

and so the kinematic model of this WMR is described by the following relations :

<sup>3</sup>In Fig. 2.7 the points  $Q$  and  $G$  are shown distinct in order to use the same Figure in all configurations with  $Q$  and  $G$  separated by distance  $b$ .

$$\dot{x}_Q = \frac{r}{2}(\dot{\theta}_r \cos \phi + \dot{\theta}_l \cos \phi) \quad (2.36a)$$

$$\dot{y}_Q = \frac{r}{2}(\dot{\theta}_r \sin \phi + \dot{\theta}_l \sin \phi) \quad (2.36b)$$

$$\dot{\phi} = \frac{r}{2a}(\dot{\theta}_r - \dot{\theta}_l) \quad (2.36c)$$

Analogously to Eq.(2.28a,b) the kinematic model (2.36a-c) can be written in the *driftless affine* form :

$$\dot{\mathbf{p}} = \begin{bmatrix} (r/2)\cos\phi \\ (r/2)\sin\phi \\ r/2a \end{bmatrix} \dot{\theta}_r + \begin{bmatrix} (r/2)\cos\phi \\ (r/2)\sin\phi \\ -r/2a \end{bmatrix} \dot{\theta}_l \quad (2.37a)$$

or

$$\dot{\mathbf{p}} = \mathbf{J}\dot{\mathbf{q}} \quad (2.37b)$$

where :

$$\dot{\mathbf{p}} = \begin{bmatrix} \dot{x}_Q \\ \dot{y}_Q \\ \dot{\phi} \end{bmatrix}, \quad \dot{\mathbf{q}} = \begin{bmatrix} \dot{\theta}_r \\ \dot{\theta}_l \end{bmatrix} \quad (2.37c)$$

and  $\mathbf{J}$  is the WMR's Jacobian :

$$\mathbf{J} = \begin{bmatrix} (r/2)\cos\phi & (r/2)\cos\phi \\ (r/2)\sin\phi & (r/2)\sin\phi \\ r/2a & -r/2a \end{bmatrix} \quad (2.37d)$$

Here, the two 3-dimensional vector fields are :

$$\mathbf{g}_1 = \begin{bmatrix} (r/2)\cos\phi \\ (r/2)\sin\phi \\ r/2a \end{bmatrix}, \quad \mathbf{g}_2 = \begin{bmatrix} (r/2)\cos\phi \\ (r/2)\sin\phi \\ -r/2a \end{bmatrix} \quad (2.38)$$

The field  $\mathbf{g}_1$  allows the rotation of the right wheel, and  $\mathbf{g}_2$  allows the rotation of the left wheel. Eliminating  $v_Q$  in Eq.(2.35) we get as usual the nonholonomic constraint (2.25) {or (2.27)}.

$$-\dot{x}_Q \sin \phi + \dot{y}_Q \cos \phi = 0 \quad (2.39)$$

which expresses the fact that the point  $Q$  is moving along  $Qx_r$ , and its velocity along the axis  $Qy_r$  is zero (no lateral motion), i.e. {see Fig. 2.7b} :

$$-(\dot{x}_Q)_1 + (\dot{y}_Q)_1 = 0$$

where  $(\dot{x}_Q)_1 = \dot{x}_Q \sin \phi$  and  $(\dot{y}_Q)_1 = \dot{y}_Q \cos \phi$ .

The Jacobian matrix  $\mathbf{J}$  in Eq.(2.37d) has three rows and two columns, and so it is not invertible. Therefore, the solution of Eq.(2.37b) for  $\dot{\mathbf{q}}$  is given by :

$$\dot{\mathbf{q}} = \mathbf{J}^\dagger \dot{\mathbf{p}} \quad (2.40)$$

where  $\mathbf{J}^\dagger$  is the generalized inverse of  $\mathbf{J}$  given by Eq.(2.8a). However, here  $\mathbf{J}^\dagger$  can be computed directly by using Eq.(2.34a), and observing from Fig. 2.7b that :

$$v_Q = \dot{x}_Q \cos \phi + \dot{y}_Q \sin \phi$$

Thus, using this equation in Eq.(2.34a) we obtain :

$$\begin{aligned} r\dot{\theta}_r &= \dot{x}_Q \cos \phi + \dot{y}_Q \sin \phi + a\dot{\phi} \\ r\dot{\theta}_l &= \dot{x}_Q \cos \phi + \dot{y}_Q \sin \phi - a\dot{\phi} \end{aligned} \quad (2.41a)$$

i.e. :

$$\begin{bmatrix} \dot{\theta}_r \\ \dot{\theta}_l \end{bmatrix} = \frac{1}{r} \begin{bmatrix} \cos \phi & \sin \phi & a \\ \cos \phi & \sin \phi & -a \end{bmatrix} \begin{bmatrix} \dot{x}_Q \\ \dot{y}_Q \\ \dot{\phi} \end{bmatrix}$$

or

$$\dot{\mathbf{q}} = \mathbf{J}^\dagger \dot{\mathbf{p}} \quad (2.41b)$$

where <sup>4</sup>:

$$\mathbf{J}^\dagger = \frac{1}{r} \begin{bmatrix} \cos \phi & \sin \phi & a \\ \cos \phi & \sin \phi & -a \end{bmatrix} \quad (2.41c)$$

The nonholonomic constraint (2.39) can be written as :

$$\mathbf{M}\dot{\mathbf{p}} = 0, \quad \mathbf{M} = \begin{bmatrix} -\sin \phi & \cos \phi & 0 \end{bmatrix} \quad (2.42)$$

Clearly, if  $\dot{\theta}_r \neq \dot{\theta}_l$ , then the difference between  $\dot{\theta}_r$  and  $\dot{\theta}_l$  determines the robot's rotation speed  $\dot{\phi}$  and its direction. The instantaneous curvature radius  $R$  is given by {see (1.1)} :

$$R = \frac{v_Q}{\dot{\phi}} = a \left( \frac{v_r + v_l}{v_r - v_l} \right), \quad v_r \geq v_l \quad (2.43a)$$

and the instantaneous curvature coefficient is :

$$\kappa = 1/R \quad (2.43b)$$

### Example 2.1

Derive the kinematic relations (2.35) using the rotation matrix concept. (2.17).

#### Solution

Here, the point  $P(x_p, y_p)$  of Fig. 2.4 is the point  $Q(x_Q, y_Q)$  in Fig. 2.7. The WMR velocities along the local coordinate axes  $Qx_r$  and  $Qy_r$  are  $\dot{x}_r$  and  $\dot{y}_r$ . The corresponding velocities in the world coordinate frame are  $\dot{x}_Q$  and  $\dot{y}_Q$ . Therefore for a given  $\phi$ , (2.17) gives :

$$\begin{bmatrix} \dot{x}_Q \\ \dot{y}_Q \end{bmatrix} = \begin{bmatrix} \cos \phi & -\sin \phi \\ \sin \phi & \cos \phi \end{bmatrix} \begin{bmatrix} \dot{x}_r \\ \dot{y}_r \end{bmatrix} \quad (2.44)$$

Now, the condition of no lateral wheel movement implies that  $\dot{y}_r = 0$  and  $\dot{x}_r = v_Q$ .

Therefore the above relation gives :

$$\dot{x}_Q = v_Q \cos \phi \quad \text{and} \quad \dot{y}_Q = v_Q \sin \phi$$

as desired.

### Example 2.2

Derive the kinematic equations and constraints of a differential drive WMR by relaxing the no-slipping condition of the wheels' motion.

#### Solution

We will work with the WMR of Fig. 2.7. Considering the rotation about the center of gravity  $G$  we get the following relations :

<sup>4</sup> As an exercise, the reader is advised to derive Eq.(2.41c) using Eq.(2.8a).

$$\dot{x}_G = \dot{x}_Q + b\dot{\phi}\sin\phi$$

$$\dot{y}_G = \dot{y}_Q - b\dot{\phi}\cos\phi$$

Therefore, the kinematic equations (2.41a) and the nonholonomic constraint (2.42) become :

$$r\dot{\theta}_r = \dot{x}_G \cos\phi + \dot{y}_G \sin\phi + a\dot{\phi}$$

$$r\dot{\theta}_l = \dot{x}_G \cos\phi + \dot{y}_G \sin\phi - a\dot{\phi}$$

$$-\dot{x}_G \sin\phi + \dot{y}_G \cos\phi + b\dot{\phi} = 0$$

Now, assume that the wheels are subject to longitudinal and lateral slip [10]. To include the slip into the kinematics of the robot, we introduce two variables  $w_r$ ,  $w_l$  for the longitudinal slip displacements of the right wheel and left wheel, respectively, and two variables  $z_r$ ,  $z_l$  for the corresponding lateral slip displacements. Thus, here :

$$\mathbf{p} = [x_G, y_G, \phi, w_r, w_l, z_r, z_l]^T$$

The slipping wheels' velocities are now given by :

$$v_r = (r\dot{\theta}_r - \dot{w}_r) \cos\zeta_r, \quad v_l = (r\dot{\theta}_l - \dot{w}_l) \cos\zeta_l$$

where  $\zeta_r$  and  $\zeta_l$  are the steering angles of the wheels.

Using these relations for  $v_r$  and  $v_l$  the above kinematic equations are written as :

$$v_r = (r\dot{\theta}_r - \dot{w}_r) \cos\zeta_r = \dot{x}_G \cos\phi + \dot{y}_G \sin\phi + a\dot{\phi}$$

$$v_l = (r\dot{\theta}_l - \dot{w}_l) \cos\zeta_l = \dot{x}_G \cos\phi + \dot{y}_G \sin\phi - a\dot{\phi}$$

and the nonholonomic constraint becomes :

$$-\dot{x}_G \sin\phi + \dot{y}_G \cos\phi + b\dot{\phi} - \dot{z}_r \cos\zeta_r = 0$$

$$-\dot{x}_G \sin\phi + \dot{y}_G \cos\phi + b\dot{\phi} - \dot{z}_l \cos\zeta_l = 0$$

In our WMR the two wheels have a common axis and are unsteered. Therefore  $\zeta_r = \zeta_l = 0$ . For WMRs with steered wheels we may have  $\zeta_r \neq 0$ ,  $\zeta_l \neq 0$ . In our case  $\cos\zeta_r = \cos\zeta_l = 1$ , and so the two kinematic equations, solved for the angular wheel velocities  $\dot{\theta}_r$  and  $\dot{\theta}_l$ , give :

$$\dot{\mathbf{q}} = \mathbf{J}^\dagger \dot{\mathbf{p}}, \quad \dot{\mathbf{q}} = \begin{bmatrix} \dot{\theta}_r \\ \dot{\theta}_l \end{bmatrix}$$

where the inverse Jacobian is :

$$\mathbf{J}^\dagger = \frac{1}{r} \begin{bmatrix} \cos\phi & \sin\phi & a & 1 & 0 & 0 & 0 \\ \cos\phi & \sin\phi & -a & 0 & 1 & 0 & 0 \end{bmatrix}$$

The nonholonomic constraints are written in Pfaffian form :

$$\mathbf{M}(\mathbf{p})\dot{\mathbf{p}} = \mathbf{0}$$

where :

$$\mathbf{M}(\mathbf{p}) = \begin{bmatrix} -\sin\phi & \cos\phi & b & 0 & 0 & -1 & 0 \\ -\sin\phi & \cos\phi & b & 0 & 0 & 0 & -1 \end{bmatrix}$$

$$\dot{\mathbf{p}} = (\dot{x}_G, \dot{y}_G, \dot{\phi} : \dot{w}_r, \dot{w}_l, \dot{z}_r, \dot{z}_l)^T$$

In the special case where only lateral slip takes place (i.e.,  $\dot{w}_r = 0$ ,  $\dot{w}_l = 0$ ), the components  $\dot{w}_r$  and  $\dot{w}_l$  are dropped from  $\dot{\mathbf{p}}$ , and the matrices  $\mathbf{J}^\dagger$  and  $\mathbf{M}(\mathbf{p})$  are



### 2.3.3 Tricycle

The orientation angle and angular velocity are  $\phi$  and  $\dot{\phi}$ , respectively. It is assumed that the vehicle has its guidance point  $Q$  in the back of the powered wheel (i.e., it has a central back axis). The state of the robot's motion is :

where  $\dot{\mathbf{\theta}} = [\dot{\theta}_w, \dot{\psi}]^T$  is the vector of joint velocities (control variables), and

$$\mathbf{J} = \begin{bmatrix} r \cos \psi \cos \phi & 0 \\ r \cos \psi \sin \phi & 0 \\ (r/D) \sin \psi & 0 \\ 0 & 1 \end{bmatrix} \quad (2.46)$$

is the Jacobian matrix. This Jacobian is again noninvertible, but we can find the inverse kinematic equations directly using the relations :

$$\dot{\phi}/v = (1/D) \operatorname{tg} \psi \text{ or } \psi = \operatorname{arctg}(D\dot{\phi}/v) \quad (2.47a)$$

and

$$\dot{\theta}_w = \frac{v_w}{r} = \frac{1}{r} \sqrt{v^2 + (D\dot{\phi})^2} \quad (2.47b)$$

The instantaneous curvature radius  $R$  is given by (see Fig. 2.8) :

$$R = D \operatorname{tg}(\pi/2 - \psi(t)) \quad (2.48)$$

From (2.45) we see that the tricycle is again a 2-input driftless affine system with vector fields :

$$\mathbf{g}_1 = \begin{bmatrix} r \cos \psi \cos \phi \\ r \cos \psi \sin \phi \\ (r/D) \sin \psi \\ 0 \end{bmatrix}, \quad \mathbf{g}_2 = \begin{bmatrix} 0 \\ 0 \\ 0 \\ 1 \end{bmatrix}$$

that allow steering wheel motion  $\dot{\theta}_w$ , and steering angle motion  $\dot{\psi}$ , respectively.

### 2.3.4 Car-Like WMR

The geometry of the car-like mobile robot is shown in Fig. 2.9a and the A.W.E.S.O.M.-9000 line-tracking car-like robot prototype (Aalborg University) in Fig. 2.9b.

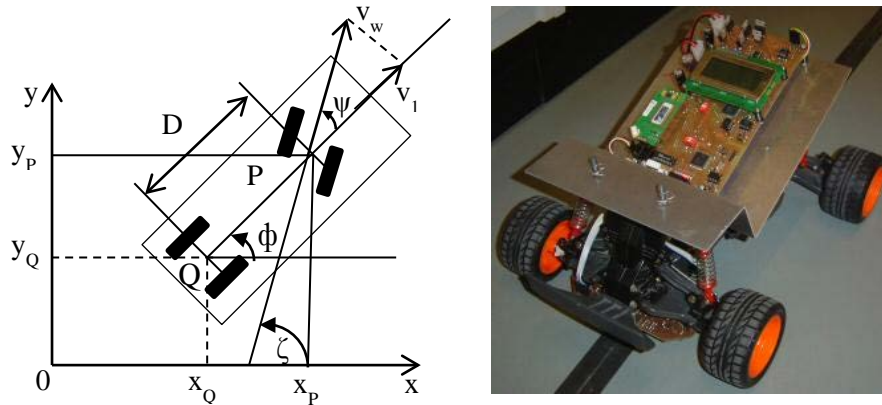


**Fig. 2.9 : (a) Kinematic structure of a car-like robot, (b) A car-like robot prototype.**  
Source : <http://sqrt-1.dk/robot/robot.php>

The state of the robot's motion is represented by the vector [20] :

$$\mathbf{p} = [x_Q, y_Q, \phi, \psi]^T \quad (2.49)$$

where  $x_Q, y_Q$  are the Cartesian coordinates of the wheel axis midpoint  $Q$ ,  $\phi$  is the orientation angle of the vehicle, and  $\psi$  is the steering angle. Here, we have two nonholonomic constraints, one for each wheel pair, i.e. :

$$-\dot{x}_Q \sin \phi + \dot{y}_Q \cos \phi = 0 \quad (2.50a)$$

$$-\dot{x}_p \sin(\phi + \psi) + \dot{y}_p \cos(\phi + \psi) = 0 \quad (2.50b)$$

where  $x_p$  and  $y_p$  are the position coordinates of the front wheels midpoint  $P$ .

From Fig. 2.9 we get :

$$x_p = x_Q + D \cos \phi, \quad y_p = y_Q + D \sin \phi$$

Using these relations the second kinematic constraint (2.50b) becomes :

$$-\dot{x}_Q \sin(\phi + \psi) + \dot{y}_Q \cos(\phi + \psi) + D(\cos \psi) \dot{\phi}$$

The two nonholonomic constraints are written in the matrix form :

$$\mathbf{M}(\mathbf{p})\dot{\mathbf{p}} = \mathbf{0} \quad (2.51a)$$

where :

$$\mathbf{M}(\mathbf{p}) = \begin{bmatrix} -\sin \phi & \cos \phi & 0 & 0 \\ -\sin(\phi + \psi) & \cos(\phi + \psi) & D \cos \psi & 0 \end{bmatrix} \quad (2.51b)$$

The kinematic equations for a rear-wheel driving car are found to be {see Fig. 2.9} :

$$\dot{x}_Q = v_1 \cos \phi$$

$$\dot{y}_Q = v_1 \sin \phi$$

$$\begin{aligned} \dot{\phi} &= \frac{1}{D} v_w \sin \psi \\ &= \frac{1}{D} v_1 \tan \psi \quad (\text{since } v_w = v_1 / \cos \psi) \end{aligned} \quad (2.52)$$

$$\dot{\psi} = v_2$$

These equations can be written in the affine form :

$$\begin{bmatrix} \dot{x}_Q \\ \dot{y}_Q \\ \dot{\phi} \\ \dot{\psi} \end{bmatrix} = \begin{bmatrix} \cos \phi \\ \sin \phi \\ (1/D) \tan \psi \\ 0 \end{bmatrix} v_1 + \begin{bmatrix} 0 \\ 0 \\ 0 \\ 1 \end{bmatrix} v_2 \quad (2.53)$$

that has the vector fields :

$$\mathbf{g}_1 = \begin{bmatrix} \cos \phi \\ \sin \phi \\ (1/D) \tan \psi \\ 0 \end{bmatrix}, \quad \mathbf{g}_2 = \begin{bmatrix} 0 \\ 0 \\ 0 \\ 1 \end{bmatrix}$$

allowing the driving motion  $v_1$  and the steering motion  $v_2 = \dot{\psi}$ , respectively. The Jacobian form of Eq.(2.53) is :

$$\dot{\mathbf{p}} = \mathbf{J}\mathbf{v}, \quad \mathbf{v} = [v_1, v_2]^T \quad (2.54)$$

with Jacobian matrix :

$$\mathbf{J} = \begin{bmatrix} \cos \phi & 0 \\ \sin \phi & 0 \\ (tg\psi)/D & 0 \\ 0 & 1 \end{bmatrix} \quad (2.55)$$

Here, there is a singularity at  $\psi = \pm\pi/2$ , which corresponds to the “jamming” of the WMR when the front wheels are normal to the longitudinal axis of its body. Actually, this singularity does not occur in practice due to the restricted range of the steering angle  $\psi$  ( $-\pi/2 < \psi < \pi/2$ ).

The kinematic model for the front wheel driving vehicle is {see Eqs.(2.45), (2.46)} [20] :

$$\dot{\mathbf{p}} = \mathbf{J}\mathbf{v}, \quad \mathbf{J} = \begin{bmatrix} \cos \phi \cos \psi & 0 \\ \sin \phi \cos \psi & 0 \\ (\sin \psi)/D & 0 \\ 0 & 1 \end{bmatrix} \quad (2.56a)$$

In this case the previous singularity does not occur, since at  $\psi = \pm\pi/2$  the car can still (in principle) pivot about its rear wheels. Using the new inputs  $u_1$  and  $u_2$  defined as :

$$u_1 = v_1, \quad u_2 = (1/D)\sin(\zeta - \phi)v_1 + v_2,$$

the above model is transformed to :

$$\begin{bmatrix} \dot{x}_p \\ \dot{y}_p \\ \dot{\phi} \\ \dot{\zeta} \end{bmatrix} = \begin{bmatrix} \cos \zeta \\ \sin \zeta \\ (1/D)\sin(\zeta - \phi) \\ 0 \end{bmatrix} u_1 + \begin{bmatrix} 0 \\ 0 \\ 0 \\ 1 \end{bmatrix} u_2 \quad (2.56b)$$

where  $\zeta = \phi + \psi$  is the total steering angle with respect to the axis Ox.

Indeed, from  $x_p = x_Q + D \cos \phi$  and  $y_p = y_Q + D \sin \phi$  (see Fig. 2.9), and Eq.(2.56a) we get :

$$\begin{aligned} \dot{x}_p &= \dot{x}_Q - D(\sin \phi)\dot{\phi} = (\cos \phi \cos \psi - \sin \phi \sin \psi)v_1 \\ &= [\cos(\phi + \psi)]v_1 = (\cos \zeta)u_1 \\ \dot{y}_p &= \dot{y}_Q + D(\cos \phi)\dot{\phi} = (\sin \phi \cos \psi + \cos \phi \sin \psi)v_1 \\ &= [\sin(\phi + \psi)]v_1 = (\sin \zeta)u_1 \\ \dot{\phi} &= \frac{1}{D}[\sin(\zeta - \phi)]v_1 = \left[\frac{1}{D}\sin(\zeta - \phi)\right]u_1 \\ \dot{\zeta} &= \dot{\phi} + \dot{\psi} = \left[\frac{1}{D}\sin(\zeta - \phi)\right]v_1 + v_2 = u_2 \end{aligned}$$

We observe, from Eq.(2.56b), that the kinematic model for  $x_p$ ,  $y_p$  and  $\zeta$  (i.e., the first, second, and fourth equation in Eq.(2.56b)) is actually a unicycle model (2.28).

Two special cases of the above car-like model are known as :

- Reeds-Shepp car
- Dubins car

The *Reeds-Shepp car* is obtained by restricting the values of the velocity  $v_1$  to three distinct values  $+1$ ,  $0$  and  $-1$ . These values appear to correspond to three distinct “gears” : “forward”, “park”, or “reverse”. The *Dubins car* is obtained when the reverse motion is not allowed in the Reeds-Shepp car, i.e., the value  $v_1 = -1$  is excluded, in which case  $v_1 = \{0, 1\}$ .

### Example 2.3

It is desired to find the steering angle  $\psi$  which is required for a rear-wheel driven car-like WMR to go from its present position  $Q(x_Q, y_Q)$  to a given goal  $F(x_f, y_f)$ . The available data, which are obtained via proper sensors, are the distance  $L$  between  $(x_f, y_f)$  and  $(x_Q, y_Q)$  and the angle  $\varepsilon$  of the vector  $\overrightarrow{QF}$  with respect to the current vehicle orientation.

### Solution

We will work with the geometry of Fig. 2.10 [19]. The kinematic equations of the WMR are given by Eq.(2.52). The WMR will go from the position  $Q$  to the goal  $F$  following a circular path with curvature :

$$\frac{1}{R_1} = \frac{1}{D} \tan \psi$$

determined using the bicycle equivalent model, that combines the two front wheels and the two rear wheels (see Fig. 2.10, left).

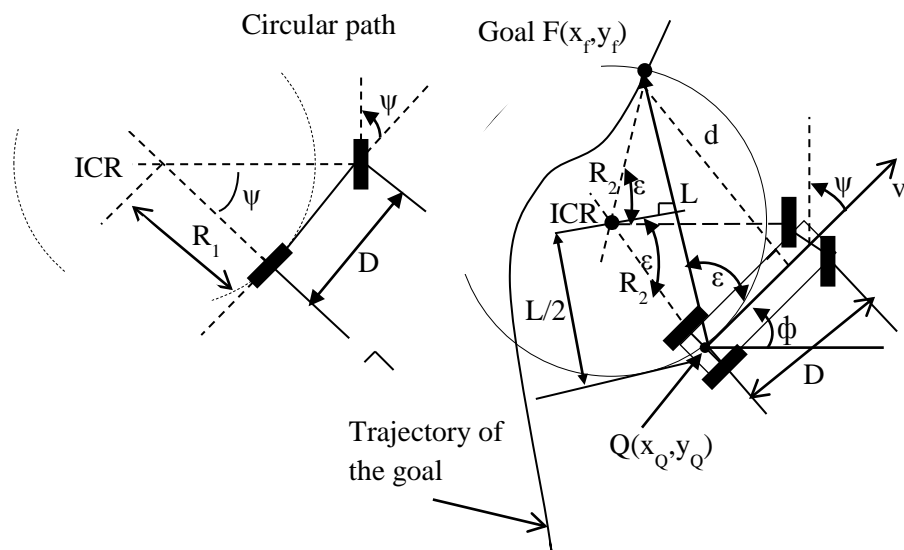


**Fig. 2.10 : Geometry of the goal tracking problem.**

On the other hand, the curvature  $1/R_2$  of the circular path that passes through the goal, is obtained from the relation (see Fig. 2.10, right) :

$$L/2 = R_2 \sin(\varepsilon)$$

i.e. :

$$\frac{1}{R_2} = \frac{2}{L} \sin(\varepsilon) \quad (2.57a)$$

To meet the goal tracking requirement the above two curvatures  $1/R_1$  and  $1/R_2$  must be the same, i.e.:

$$\frac{1}{D}tg\psi = \frac{2}{L}\sin(\varepsilon)$$

Therefore :

$$\psi = tg^{-1}\left(\frac{2D}{L}\sin(\varepsilon)\right) \quad (2.57b)$$

Equation (2.57b) gives the steering angle  $\psi$  in terms of the data  $L$  and  $\varepsilon$ , and can be used to pursuit tracking of goals (targets) that are moving along given trajectories. In these cases the goal  $F$  lies at the intersection of the goal trajectory and the look-ahead circle. To get a better interpretation of (2.57a), we use the lateral distance  $d$  between the vehicles orientation (heading) vector and the goal point, which is given by (see Fig. 2.10) :

$$d = L\sin(\varepsilon)$$

Then, the curvature  $1/R_2$  in Eq.(2.57a) is given by :

$$\frac{1}{R_2} = \frac{2d}{L^2}$$

This indicates that the curvature  $1/R_1$  of the path resulting from the steering angle  $\psi$  should be :

$$\frac{1}{R_1} = \left(\frac{2}{L^2}\right)d \quad (2.57c)$$

Equation (2.57c) is a “*proportional control law*” and shows that the curvature  $1/R_1$  of the robot’s path should be proportional to the cross track error  $d$  some look-ahead distance in front of the WMR with a gain  $2/L^2$ .

### 2.3.5 Chain and Brockett – Integrator models

The general 2-input n-dimensional chain model (briefly  $(2,n)$ -chain model) is :

$$\begin{aligned} \dot{x}_1 &= u_1 \\ \dot{x}_2 &= u_2 \\ \dot{x}_3 &= x_2 u_1 \\ &\vdots \\ \dot{x}_n &= x_{n-1} u_1 \end{aligned} \quad (2.58)$$

The *Brockett* (single) *integrator* model is :

$$\begin{aligned} \dot{x}_1 &= u_1 \\ \dot{x}_2 &= u_2 \\ \dot{x}_3 &= x_1 u_2 - x_2 u_1 \end{aligned} \quad (2.59)$$

and the *double integrator* model is :

$$\begin{aligned} \ddot{x}_1 &= u_1 \\ \ddot{x}_2 &= u_2 \\ \dot{x}_3 &= x_1 \dot{x}_2 - x_2 \dot{x}_1 \end{aligned} \quad (2.60)$$

The nonholonomic WMR kinematic models can be transformed to the above models. Here, the unicycle model (which also covers the differential drive model) and the car-like model will be considered.

### 2.3.5.1 Unicycle WMR

The unicycle kinematic model is given by Eq.(2.26) :

$$\dot{x}_Q = v_Q \cos \phi, \quad \dot{y}_Q = v_Q \sin \phi, \quad \dot{\phi} = v_\phi \quad (2.61)$$

Using the transformation :

$$\begin{aligned} z_1 &= \phi \\ z_2 &= x_Q \cos \phi + y_Q \sin \phi \end{aligned} \quad (2.62)$$

$$z_3 = x_Q \sin \phi - y_Q \cos \phi$$

the unicycle model is converted to the (2,3)-chain form :

$$\begin{aligned} \dot{z}_1 &= u_1 \\ \dot{z}_2 &= u_2 \\ \dot{z}_3 &= z_2 u_1 \end{aligned} \quad (2.63)$$

where  $u_1 = v_\phi$  and  $u_2 = v_Q - z_3 u_1$ .

Defining new state variables :

$$x_1 = z_1, \quad x_2 = z_2, \quad x_3 = -2z_3 + z_1 z_2 \quad (2.64)$$

the (2,3)-chain model is converted to the *Brockett integrator* :

$$\begin{aligned} \dot{x}_1 &= u_1 \\ \dot{x}_2 &= u_2 \\ \dot{x}_3 &= x_1 u_2 - x_2 u_1 \end{aligned} \quad (2.65)$$

### 2.3.5.2 Rear-wheel driving car

The rear-wheel driven car model is given by Eq.(2.52) :

$$\dot{x}_Q = v_1 \cos \phi, \quad \dot{y}_Q = v_1 \sin \phi, \quad \dot{\phi} = \frac{v_1}{D} \tan \psi, \quad \dot{\psi} = v_2 \quad (2.66)$$

Using the state transformation :

$$x_1 = x_Q, \quad x_2 = \frac{\tan \psi}{D \cos^3 \phi}, \quad x_3 = \tan \phi, \quad x_4 = y_Q \quad (2.67)$$

and input transformation :

$$v_1 = u_1 / \cos \phi \quad (2.68)$$

$$v_2 = -\frac{3 \sin^2 \psi \sin \phi}{D \cos^2 \phi} u_1 + D \cos^2 \psi (\cos^3 \phi) u_2$$

for  $\phi \neq \pi/2 \pm k\pi$  and  $\psi \neq \pi/2 \pm k\pi$ , the model (2.66) is converted to the (2,4) – chain form :

$$\begin{aligned}
\dot{x}_1 &= u_1 \\
\dot{x}_2 &= u_2 \\
\dot{x}_3 &= x_2 u_1 \\
\dot{x}_4 &= x_3 u_1
\end{aligned} \tag{2.69}$$

### 2.3.6 Car-Pulling Trailer WMR

This is an extension of the car-like WMR, where  $N$  one-axis trailers are attached to a car-like robot with rear wheel drive. This type of trailer is used, for example, at airports for transporting luggage. The form of equations depend crucially on the exact point at which the trailer is attached and on the choice of body frames. Here, for simplicity each trailer will be assumed to be connected to the axle midpoint of the previous trailer (*zero hooking*) as shown in Fig. 2.11 [20].

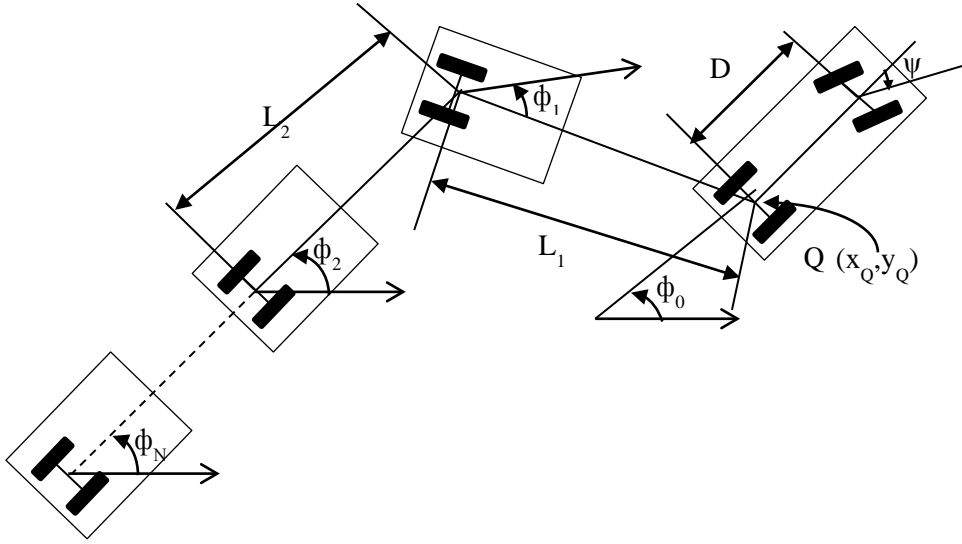


**Fig. 2.11 : Geometrical structure of the N-trailer WMR.**

The new parameter introduced here is the distance from the center of the back axle of trailer  $i$  to the point at which is hitched to the next body. This is called the *hitch* (or *hinge-to-hinge*) length denoted by  $L_i$ . The car length is  $D$ . Let  $\phi_i$  be the orientation of the  $i$ th trailer, expressed with respect to the world coordinate frame. Then from the geometry of Fig. 2.11 we get the following equations :

$$\begin{aligned}
x_i &= x_Q - \sum_{j=1}^i L_j \cos \phi_j \\
y_i &= y_Q - \sum_{j=1}^i L_j \sin \phi_j
\end{aligned} \quad i = 1, 2, \dots, N$$

which give the following nonholonomic constraints :

$$\begin{aligned}
\dot{x}_Q \sin \phi_0 - \dot{y}_Q \cos \phi_0 &= 0 \\
\dot{x}_Q \sin(\phi_0 + \psi) - \dot{y}_Q \cos(\phi_0 + \psi) - \dot{\phi}_0 D \cos \psi &= 0 \\
\dot{x}_Q \sin \phi_i - \dot{y}_Q \cos \phi_i + \sum_{j=1}^i \dot{\phi}_j L_j \cos(\phi_i - \phi_j) &= 0
\end{aligned}$$

for  $i = 1, 2, \dots, N$ .



In analogy to Eq.(2.52) the kinematic equations of the N-trailer are found to be :

$$\begin{aligned}
\dot{x}_Q &= v_1 \cos \phi_0 \\
\dot{y}_Q &= v_1 \sin \phi_0 \\
\dot{\phi}_0 &= (1/D) v_1 \tan \psi \\
\dot{\psi} &= v_2 \\
\dot{\phi}_1 &= \frac{1}{L_1} \sin(\phi_0 - \phi_1) \\
\dot{\phi}_2 &= \frac{1}{L_2} \cos(\phi_0 - \phi_1) \sin(\phi_1 - \phi_2) \\
&\vdots \\
\dot{\phi}_i &= \frac{1}{L_i} \prod_{j=1}^{i-1} \cos(\phi_{j-1} - \phi_j) \sin(\phi_{i-1} - \phi_i) \\
&\vdots \\
\dot{\phi}_N &= \frac{1}{L_N} \prod_{j=1}^{N-1} \cos(\phi_{j-1} - \phi_j) \sin(\phi_{N-1} - \phi_N)
\end{aligned} \tag{2.70}$$

which, obviously, represent a driftless affine system with two inputs  $u_1 = v_1$  and  $u_2 = v_2$ , and  $N + 4$  states :

$$\dot{\mathbf{x}} = \mathbf{g}_1(\mathbf{x})u_1 + \mathbf{g}_2(\mathbf{x})u_2$$

We observe that the first four lines of the fields  $\mathbf{g}_1$  and  $\mathbf{g}_2$  represent the (powered) car-like WMR itself.

## 2.4 Omnidirectional WMR Kinematic Modeling

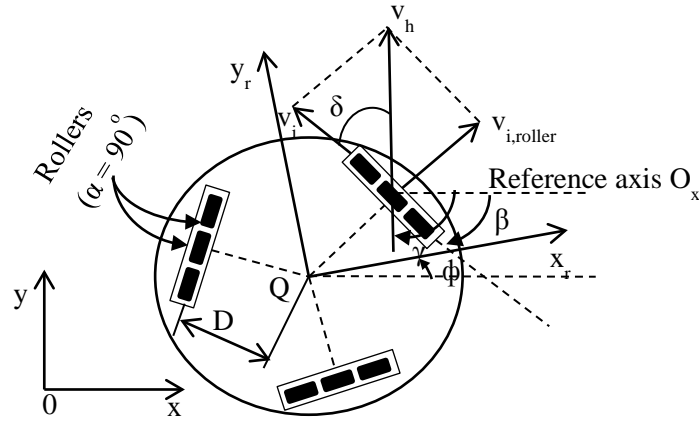
The following WMRs will be considered :

- Multi-wheel omnidirectional WMR with orthogonal (universal) wheels
- Four-wheel omnidirectional WMR with mecanum wheels that have a roller angle  $\pm 45^\circ$ .

### 2.4.1 Universal Multi-Wheel Omnidirectional WMR

The geometric structure of a multi-wheel omnirobot is shown in Fig. 2.12a. Each wheel has three velocity components [16] :

- Its own velocity  $v_i = r\dot{\theta}_i$ , where  $r$  is the common wheel radius and  $\dot{\theta}_i$  its own angular velocity.
- An induced velocity  $v_{i,roller}$  which is due to the free rollers (here assumed of the universal type; roller angle  $\pm 90^\circ$ ).
- A velocity component  $v_\phi$  which is due to the rotation of the robotic platform about its center of gravity  $Q$ , i.e.,  $v_\phi = D\dot{\phi}$ , where  $\dot{\phi}$  is the angular velocity of the platform and  $D$  is the distance of the wheel from  $Q$ .



(a)



(b)

**Fig. 2.12 : (a) Velocity vector of wheel  $i$ . The velocity  $v_h$  is the robot vehicle velocity due to the wheel motion, (b) An example of a 3-wheel set-up.**

Source : <http://deviceguru.com/files/rovio-3.jpg>

Here, the roller angle is  $\pm 90^\circ$ , and so :

$$v_h^2 = v_i^2 + v_{i,roller}^2 \quad (2.71a)$$

where :

$$\begin{aligned} v_i &= v_h \cos(\delta) \\ &= v_h \cos(\gamma - \beta) \\ &= v_h (\cos \gamma \cos \beta + \sin \gamma \sin \beta) \end{aligned} \quad (2.71b)$$

Thus the total velocity of the wheel  $i$  is :

$$\begin{aligned} v_i &= v_h (\cos \gamma \cos \beta + \sin \gamma \sin \beta) + D\dot{\phi} \\ &= v_{hx} \cos \beta + v_{hy} \sin \beta + D\dot{\phi} \end{aligned} \quad (2.72)$$

where  $v_{hx}$  and  $v_{hy}$  are the  $x, y$  components of  $v_h$ , i.e. :

$$v_{hx} = v_h \cos \gamma, \quad v_{hy} = v_h \sin \gamma$$

Equation (2.72) is general and can be used in WMRs with any number of wheels.

Thus, for example, in the case of a 3-wheel robot we may choose the angle  $\beta$  for the wheels 1, 2 and 3 as  $0^\circ$ ,  $120^\circ$  and  $240^\circ$ , respectively, and get the equations :

$$v_1 = v_{hx} + D\dot{\phi}, \quad v_2 = -\frac{1}{2}v_{hx} + \frac{\sqrt{3}}{2}v_{hy} + D\dot{\phi}, \quad v_3 = -\frac{1}{2}v_{hx} - \frac{\sqrt{3}}{2}v_{hy} + D\dot{\phi} \quad (2.73)$$

with  $v_i = r\dot{\theta}_i$ . Now, defining the vectors :

$$\dot{\mathbf{p}}_h = \begin{bmatrix} v_{hx} & v_{hy} & \dot{\phi} \end{bmatrix}^T, \quad \dot{\mathbf{q}} = \begin{bmatrix} \dot{\theta}_1 & \dot{\theta}_2 & \dot{\theta}_3 \end{bmatrix}^T$$

we can write Eq.(2.73) in the inverse Jacobian form :

$$\dot{\mathbf{q}} = \mathbf{J}^{-1} \dot{\mathbf{p}}_h \quad (2.74a)$$

where :

$$\mathbf{J}^{-1} = \frac{1}{r} \begin{bmatrix} 1 & 0 & D \\ -1/2 & \sqrt{3}/2 & D \\ -1/2 & -\sqrt{3}/2 & D \end{bmatrix} \quad (2.74b)$$

Here  $\det \mathbf{J} \neq 0$ , and Eq.(2.74a) can be inverted to give  $\dot{\mathbf{p}}_h = \mathbf{J}\dot{\mathbf{q}}$ .

It is remarked that using omniwheels at different angles we can obtain an overall velocity of the WMR's platform which is greater than the maximum angular velocity of each wheel. For example, selecting in the above 3-wheel case  $\beta = 60^\circ$  and  $\gamma = 90^\circ$  we get from Eq.(2.71b) :

$$v_i = \frac{\sqrt{3}}{2}v_h, \text{ i.e. } v_h = \frac{2}{\sqrt{3}}v_i > v_i$$

The ratio  $v_h / v_i$  is called the *velocity augmentation factor* [16] :

$$VAF = v_h / v_i$$

and depends on the number of wheels used and their angular positions on the robot's body. As a further example, consider a 4-wheel robot with  $\beta = 45^\circ$  and  $\gamma = 90^\circ$ . Then, Eq.(2.71b) gives :

$$VAF = \sqrt{2}$$

#### Example 2.4

We are given the 4-universal – wheel omnidirectional robot of Fig. 2.13, where the angles of the wheels with respect to the axis  $Qx_r$  of the vehicle's coordinate frame are  $\beta_i$  ( $i=1,2,3,4$ ). Derive the kinematic equations of the robot in terms of the unit directional vectors  $\mathbf{u}_i$  ( $i=1,2,3,4$ ) of the wheel velocities, with respect to the local coordinate frame  $Qx_r y_r$ .

#### Solution

Let  $\dot{\phi}$  be the robot's angular velocity, and  $\mathbf{v}_Q$  its linear velocity with world-frame coordinates  $\dot{x}_Q$  and  $\dot{y}_Q$ .

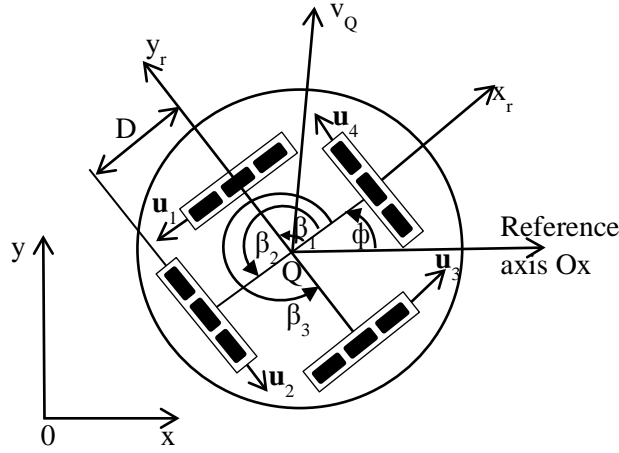


**Fig. 2.13 : Four-wheel omnidirectional robot.**

The unit directional vectors of the wheel velocities are :

$$\mathbf{u}_1 = \begin{bmatrix} -\sin \beta_1 \\ \cos \beta_1 \end{bmatrix}, \mathbf{u}_2 = \begin{bmatrix} -\sin \beta_2 \\ \cos \beta_2 \end{bmatrix}, \mathbf{u}_3 = \begin{bmatrix} -\sin \beta_3 \\ \cos \beta_3 \end{bmatrix}, \mathbf{u}_4 = \begin{bmatrix} 0 \\ 1 \end{bmatrix}$$

where it was assumed that the axis of wheel 4 coincides with axis  $Qx_r$ .

The relation between  $\dot{x}_Q, \dot{y}_Q$  and  $\dot{x}_r, \dot{y}_r$  is given by the rotational matrix  $\mathbf{R}(\phi)$  {see Eq.(2.17)}, i.e. :

$$\begin{bmatrix} \dot{x}_Q \\ \dot{y}_Q \end{bmatrix} = \begin{bmatrix} \cos \phi & -\sin \phi \\ \sin \phi & \cos \phi \end{bmatrix} \begin{bmatrix} \dot{x}_r \\ \dot{y}_r \end{bmatrix} = \mathbf{R}(\phi) \begin{bmatrix} \dot{x}_r \\ \dot{y}_r \end{bmatrix}$$

or

$$\begin{bmatrix} \dot{x}_r \\ \dot{y}_r \end{bmatrix} = \begin{bmatrix} \cos \phi & \sin \phi \\ -\sin \phi & \cos \phi \end{bmatrix} \begin{bmatrix} \dot{x}_Q \\ \dot{y}_Q \end{bmatrix} = \mathbf{R}^{-1}(\phi) \begin{bmatrix} \dot{x}_Q \\ \dot{y}_Q \end{bmatrix}$$

Now, we have :

$$v_1 = r\dot{\theta}_1 = \mathbf{u}_1^T \begin{bmatrix} \dot{x}_r \\ \dot{y}_r \end{bmatrix} + D\dot{\phi} = \mathbf{u}_1^T \mathbf{R}^{-1}(\phi) \begin{bmatrix} \dot{x}_Q \\ \dot{y}_Q \end{bmatrix} + D\dot{\phi}$$

$$v_2 = r\dot{\theta}_2 = \mathbf{u}_2^T \begin{bmatrix} \dot{x}_r \\ \dot{y}_r \end{bmatrix} + D\dot{\phi} = \mathbf{u}_2^T \mathbf{R}^{-1}(\phi) \begin{bmatrix} \dot{x}_Q \\ \dot{y}_Q \end{bmatrix} + D\dot{\phi}$$

$$v_3 = r\dot{\theta}_3 = \mathbf{u}_3^T \begin{bmatrix} \dot{x}_r \\ \dot{y}_r \end{bmatrix} + D\dot{\phi} = \mathbf{u}_3^T \mathbf{R}^{-1}(\phi) \begin{bmatrix} \dot{x}_Q \\ \dot{y}_Q \end{bmatrix} + D\dot{\phi}$$

$$v_4 = r\dot{\theta}_4 = \mathbf{u}_4^T \begin{bmatrix} \dot{x}_r \\ \dot{y}_r \end{bmatrix} + D\dot{\phi} = \mathbf{u}_4^T \mathbf{R}^{-1}(\phi) \begin{bmatrix} \dot{x}_Q \\ \dot{y}_Q \end{bmatrix} + D\dot{\phi}$$

or, in compact, form :

$$\dot{\mathbf{q}} = \mathbf{J}^{-1} \dot{\mathbf{p}}_Q \quad (2.75a)$$

where :

$$\dot{\mathbf{q}} = \begin{bmatrix} \dot{\theta}_1 \\ \dot{\theta}_2 \\ \dot{\theta}_3 \\ \dot{\theta}_4 \end{bmatrix}, \dot{\mathbf{p}}_Q = \begin{bmatrix} \dot{x}_Q \\ \dot{y}_Q \\ \dot{\phi} \end{bmatrix} \quad (2.75b)$$

$$\mathbf{J}^{-1} = \frac{1}{r} (\mathbf{U}^T \mathbf{R}^{-1}(\phi) + \bar{\mathbf{D}}) \quad (2.75c)$$

with :

$$\mathbf{U} = [\mathbf{u}_1 \mid \mathbf{u}_2 \mid \mathbf{u}_3 \mid \mathbf{u}_4], \bar{\mathbf{D}} = [D, D, D, D]^T \quad (2.75d)$$

As usual, this inverse Jacobian equation gives the required angular wheel speeds  $\dot{\theta}_i$  ( $i=1,2,3,4$ ) that lead to the desired linear velocity  $[\dot{x}_Q, \dot{y}_Q]$ , and angular velocity  $\dot{\phi}$  of the robot. A discussion of the modeling and control problem of a WMR with this structure is provided in [17].

### 2.4.2 Four – Wheel Omnidirectional WMR with Mecanum Wheels

Consider the 4-wheel WMR of Fig. 2.14, where the mecanum wheels have roller angle  $\pm 45^\circ$  [2,4].

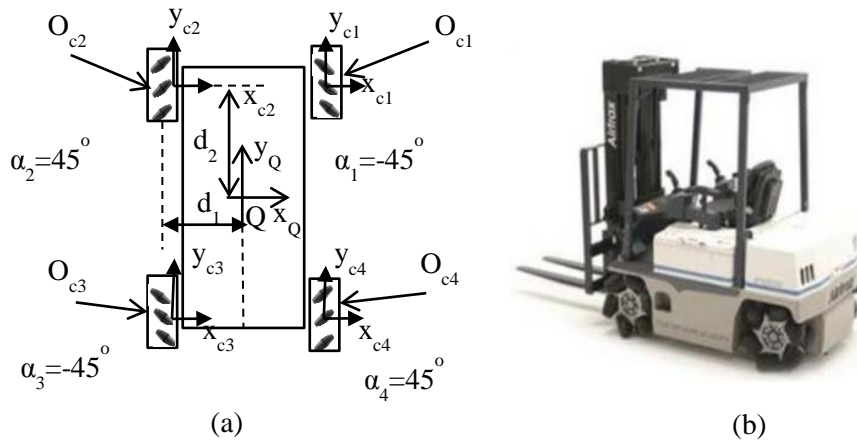


**Fig. 2.14 : Four-mecanum-wheel WMR**

(a) Kinematic geometry

(b) A real 4-mecanum-wheel WMR.

Source: <http://www.automotto.com/entry/airtrax-wheels-go-in-any-direction>

Here, we have four wheel coordinate frames  $O_{ci}$  ( $i=1,2,3,4$ ). The angular velocity  $\dot{q}_i$  of the wheel  $i$  has three components :

- $\dot{\theta}_{ix}$  : rotation speed around the hub.
- $\dot{\theta}_{ir}$  : rotation speed of the roller  $i$ .
- $\dot{\theta}_{iz}$  : rotation speed of the wheel around the contact point.

The wheel velocity vector  $\mathbf{v}_{ci} = [\dot{x}_{ci}, \dot{y}_{ci}, \dot{\phi}_{ci}]^T$  in  $O_{ci}$  coordinates is given by:

$$\begin{bmatrix} \dot{x}_{ci} \\ \dot{y}_{ci} \\ \dot{\phi}_{ci} \end{bmatrix} = \begin{bmatrix} 0 & r_i \sin \alpha_i & 0 \\ R_i & -r_i \cos \alpha_i & 0 \\ 0 & 0 & 1 \end{bmatrix} \begin{bmatrix} \dot{\theta}_{ix} \\ \dot{\theta}_{ir} \\ \dot{\theta}_{iz} \end{bmatrix} \quad (2.76)$$

for  $i=1,2,3,4$ , where  $R_i$  is the wheel radius,  $r_i$  is the roller radius, and  $\alpha_i$  the roller angle. The robot velocity vector  $\dot{\mathbf{p}}_Q = [\dot{x}_Q, \dot{y}_Q, \dot{\phi}_Q]^T$  in the  $Ox_Qy_Q$  coordinate frame {see Eqs.(2.9)-(2.13)} is :

$$\dot{\mathbf{p}}_Q = \begin{bmatrix} \dot{x}_Q \\ \dot{y}_Q \\ \dot{\phi}_Q \end{bmatrix} = \begin{bmatrix} \cos \phi_{ci}^Q & -\sin \phi_{ci}^Q & d_{ciy}^Q \\ \sin \phi_{ci}^Q & \cos \phi_{ci}^Q & -d_{cix}^Q \\ 0 & 0 & 1 \end{bmatrix} \begin{bmatrix} \dot{x}_{ci} \\ \dot{y}_{ci} \\ \dot{\phi}_{ci} \end{bmatrix} \quad (2.77)$$

where  $\phi_{ci}^Q$  denotes the rotation angle (orientation) of the frame  $O_{ci}$  with respect to  $Qx_Qy_Q$ , and  $d_{cix}^Q, d_{ciy}^Q$  are the translations of  $O_{ci}$  with respect to  $Qx_Qy_Q$ . Introducing Eq.(2.76) into Eq.(2.77) we get :

$$\dot{\mathbf{p}}_Q = \mathbf{J}_i \dot{\mathbf{q}}_i \quad (i=1,2,3,4) \quad (2.78)$$

where  $\dot{\mathbf{q}}_i = [\dot{\theta}_{ix}, \dot{\theta}_{ir}, \dot{\theta}_{iz}]^T$ , and

$$\mathbf{J}_i = \begin{bmatrix} -R_i \sin \phi_{ci}^Q & r_i \sin(\phi_{ci}^Q + \alpha_i) & d_{ciy}^Q \\ R_i \cos \phi_{ci}^Q & -r_i \cos(\phi_{ci}^Q + \alpha_i) & -d_{cix}^Q \\ 0 & 0 & 1 \end{bmatrix} \quad (2.79)$$

is the Jacobian matrix of wheel  $i$ , which is square and invertible. If all wheels are identical (except for the orientation of the rollers), the kinematic parameters of the robot in the configuration shown in Fig. 2.14 are :

$$R_i = R, \quad r_i = r, \quad \phi_{ci}^Q = 0 \\ |d_{cix}^Q| = d_1, \quad |d_{ciy}^Q| = d_2 \quad (2.80)$$

$$\alpha_1 = \alpha_3 = -45^\circ, \quad \alpha_2 = \alpha_4 = 45^\circ$$

Thus, the Jacobian matrices (2.79) are :

$$\mathbf{J}_1 = \begin{bmatrix} 0 & -r\sqrt{2}/2 & d_2 \\ R & -r\sqrt{2}/2 & d_1 \\ 0 & 0 & 1 \end{bmatrix}, \quad \mathbf{J}_2 = \begin{bmatrix} 0 & r\sqrt{2}/2 & d_2 \\ R & -r\sqrt{2}/2 & -d_1 \\ 0 & 0 & 1 \end{bmatrix} \\ \mathbf{J}_3 = \begin{bmatrix} 0 & -r\sqrt{2}/2 & -d_2 \\ R & -r\sqrt{2}/2 & -d_1 \\ 0 & 0 & 1 \end{bmatrix}, \quad \mathbf{J}_4 = \begin{bmatrix} 0 & r\sqrt{2}/2 & -d_2 \\ R & -r\sqrt{2}/2 & d_1 \\ 0 & 0 & 1 \end{bmatrix} \quad (2.81)$$

The robot motion is produced by the simultaneous motion of all wheels.

In terms of  $\dot{\theta}_{ix}$  (i.e., the wheels' angular velocities around their axles) the velocity vector  $\dot{\mathbf{p}}_Q$  is given by :

$$\begin{bmatrix} \dot{x}_Q \\ \dot{y}_Q \\ \dot{\phi}_Q \end{bmatrix} = \frac{R}{4} \begin{bmatrix} -1 & 1 & -1 & 1 \\ 1 & 1 & 1 & 1 \\ 1 & -1 & -1 & 1 \\ \frac{1}{d_1+d_2} & \frac{-1}{d_1+d_2} & \frac{-1}{d_1+d_2} & \frac{1}{d_1+d_2} \end{bmatrix} \begin{bmatrix} \dot{\theta}_{1x} \\ \dot{\theta}_{2x} \\ \dot{\theta}_{3x} \\ \dot{\theta}_{4x} \end{bmatrix} \quad (2.82)$$

The robot speed vector  $\dot{\mathbf{p}} = [\dot{x}, \dot{y}, \dot{\phi}]^T$  in the world coordinate frame is obtained as :

$$\begin{bmatrix} \dot{x} \\ \dot{y} \\ \dot{\phi} \end{bmatrix} = \begin{bmatrix} \cos \phi & -\sin \phi & 0 \\ \sin \phi & \cos \phi & 0 \\ 0 & 0 & 1 \end{bmatrix} \begin{bmatrix} \dot{x}_Q \\ \dot{y}_Q \\ \dot{\phi}_Q \end{bmatrix} \quad (2.83)$$

where  $\phi$  is the rotation angle of the platform's coordinate frame  $Qx_Qy_Q$  around the  $z$  axis which is orthogonal to  $Oxy$ . Inverting Eqs.(2.82) and (2.83) we get the inverse kinematic model, which gives the angular speeds  $\dot{\theta}_{ix}$  ( $i=1,2,3,4$ ) of the wheels around their hubs required to get a desired speed  $[\dot{x}, \dot{y}, \dot{\phi}]^T$  of the robot :

$$\begin{bmatrix} \dot{\theta}_{1x} \\ \dot{\theta}_{2x} \\ \dot{\theta}_{3x} \\ \dot{\theta}_{4x} \end{bmatrix} = \frac{1}{R} \begin{bmatrix} -1 & 1 & (d_1+d_2) \\ 1 & 1 & -(d_1+d_2) \\ -1 & 1 & -(d_1+d_2) \\ 1 & 1 & (d_1+d_2) \end{bmatrix} \begin{bmatrix} \dot{x}_Q \\ \dot{y}_Q \\ \dot{\phi}_Q \end{bmatrix} \quad (2.84)$$

$$\begin{bmatrix} \dot{x}_Q \\ \dot{y}_Q \\ \dot{\phi}_Q \end{bmatrix} = \begin{bmatrix} \cos \phi & \sin \phi & 0 \\ -\sin \phi & \cos \phi & 0 \\ 0 & 0 & 1 \end{bmatrix} \begin{bmatrix} \dot{x} \\ \dot{y} \\ \dot{\phi} \end{bmatrix} \quad (2.85)$$

For historical awareness, we mention here that the mecanum wheel was invented by the Swedish engineer *Bengt Ilon* in 1973 during his work at the Swedish company Mecanum AB. For this reason it is also known as *Ilon wheel* or *Swedish wheel*.

### Example 2.5

It is desired to construct a mecanum wheel with  $n$  rollers of angle  $\alpha$ . Determine the roller length  $D_r$  and the thickness  $d$  of the wheel.

### Solution

We consider the wheel geometry shown in Fig. 2.15, where  $R$  is the wheel radius [18].

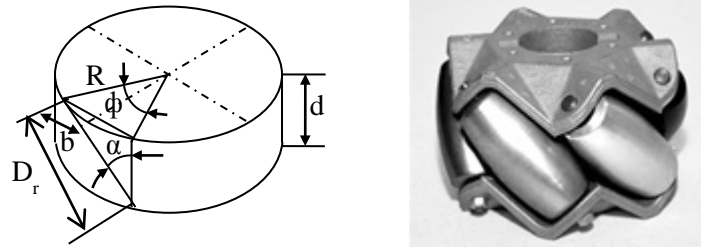


**Fig. 2.15 : (a) Geometry of mecanum wheel where the rollers are assumed to be placed peripherally, (b) A 6-roller wheel example.**

Source : <http://store.kornylak.com/SearchResults.asp?Cat=7>

From this figure we get the following relations :

$$n = 2\pi / \phi \quad (2.86a)$$

$$\sin(\phi / 2) = b / R \quad (2.86b)$$

$$2b = D_r \sin \alpha \quad (2.86c)$$

$$d = D_r \cos \alpha \quad (2.86d)$$

From Eq.(2.86a-c) we have :

$$\sin\left(\frac{\pi}{n}\right) = \left(\frac{D_r}{2R}\right) \sin \alpha \quad (2.87)$$

whence :

$$D_r = 2R \frac{\sin(\pi / n)}{\sin \alpha} \quad (2.88)$$

Solving (2.87) for  $\sin \alpha$  and noting that  $\cos \alpha = \sin \alpha / \tan \alpha$ , (2.86d) gives :

$$d = 2R \frac{\sin(\pi / n)}{\tan \alpha} \quad (2.89)$$

For a roller angle  $\alpha = 45^\circ$ , Eqs.(2.88) and (2.89) give :

$$D_r = 2\sqrt{2}R \sin(\pi / n) \quad (2.90a)$$

$$d = 2R \sin(\pi / n) \quad (2.90b)$$

For a roller angle  $\alpha = 90^\circ$  (universal wheel) we get :

$$D_r = 2R \sin(\pi / n) \quad (2.91a)$$

$$d = 0 \quad (\text{ideally}) \quad (2.91b)$$

In this case,  $d$  can have any convenient value required by other design considerations.

## References

- [1]Angelo A. Robotics: A reference Guide to New Technology. Boston, MA: Greenwood Press;2007.
- [2]Muir P F, Neuman C P. Kinematic modeling of wheeled mobile robots. Journal of Robotic Systems 1987; 4(2):281-329.
- [3]Alexander J C, Maddocks J H. On the kinematics of wheeled mobile robots. International Journal of Robotics Research 1981; 8(5): 15-27.
- [4]Muir P F, Neuman C. Kinematic modeling for feedback control of an omnidirectional wheeled mobile robot. Proceedings of IEEE International Conference on Robotics and Automation. Raileigh, USA,1987;1772-78.
- [5]Kim D S, Hyun Kwon W, Park H S. Geometric kinematics and applications of a mobile robot. International Journal of Control Automation and Systems 2003; 1(3): 376-84.
- [6]Rajagopalan R. A generic kinematic formulation for wheeled mobile robots. Journal of Robotic Systems 1997; 14:77-91.
- [7]Sreenivasan S V. Kinematic geometry of wheeled vehicle systems. Proceedings of 24<sup>th</sup> ASME Mechanism Conference. Irvine, CA, 96-DETC-MECH-1137, 1996.
- [8]Balakrishna R, Ghosal A. Two dimensional wheeled vehicle kinematics. IEEE Transactions Robotics and Automation 1995; 11(1):126-130.
- [9]Killough S M, Pin F G. Design of an omnidirectional and holonomic wheeled platform design. Proceedings of IEEE Conference on Robotics and Automation, Nice, France, 1992,p.84-90.



- [10]Sidek N, Sarkar N. Dynamic modeling and control of nonholonomic mobile robot with lateral slip. Proceedings of 7<sup>th</sup> WSEAS International Conference on Signal Processing Robotics and Automation (ISPRA'08), Cambridge, Feb.20-22, 2008,p.66-74.
- [11]Giovanni I. Swedish wheeled omnidirectional mobile robots: Kinematics Analysis and Control. IEEE Transactions on Robotics 2009;25(1): 164-171.
- [12]West M, Asada H. Design of a holonomic omnidirectional vehicle. Proceedings of IEEE Conference on Robotics and Automation, Nice, France, May, 1992,p.97-103.
- [13]Chakraborty N, Ghosal A. Kinematics of wheeled mobile robots on uneven terrain. Mechanism and Machine Theory 2004; 39: 1273-1287.
- [14]Sordalen O J, Egeland O. Exponential stabilization of nonholonomic chained systems. IEEE Transactions Automatic Control 1995; 40(1):35-49.
- [15]Khalil H. Nonlinear Systems. Upper Saddle River, N.J: Prentice Hall;2001.
- [16]Ashmore M, Barnes N. Omni-drive robot motion on curved paths : The fastest path between two points is not a straight line. Proceedings of 15<sup>th</sup> Australian Joint Conference on Artificial Intelligence : Advances in Artificial Intelligence (AI'02) (Springer, London, 2002), p.225-236.
- [17]Huang L, Lim Y S, Li D, Teoh C.E.L. Design and analysis of a four-wheel omnidirectional mobile robot. Proceedings of 2<sup>nd</sup> International Conference on Autonomous Robots and Agents. Palmerston North, New Zealand, Dec., 2004, p.425-28.
- [18]Doroftei I, Grosu V, Spinu V. Omnidirectional mobile robot: Design and Implementation, In: Habib M K, editor. Bioinspiration and Robotics : Walking and Climbing Robots. Vienna, Austria In-Tech,2007, p.512-27.
- [19]Phairoh T, Williamson K. Autonomous mobile robots using real time kinematic signal correction and global positioning system control. Proceedings of 2008 IAJC-IJME International Conference on Engineering and Technology, Sheraton, Nashville, TN, USA, November, 2008, Paper 087 / IT304.
- [20]De Luca A, Oriolo G, Samson C. Feedback control of a nonholonomic car-like robot. In : Laumond J-P editor. Robot Motion Planning and Control. Berlin / New York: Springer; 1998: 171-253.

## Chapter 3

# Mobile Robot Dynamics

### 3.1 Introduction

The next problem in the study of all types of robots, after kinematics, is the *dynamic modeling*. Dynamic modeling is performed using the laws of mechanics that are based on the three physical elements: inertia, elasticity and friction that are present in any real mechanical system such as the robot. Mobile robot dynamics is a challenging field on its own and has attracted considerable attention by researchers and engineers over the years. Most mobile robots, employed in practice, use conventional wheels and are subject to nonholonomic constraints that need particular treatment. Delicate stability and control problems, that often have to be faced in the design of a mobile robot, are due to the existence of longitudinal and lateral slip in the movement of the WMRs wheels.

This chapter has the following objectives:

- To present the general dynamic modeling concepts and techniques of robots.
- To study the Newton-Euler and Lagrange dynamic models of differential – drive mobile robots
- To study the dynamics of differential –drive mobile robots with longitudinal and lateral slip.
- To derive a dynamic model of car-like WMRs
- To derive a dynamic model of 3-wheel omnidirectional robots
- To derive a dynamic model of 4-wheel mecanum omnidirectional robots.

### 3.2 General Robot Dynamic Modeling

Robot dynamic modeling deals with the derivation of the dynamic equations of the robot motion. This can be done using two methodologies:

- Newton-Euler method
- Lagrange method

The complexity of the Newton-Euler method is  $O(n)$ , whereas the complexity of the Lagrange method can only be reduced up to  $O(n^3)$ , where  $n$  is the number of degrees of freedom.

Like kinematics, dynamics is distinguished in:

- Direct dynamics
- Inverse dynamics

*Direct dynamics* provides the dynamic equations that describe the dynamic responses of the robot to given forces/torques  $\tau_1, \tau_2, \dots, \tau_m$  that are exerted by the motors.

*Inverse dynamics* provides the forces /torques that are needed to get desired trajectories of the robot links. Direct and inverse dynamic modeling is pictorially illustrated in Fig.3.1.

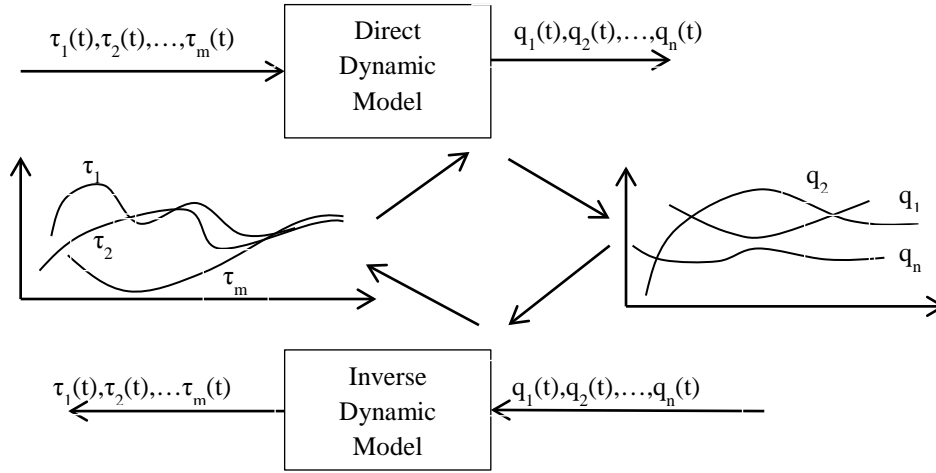


**Fig. 3.1 : Direct and inverse dynamic modeling**

In the inverse dynamic model the inputs are the desired trajectories of the link variables, and outputs the motor torques.

### 3.2.1 Newton-Euler Dynamic Model

This model is derived by direct application of the Newton-Euler equations for translational and rotational motion. Consider the object  $B_i$  (robotic link, WMR, etc) of Fig.3.2 to which a total force  $\mathbf{f}_i$  is applied at its *center of gravity* (**COG**).

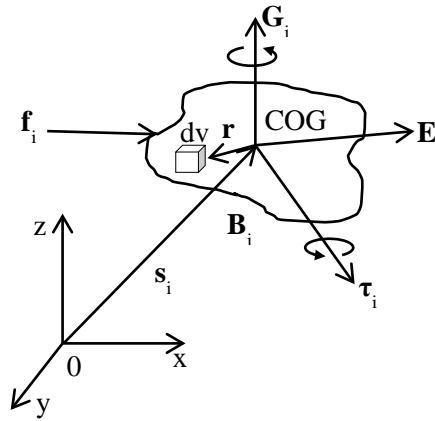


**Fig. 3.2 : A solid body  $B_i$  and the inertial coordinate frame Oxyz.**

Then, its translational motion is described by:

$$\frac{d\mathbf{E}_i}{dt} = \mathbf{f}_i \quad (3.1)$$

Here,  $\mathbf{E}_i$  is the *linear momentum* given by:

$$\mathbf{E}_i = m_i \dot{\mathbf{s}}_i \quad (3.2)$$

where  $m_i$  is the mass of the body and  $\mathbf{s}_i$  is the position of the center of gravity with respect to the world (inertial) coordinate frame Oxyz. Assuming that  $m_i$  is constant, then Eqs.(3.1) and (3.2) give:

$$m_i \ddot{\mathbf{s}}_i = \mathbf{F}_i \quad (3.3)$$

which is the general *translational dynamic model*.

The rotational motion of  $B_i$  is described by:

$$\frac{d\mathbf{G}_i}{dt} = \boldsymbol{\tau}_i \quad (3.4)$$

where  $\mathbf{G}_i$  is the total angular momentum of  $B_i$  with respect to COG, and  $\boldsymbol{\tau}_i$  is the total external torque that produces the rotational motion of the body. The total momentum  $\mathbf{G}_i$  is given by:

$$\mathbf{G}_i = \mathbf{I}_i \boldsymbol{\omega}_i \quad (3.5)$$

Here,  $\mathbf{I}_i$  is the inertia tensor given by the volume integral:

$$\mathbf{I}_i = \int_{V_i} [\mathbf{r}^T \mathbf{r} \mathbf{I}_3 - \mathbf{r} \mathbf{r}^T] \rho_i dV \quad (3.6)$$

where  $\rho_i$  is the mass density of  $B_i$ ,  $dV$  is the volume of an infinitesimal element of  $B_i$  lying at the position  $\mathbf{r}$  with respect to COG,  $\boldsymbol{\omega}_i$  is the angular velocity vector about the inertial axis passing from COG,  $\mathbf{I}_3$  is the 3x3 unit matrix, and  $V_i$  is the volume of  $B_i$ .

### 3.2.2 Lagrange Dynamic Model

The general Lagrange dynamic model of a solid body (multi-link robot, WMR, etc) is described by<sup>5</sup>

$$\frac{d}{dt} \left( \frac{\partial L}{\partial \dot{\mathbf{q}}} \right) - \frac{\partial L}{\partial \mathbf{q}} = \boldsymbol{\tau}, \quad \mathbf{q} = [q_1, q_2, \dots, q_n]^T \quad (3.7)$$

where  $q_i$  is the  $i$ th-degree of freedom variable,  $\boldsymbol{\tau}$  is the external generalized force vector applied to the body (i.e. force for translational motion, and torque for rotational motion), and  $L$  is the Lagrangian function defined by:

$$L = K - P \quad (3.8)$$

Here,  $K$  is the total kinetic energy, and  $P$  the total potential energy of the body given by:

$$\begin{aligned} K &= K_1 + K_2 + \dots + K_n \\ P &= P_1 + P_2 + \dots + P_n \end{aligned} \quad (3.9)$$

where  $K_i$  is the kinetic energy of link (degree of freedom)  $i$ , and  $P_i$  its potential energy. The kinetic energy  $K$  of the body is equal to:

$$K = \frac{1}{2} m \dot{\mathbf{s}}^T \dot{\mathbf{s}} + \frac{1}{2} \boldsymbol{\omega}^T \mathbf{I} \boldsymbol{\omega} \quad (3.10)$$

where  $\dot{\mathbf{s}}$  is the linear velocity of the center of gravity,  $\boldsymbol{\omega}$  is the angular velocity of the rotation,  $m$  is the mass, and  $\mathbf{I}$  the inertia tensor of the body.

### 3.2.3 Lagrange Model of a multi-Link Robot

---

<sup>5</sup> Derivations of Eq.(3.7) from first principles are provided in textbooks on mechanics.

Given a general multi-link robot, the application of Eq.(3.7) leads (always) to a dynamic model of the form:

$$\mathbf{D}(\mathbf{q})\ddot{\mathbf{q}} + \mathbf{h}(\mathbf{q}, \dot{\mathbf{q}}) + \mathbf{g}(\mathbf{q}) = \boldsymbol{\tau} \quad (3.11a)$$

where, for any  $\dot{\mathbf{q}} \neq \mathbf{0}$ ,  $\mathbf{D}(\mathbf{q})$  is a  $n \times n$  positive definite matrix, and:

$$\mathbf{q} = [q_1, q_2, \dots, q_n]^T \quad (3.11b)$$

is the vector of generalized variables (linear, angular)  $q_i$ ,  $\mathbf{D}(\mathbf{q})\ddot{\mathbf{q}}$  represents the inertia force,  $\mathbf{h}(\mathbf{q}, \dot{\mathbf{q}})$  represents the centrifugal and Coriolis force, and  $\mathbf{g}(\mathbf{q})$  stands for the gravitational force. Since  $\boldsymbol{\tau}$  is the net force/torque applied to the robot, if there is also friction force/torque  $\boldsymbol{\tau}_f$ , then  $\boldsymbol{\tau} = \boldsymbol{\tau}' - \boldsymbol{\tau}_f$  where  $\boldsymbol{\tau}'$  is the force/torque exerted by the actuators at the joints.

It is useful to note that given the model (3.11a,b) one can express the kinetic energy of the robot as:

$$K = \frac{1}{2} \dot{\mathbf{q}}^T(t) \mathbf{D}(\mathbf{q}) \dot{\mathbf{q}}(t) \quad (3.12)$$

The expressions of  $\mathbf{D}(\mathbf{q})$ ,  $\mathbf{h}(\mathbf{q}, \dot{\mathbf{q}})$  and  $\mathbf{g}(\mathbf{q})$  have to be derived in each particular case. General derivations of Eq.(3.11a) from Eq.(3.7) are given in standard industrial (fixed) robotics books.

Typically, the function  $\mathbf{h}(\mathbf{q}, \dot{\mathbf{q}})$  can be written in the form:

$$\mathbf{h}(\mathbf{q}, \dot{\mathbf{q}}) = \mathbf{C}(\mathbf{q}, \dot{\mathbf{q}}) \dot{\mathbf{q}} \quad (3.13)$$

A useful universal property of the Lagrange model given by Eqs.(3.11a)-(3.13) is that the  $n \times n$  matrix  $\mathbf{A} = \dot{\mathbf{D}} - 2\mathbf{C}$  is antisymmetric, i.e.  $\mathbf{A}^T = -\mathbf{A}$ .

### 3.2.4 Dynamic Modeling of Nonholonomic Robots

The Lagrange dynamic model of a nonholonomic robot (fixed or mobile) has the form (3.7):

$$\frac{d}{dt} \left( \frac{\partial L}{\partial \dot{\mathbf{q}}} \right) - \frac{\partial L}{\partial \mathbf{q}} + \mathbf{M}^T(\mathbf{q}) \boldsymbol{\lambda} = \mathbf{E} \boldsymbol{\tau} \quad (3.14)$$

where  $\mathbf{M}(\mathbf{q})$  is the  $m \times n$  matrix of the  $m$  nonholonomic constraints:

$$\mathbf{M}(\mathbf{q}) \dot{\mathbf{q}} = \mathbf{0} \quad (3.15)$$

and  $\boldsymbol{\lambda}$  is the vector Lagrange multiplier. This model leads to:

$$\mathbf{D}(\mathbf{q})\ddot{\mathbf{q}} + \mathbf{C}(\mathbf{q}, \dot{\mathbf{q}}) \dot{\mathbf{q}} + \mathbf{g}(\mathbf{q}) + \mathbf{M}^T(\mathbf{q}) \boldsymbol{\lambda} = \mathbf{E} \boldsymbol{\tau} \quad (3.16)$$

where  $\mathbf{E}$  is a nonsingular transformation matrix. To eliminate the constraint term  $\mathbf{M}^T(\mathbf{q}) \boldsymbol{\lambda}$  in Eq.(3.16) and get a constraint-free model we use a  $n \times (n-m)$  matrix  $\mathbf{B}(\mathbf{q})$  which is defined such that:

$$\mathbf{B}^T(\mathbf{q}) \mathbf{M}^T(\mathbf{q}) = \mathbf{0} \quad (3.17)$$

From Eqs.(3.15) and (3.17) one can verify that there exists a  $(n-m)$ -dimensional vector  $\mathbf{v}(t)$  such that:

$$\dot{\mathbf{q}}(t) = \mathbf{B}(\mathbf{q}) \mathbf{v}(t) \quad (3.18)$$

Now, premultiplying Eq.(3.16) by  $\mathbf{B}^T(\mathbf{q})$  and using Eqs.(3.15), (3.17) and (3.18) we get:

$$\bar{\mathbf{D}}(\mathbf{q})\dot{\mathbf{v}} + \bar{\mathbf{C}}(\mathbf{q}, \dot{\mathbf{q}})\mathbf{v} + \bar{\mathbf{g}}(\mathbf{q}) = \bar{\mathbf{E}}\boldsymbol{\tau} \quad (3.19a)$$

where:

$$\bar{\mathbf{D}} = \mathbf{B}^T \mathbf{D} \mathbf{B}$$

$$\bar{\mathbf{C}} = \mathbf{B}^T \mathbf{D} \dot{\mathbf{B}} + \mathbf{B}^T \mathbf{C} \mathbf{B} \quad (3.19b)$$

$$\bar{\mathbf{g}} = \mathbf{B}^T \mathbf{g}$$

$$\bar{\mathbf{E}} = \mathbf{B}^T \mathbf{E}$$

The reduced (unconstrained) model (3.19a,b) describes the dynamic evolution of the  $n$ -dimensional vector  $\mathbf{q}(t)$  in terms of the dynamic evolution of the  $(n-m)$ -dimensional vector  $\mathbf{v}(t)$ .

### 3.3 Differential Drive WMR

The dynamic model of the differential drive WMR will be derived here by both the Newton –Euler and Lagrange methods.

#### 3.3.1 Newton-Euler Dynamic Model

In the present case use will be made of the Newton-Euler equations:

$$m\dot{\mathbf{v}} = \mathbf{F} \quad (\text{Translational motion}) \quad (3.20a)$$

$$\mathbf{I}\dot{\boldsymbol{\omega}} = \mathbf{N} \quad (\text{Rotational motion}) \quad (3.20b)$$

where  $\mathbf{F}$  is the total force applied at the center of gravity G,  $\mathbf{N}$  is the total torque with respect to the center of gravity  $m$  is the mass of the WMR, and  $\mathbf{I}$  is the inertia of the WMR. Referring to Fig.2.7, and assuming that the center of gravity G coincides with the midpoint Q (i.e.,  $b=0$ ), we find:

$$\mathbf{F} = F_r + F_l, \quad \tau_r = rF_r, \quad \tau_l = rF_l \quad (3.21a)$$

i.e:

$$F = \frac{1}{r}(\tau_r + \tau_l) \quad (3.21b)$$

where  $F_r$  and  $F_l$  are the forces that produce the torques  $\tau_r$  and  $\tau_l$ , respectively.

Also:

$$N = (F_r - F_l)2a = \frac{2a}{r}(\tau_r - \tau_l) \quad (3.22)$$

Therefore, (3.20a,b) give the WMR's dynamic model:

$$\dot{\mathbf{v}} = \frac{1}{mr}(\tau_r + \tau_l) \quad (3.23a)$$

$$\dot{\boldsymbol{\omega}} = \frac{2a}{Ir}(\tau_r - \tau_l) \quad (3.23b)$$

#### 3.3.2 Lagrange Dynamic Model

We refer to Fig.2.7 and assume again that the point Q is at the position of point G. Here, the nonholonomic constraint matrix is {see (2.42)}:

$$\mathbf{M}(\mathbf{q}) = \begin{bmatrix} -\sin \phi & \cos \phi & 0 \end{bmatrix} \quad (3.24)$$

Since the WMR moves on an horizontal planar terrain, the terms  $\mathbf{C}(\mathbf{q}, \dot{\mathbf{q}})$  and  $\mathbf{g}(\mathbf{q})$  in Eq.(3.16) are zero. Therefore, the model (3.16) becomes:

$$\mathbf{D}(\mathbf{q})\ddot{\mathbf{q}} + \mathbf{M}^T(\mathbf{q})\boldsymbol{\lambda} = \mathbf{E}\boldsymbol{\tau} \quad (3.25)$$

where:

$$\mathbf{q} = \begin{bmatrix} x_Q \\ y_Q \\ \phi \end{bmatrix}, \boldsymbol{\tau} = \begin{bmatrix} \tau_r \\ \tau_l \end{bmatrix} \quad (3.26a)$$

$$\mathbf{D}(\mathbf{q}) = \begin{bmatrix} m & 0 & 0 \\ 0 & m & 0 \\ 0 & 0 & I \end{bmatrix}, \mathbf{E} = \frac{1}{r} \begin{bmatrix} \cos \phi & \cos \phi \\ \sin \phi & \sin \phi \\ 2a & -2a \end{bmatrix} \quad (3.26b)$$

To convert the model (3.25) to the corresponding unconstrained model (3.19a,b) we need the matrix  $\mathbf{B}(\mathbf{q})$  in (3.17). Here, this matrix is:

$$\mathbf{B}(\mathbf{q}) = \begin{bmatrix} \cos \phi & 0 \\ \sin \phi & 0 \\ 0 & 1 \end{bmatrix} \quad (3.27)$$

which satisfies Eq.(3.17). Therefore, Eq.(3.19b) gives:

$$\bar{\mathbf{D}} = \mathbf{B}^T \mathbf{D} \mathbf{B} = \begin{bmatrix} m & 0 \\ 0 & I \end{bmatrix}, \bar{\mathbf{E}} = \frac{1}{r} \begin{bmatrix} 1 & 1 \\ 2a & -2a \end{bmatrix} \quad (3.28)$$

and the model (3.19a) becomes:

$$\begin{bmatrix} m & 0 \\ 0 & I \end{bmatrix} \begin{bmatrix} \dot{v}_1 \\ \dot{v}_2 \end{bmatrix} = \frac{1}{r} \begin{bmatrix} 1 & 1 \\ 2a & -2a \end{bmatrix} \begin{bmatrix} \tau_r \\ \tau_l \end{bmatrix} \quad (3.29)$$

Noting that  $v_1$  is the translation velocity  $v$ , and  $v_2$  the angular velocity  $\omega$  of the robot, Eq.(3.29) gives the model:

$$\dot{v} = \frac{1}{mr} (\tau_r + \tau_l) \quad (3.30a)$$

$$\dot{\omega} = \frac{2a}{Ir} (\tau_r - \tau_l) \quad (3.30b)$$

which is identical to Eq.(3.23a,b), as expected. Finally, using Eq.(3.18) we get:

$$\begin{bmatrix} \dot{x}_Q \\ \dot{y}_Q \\ \dot{\phi} \end{bmatrix} = \begin{bmatrix} \cos \phi & 0 \\ \sin \phi & 0 \\ 0 & 1 \end{bmatrix} \begin{bmatrix} v \\ \omega \end{bmatrix} = \begin{bmatrix} v \cos \phi \\ v \sin \phi \\ \omega \end{bmatrix} \quad (3.31)$$

which is the WMR's kinematic model. The dynamic and kinematic equations (3.30a,b) and (3.31) describe fully the motion of the differential drive WMR.

### Example 3.1

The problem is to derive the Lagrange dynamic model using directly the Lagrangian function  $L$  for a differential drive WMR in which:

1. There is linear friction in the wheels with the same friction coefficient.
2. The wheel midpoint  $Q$  does not coincide with the center of gravity  $G$ .
3. The wheel –motor assemblies have nonzero inertia.

### Solution

We will work with the WMR of Fig. 2.7. The kinetic energy  $K$  of the robot is given by:

$$K = K_1 + K_2 + K_3 \quad (3.32)$$

where:

$$K_1 = \frac{1}{2} m v_G^2 = \frac{1}{2} m (\dot{x}_G^2 + \dot{y}_G^2)$$

$$K_2 = \frac{1}{2} I_Q \dot{\phi}^2 \quad (3.33)$$

$$K_3 = \frac{1}{2} I_o \dot{\theta}_r^2 + \frac{1}{2} I_o \dot{\theta}_l^2$$

and (see example 2.2):

$$\dot{x}_G = \dot{x}_Q + b \dot{\phi} \sin \phi$$

$$\dot{y}_G = \dot{y}_Q - b \dot{\phi} \cos \phi$$

with:

$m$  = mass of the entire robot

$v_G$  = linear velocity of the center of gravity  $G$

$I_Q$  = moment of inertia of the robot with respect to  $Q$

$I_o$  = moment of inertia of each wheel plus the corresponding motor's rotor moment of inertia.

The velocities  $\dot{x}_Q$ ,  $\dot{y}_Q$  and  $\dot{\phi}$  are given by Eq.(2.36a-c):

$$\dot{x}_Q = \frac{r}{2} (\dot{\theta}_r \cos \phi + \dot{\theta}_l \cos \phi) = \frac{r}{2} (\dot{\theta}_r + \dot{\theta}_l) \cos \phi$$

$$\dot{y}_Q = \frac{r}{2} (\dot{\theta}_r \sin \phi + \dot{\theta}_l \sin \phi) = \frac{r}{2} (\dot{\theta}_r + \dot{\theta}_l) \sin \phi \quad (3.34)$$

$$\dot{\phi} = \frac{r}{2a} (\dot{\theta}_r - \dot{\theta}_l)$$

Using Eqs.(3.33) and (3.34) in Eq.(3.32) the total kinetic energy  $K$  of the robot is found to be:

$$K(\dot{\theta}_r, \dot{\theta}_l) = \left[ \frac{mr^2}{8} + \frac{(I_Q + mb^2)r^2}{8a^2} + \frac{I_o}{2} \right] \dot{\theta}_r^2$$

$$+ \left[ \frac{mr^2}{8} + \frac{(I_Q + mb^2)r^2}{8a^2} + \frac{I_o}{2} \right] \dot{\theta}_l^2 \quad (3.35)$$

$$+ \left[ \frac{mr^2}{4} - \frac{(I_Q + mb^2)r^2}{4a^2} \right] \dot{\theta}_r \dot{\theta}_l$$

Here, the kinetic energy is expressed directly in terms of the angular velocities  $\dot{\theta}_r$  and  $\dot{\theta}_l$  of the driving wheels. The Lagrangian  $L$  is equal to  $K$ , since the robot is moving on an horizontal plane and so the potential energy  $P$  is zero. Therefore, the Lagrange dynamic equations of this robot are:



$$\begin{aligned}\frac{d}{dt}\left(\frac{\partial K}{\partial \dot{\theta}_r}\right) - \frac{\partial K}{\partial \theta_r} &= \tau_r - \beta \dot{\theta}_r \\ \frac{d}{dt}\left(\frac{\partial K}{\partial \dot{\theta}_l}\right) - \frac{\partial K}{\partial \theta_l} &= \tau_l - \beta \dot{\theta}_l\end{aligned}\tag{3.36}$$

where  $\beta$  is the wheels' common friction coefficient, and  $\tau_r, \tau_l$  are the right and left actuation torques. Using (3.35) in (3.36) we get:

$$\begin{aligned}D_{11}\ddot{\theta}_r + D_{12}\ddot{\theta}_l + \beta\dot{\theta}_r &= \tau_r \\ D_{21}\ddot{\theta}_r + D_{22}\ddot{\theta}_l + \beta\dot{\theta}_l &= \tau_l\end{aligned}\tag{3.37}$$

where:

$$\begin{aligned}D_{11} = D_{22} &= \left[ \frac{mr^2}{4} + \frac{(I_o + mb^2)r^2}{8a^2} + I_o \right] \\ D_{12} = D_{21} &= \left[ \frac{mr^2}{4} - \frac{(I_o + mb^2)r^2}{8a^2} \right]\end{aligned}\tag{3.38}$$

Using the known relations:

$v_r = r\dot{\theta}_r, v_l = r\dot{\theta}_l, v = (v_r + v_l)/2, \omega = (v_r - v_l)/2a$ , one can easily verify that in the case where the above conditions 1,2, and 3 are relaxed (i.e.,  $\beta=0, b=0, I_o = 0$ ), the above dynamic model reduces to the model (3.30 a,b). This model was implemented and validated using MATLAB / SIMULINK in [16].

### 3.3.3 Dynamics of WMR with Slip

Here we will derive the Newton –Euler dynamic model of the slipping differential drive WMR considered in Example 2.2. The case where both longitudinal slip (variables  $w_r, w_l$ ) and lateral slip (variables  $z_r, z_l$ ) are present will be considered [5].

For convenience we write again the kinematic equations of the robot (with steering angles  $\zeta_r = \zeta_l = 0$ ):

$$\begin{aligned}\dot{\gamma}_r &= \dot{x}_G \cos \phi + \dot{y}_G \sin \phi + a\dot{\phi}, & \gamma_r &= r\theta_r - w_r \\ \dot{\gamma}_l &= \dot{x}_G \cos \phi + \dot{y}_G \sin \phi - a\dot{\phi}, & \gamma_l &= r\theta_l - w_l \\ \dot{z}_r &= -\dot{x}_G \sin \phi + \dot{y}_G \cos \phi + b\dot{\phi} \\ \dot{z}_l &= -\dot{x}_G \sin \phi + \dot{y}_G \cos \phi + b\dot{\phi}\end{aligned}$$

Defining the generalized variables' vector  $\mathbf{q}$  as:

$$\mathbf{q} = [x_G, y_G, \phi, z_r, z_l, \gamma_r, \gamma_l, \theta_r, \theta_l]\tag{3.39}$$

the above relations can be written in the following Pfaffian matrix form:

$$\mathbf{M}(\mathbf{q})\dot{\mathbf{q}} = \mathbf{0}$$

where:

$$\mathbf{M}(\mathbf{q}) = \begin{bmatrix} -\sin \phi & \cos \phi & b & -1 & 0 & 0 & 0 & 0 & 0 \\ -\sin \phi & \cos \phi & b & 0 & -1 & 0 & 0 & 0 & 0 \\ \cos \phi & \sin \phi & a & 0 & 0 & -1 & 0 & 0 & 0 \\ \cos \phi & \sin \phi & -a & 0 & 0 & 0 & -1 & 0 & 0 \end{bmatrix}\tag{3.40}$$

The matrix  $\mathbf{B}(\mathbf{q})$  and the velocity vector  $\mathbf{v}(t)$  that satisfy the relations {see Eqs.(3.17)-(3.18)}:

$$\mathbf{B}^T(\mathbf{q})\mathbf{M}^T(\mathbf{q}) = \mathbf{0}, \quad \dot{\mathbf{q}} = \mathbf{B}(\mathbf{q})\mathbf{v}(t) \quad (3.41)$$

are found to be:

$$\mathbf{B}(\mathbf{q}) = \begin{bmatrix} -\sin \phi & A & C & 0 & 0 \\ \cos \phi & B & D & 0 & 0 \\ 0 & \frac{1}{2a} & -\frac{1}{2a} & 0 & 0 \\ 1 & 0 & 0 & 0 & 0 \\ 1 & 0 & 0 & 0 & 0 \\ 0 & 1 & 0 & 0 & 0 \\ 0 & 0 & 1 & 0 & 0 \\ 0 & 0 & 0 & 1 & 0 \\ 0 & 0 & 0 & 0 & 1 \end{bmatrix} \quad (3.42)$$

where:

$$\mathbf{v} = [\dot{z}_l, \dot{\gamma}_r, \dot{\gamma}_l, \dot{\theta}_r, \dot{\theta}_l]^T \quad (\text{note that } z_r = z_l = y_r) \quad (3.43a)$$

$$A = \frac{a \cos \phi - b \sin \phi}{2a}, \quad B = \frac{b \cos \phi + a \sin \phi}{2a} \quad (3.43b)$$

$$C = \frac{a \cos \phi + b \sin \phi}{2a}, \quad D = \frac{a \sin \phi - b \cos \phi}{2a}$$

To derive the Newton-Euler dynamic model we draw the free-body diagram of the WMR body without the wheels (Fig.3.3), and the free-body diagram of the two wheels (Fig.3.4).

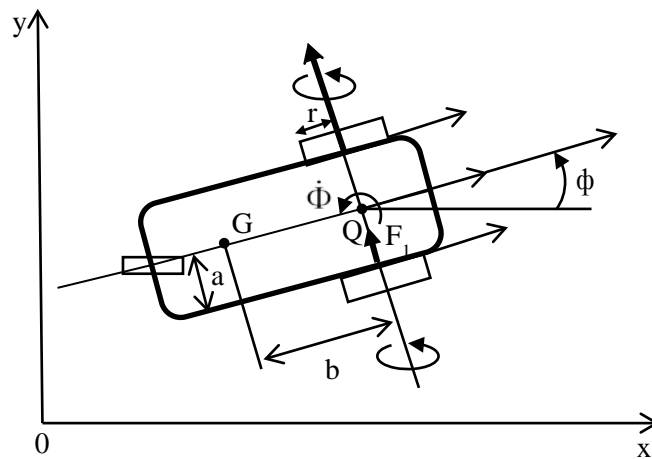


**Fig. 3.3 : Force-torque diagram of the body of the WMR (without the wheels).**

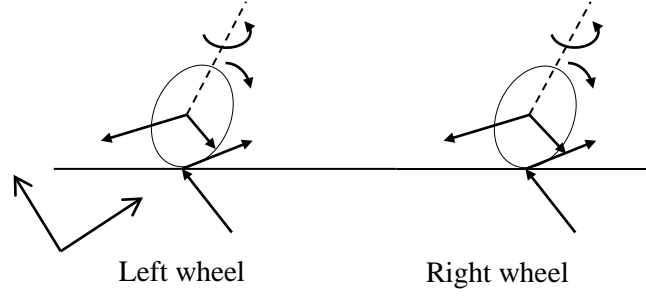


**Fig. 3.4 : Force-torque diagram of the two wheels. The coordinate frame  $O_w \gamma z$  is fixed at the driving wheels' midpoint.**

In figures 3.3 and 3.4 we have the following dynamic parameters and variables:

$\tau_b$  : The torque given to the wheels by the body of the WMR

$\tau_r, \tau_l$  : The driving torques exerted to the right and left wheel by their motors.

$m_b$  : The mass of the WMR body without the wheels.

$m_w$  : The mass of each driving wheel assembly (wheel plus DC motor of the robot body)

$I_{bz}$  : The moment of inertia about a vertical axis passing via G (without the wheels)

$I_{wy}$  : The wheel moment of inertia about its axis

$I_{wz}$  : The wheel moment of inertia about its diameter.

$F_i$  : The reaction forces between the WMR body and the wheels.

$F_{lat,r}, F_{lat,l}$  : The lateral traction force at each wheel.

$F_{long,r}, F_{long,l}$  : The longitudinal traction force at each wheel.

Using the above notation, the Newton- Euler dynamic equations of the robot, written down for each generalized variable in the vector (3.39), are:

$$m_b \ddot{x}_G = (F_1 + F_2) \sin \phi - (F_3 + F_4) \cos \phi$$

$$m_b \ddot{y}_G = -(F_1 + F_2) \cos \phi - (F_3 + F_4) \sin \phi$$

$$(I_{bz} + 2I_{wz}) \ddot{\phi} = (F_1 + F_2) b - (F_3 + F_4) a$$

$$m_w \ddot{z}_r + m_w \dot{\phi} \dot{\gamma}_r = F_{lat,r} - F_1$$

$$m_w \ddot{z}_l + m_w \dot{\phi} \dot{\gamma}_l = F_{lat,l} - F_2 \quad (3.44)$$

$$m_w \ddot{\gamma}_r - m_w \dot{\phi} \dot{z}_r = F_{long,r} - F_3$$

$$m_w \ddot{\gamma}_l - m_w \dot{\phi} \dot{z}_l = F_{long,l} - F_4$$

$$I_{wy} \ddot{\theta}_r = \tau_r - F_{long,r} r$$

$$I_{wy} \ddot{\theta}_l = \tau_l - F_{long,l} r$$

$$\text{where } \tau_b = I_{wz} \ddot{\phi}.$$

The detailed equations (3.44) can be written in the compact form of Eq.(3.16), namely:

$$\mathbf{D}(\mathbf{q}) \ddot{\mathbf{q}} + \mathbf{h}(\mathbf{q}, \dot{\mathbf{q}}) = \mathbf{E}(\mathbf{q}) \boldsymbol{\tau} + \mathbf{f}(\dot{\mathbf{q}}) + \mathbf{M}^T(\mathbf{q}) \mathbf{F} \quad (3.45)$$

where  $\mathbf{M}(\mathbf{q})$  is given by (3.40), and:

$$\mathbf{D} = \text{diag} \left[ m_b, m_b, \mathbf{I}_{bz} + 2\mathbf{I}_{wz}, m_w, m_w, m_w, m_w, \mathbf{I}_{wy}, \mathbf{I}_{wy} \right]$$

$$\mathbf{h} = \left[ 0, 0, 0, m_w \dot{\phi} \dot{\gamma}_r, m_w \dot{\phi} \dot{\gamma}_l, -m_w \dot{\phi} \dot{z}_r, -m_w \dot{\phi} \dot{z}_l, 0, 0 \right]$$

$$\mathbf{E} = \begin{bmatrix} -\frac{\mathbf{O}_{2 \times 7}}{\mathbf{I}_{2 \times 2}} \end{bmatrix}, \boldsymbol{\tau} = \begin{bmatrix} \tau_r \\ \tau_l \end{bmatrix}$$

$$\mathbf{f} = \left[ 0, 0, 0, F_{lat,r}, F_{lat,l}, F_{long,r}, F_{long,l}, -rF_{long,r}, -rF_{long,l} \right]^T$$

$$\mathbf{F} = \left[ F_1, F_2, F_3, F_4 \right]^T$$

Applying to Eq.(3.45) the procedure of section 3.2.4. we get the following reduced model (3.19 a,b):

$$\bar{\mathbf{D}}(\mathbf{q}) \dot{\mathbf{v}} + \bar{\mathbf{C}}_1(\mathbf{q}, \dot{\mathbf{q}}) \mathbf{v} + \bar{\mathbf{h}}(\mathbf{q}, \dot{\mathbf{q}}) = \bar{\mathbf{E}} \boldsymbol{\tau} + \bar{\mathbf{f}}(\mathbf{q}) \quad (3.46)$$

where:

$$\bar{\mathbf{D}}(\mathbf{q}) = \mathbf{B}^T \mathbf{D} \mathbf{B}, \quad \bar{\mathbf{C}}_1(\mathbf{q}, \dot{\mathbf{q}}) = \mathbf{B}^T \mathbf{D} \dot{\mathbf{B}}$$

$$\bar{\mathbf{h}}(\mathbf{q}, \dot{\mathbf{q}}) = \mathbf{B}^T \mathbf{h}, \quad \bar{\mathbf{E}} = \mathbf{B}^T \mathbf{E}, \quad \bar{\mathbf{f}}(\mathbf{q}) = \mathbf{B}^T \mathbf{f}$$

The model (3.46) can be splitted as:

$$\hat{\bar{\mathbf{D}}}(\hat{\mathbf{q}}) \dot{\hat{\mathbf{v}}} + \hat{\bar{\mathbf{C}}}_1(\hat{\mathbf{q}}, \dot{\hat{\mathbf{q}}}) \hat{\mathbf{v}} + \hat{\bar{\mathbf{h}}}(\hat{\mathbf{q}}, \dot{\hat{\mathbf{q}}}) = \hat{\bar{\mathbf{f}}} \quad (3.47a)$$

$$\mathbf{I}_{wy} \ddot{\theta}_r = \tau_r - rF_{long,r}$$

$$(3.47b)$$

$$\mathbf{I}_{wy} \ddot{\theta}_l = \tau_l - rF_{long,l} \quad (3.47c)$$

where:

$$\hat{\bar{\mathbf{D}}} = \hat{\mathbf{B}}^T \hat{\mathbf{D}} \hat{\mathbf{B}}, \quad \hat{\bar{\mathbf{C}}}_1 = \hat{\mathbf{B}}^T \hat{\mathbf{D}} \dot{\hat{\mathbf{B}}}$$

$$\hat{\bar{\mathbf{h}}} = \hat{\mathbf{B}}^T \hat{\mathbf{h}}, \quad \hat{\bar{\mathbf{f}}} = \hat{\mathbf{B}}^T \hat{\mathbf{f}}$$

$$\hat{\mathbf{D}} = \text{diag} \left[ m_b, m_b, \mathbf{I}_{bz} + 2\mathbf{I}_{wz}, m_w, m_w, m_w, m_w \right]^T$$

$$\hat{\mathbf{v}} = \left[ \dot{z}_l, \dot{\gamma}_r, \dot{\gamma}_l \right]^T$$

$$\hat{\mathbf{h}} = \left[ 0, 0, 0, m_w \dot{\phi} \dot{\gamma}_r, m_w \dot{\phi} \dot{\gamma}_l, -m_w \dot{\phi} \dot{z}_r, -m_w \dot{\phi} \dot{z}_l \right]^T$$

$$\hat{\mathbf{f}} = \left[ 0, 0, 0, F_{lat,r}, F_{lat,l}, F_{long,r}, F_{long,l} \right]^T$$

$$\hat{\mathbf{q}} = \left[ x_G, y_G, \phi, z_r, z_l, \gamma_r, \gamma_l \right]^T$$

$$\mathbf{B}(\hat{\mathbf{q}}) = \begin{bmatrix} -\sin \phi & A & C \\ \cos \phi & B & D \\ 0 & \frac{1}{2a} & -\frac{1}{2a} \\ 1 & 0 & 0 \\ 1 & 0 & 0 \\ 0 & 1 & 0 \\ 0 & 0 & 1 \end{bmatrix} \quad (3.48)$$

with A,B,C and D as in Eq.(3.43b). Writing  $\hat{\mathbf{h}}(\hat{\mathbf{q}},\dot{\hat{\mathbf{q}}})$  in the form of Eq.(3.13), i.e.,  $\hat{\mathbf{h}}(\hat{\mathbf{q}},\dot{\hat{\mathbf{q}}}) = \hat{\mathbf{C}}_2(\hat{\mathbf{q}},\dot{\hat{\mathbf{q}}})\dot{\hat{\mathbf{q}}}$ , the model (3.47a) takes the form:

$$\bar{\mathbf{D}}(\hat{\mathbf{q}})\dot{\hat{\mathbf{v}}} + \bar{\mathbf{C}}(\hat{\mathbf{q}},\dot{\hat{\mathbf{q}}})\hat{\mathbf{v}} = \bar{\mathbf{f}} \quad (3.49)$$

where:

$$\bar{\mathbf{C}}(\hat{\mathbf{q}},\dot{\hat{\mathbf{q}}}) = \bar{\mathbf{C}}_1(\hat{\mathbf{q}},\dot{\hat{\mathbf{q}}}) + \bar{\mathbf{C}}_2(\hat{\mathbf{q}},\dot{\hat{\mathbf{q}}}), \quad \bar{\mathbf{C}}_2(\hat{\mathbf{q}},\dot{\hat{\mathbf{q}}}) = \mathbf{B}^T \hat{\mathbf{C}}_2(\hat{\mathbf{q}},\dot{\hat{\mathbf{q}}})$$

Finally, Eq.(3.47b,c) can be written in the matrix form:

$$\mathbf{I}\dot{\boldsymbol{\theta}} = \boldsymbol{\tau} - r\mathbf{f} \quad (3.50)$$

where:

$$\mathbf{I} = \begin{bmatrix} I_{wy} & 0 \\ 0 & I_{wy} \end{bmatrix}, \boldsymbol{\theta} = \begin{bmatrix} \dot{\theta}_r \\ \dot{\theta}_l \end{bmatrix}, \boldsymbol{\tau} = \begin{bmatrix} \tau_r \\ \tau_l \end{bmatrix}, \mathbf{f} = \begin{bmatrix} F_{long,r} \\ F_{long,l} \end{bmatrix} \quad (3.51)$$

To summarize, the dynamic model of the differential drive WMR with slip is:

$$\bar{\mathbf{D}}(\hat{\mathbf{q}})\dot{\hat{\mathbf{v}}} + \bar{\mathbf{C}}(\hat{\mathbf{q}},\dot{\hat{\mathbf{q}}})\hat{\mathbf{v}} = \bar{\mathbf{f}} \quad (3.52a)$$

$$\mathbf{I}\dot{\boldsymbol{\theta}} = \boldsymbol{\tau} - r\mathbf{f} \quad (3.52b)$$

with:

$$\hat{\mathbf{q}} = [x_G, y_G, \phi, z_r, z_l, \gamma_r, \gamma_l]^T \quad (3.52c)$$

$$\hat{\mathbf{v}} = [\dot{z}_l, \dot{\gamma}_r, \dot{\gamma}_l]^T$$

### 3.4 Car-Like WMR Dynamic Model

The kinematic equations of the car-like WMR were derived in Section 2.6. Here, we will derive the Newton-Euler dynamic model for a 4-wheel rear-drive front-steer WMR [17]. The equivalent bicycle model shown in Fig.3.5 will be used.

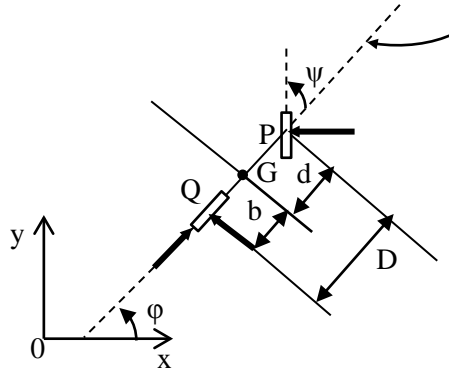


**Fig. 3.5 : Free-body diagram of the equivalent bicycle.**

The WMR is subject to the driving force  $F_d$  and two lateral slip forces  $F_r$  and  $F_f$  applied perpendicular to the corresponding wheels. Before presenting the dynamic equations we derive the nonholonomic constraints that apply to the center of gravity G which lies at a distance b from Q, and a distance d from P. To this end, we start with the nonholonomic constraints (2.50a,b) that refer to the points Q and P:

$$\begin{aligned}\dot{x}_Q \sin \phi - \dot{y}_Q \cos \phi &= 0 \\ \dot{x}_P \sin(\phi + \psi) - \dot{y}_P \cos(\phi + \psi) &= 0\end{aligned}\tag{3.53}$$

Denoting by  $x_G$  and  $y_G$  the coordinates of the point G in the world coordinate frame we get:

$$\begin{aligned}x_Q &= x_G - b \cos \phi, & x_P &= x_G + d \cos \phi \\ y_Q &= y_G - b \sin \phi, & y_P &= y_G + d \sin \phi \\ \dot{x}_Q &= \dot{x}_G + b\dot{\phi} \sin \phi, & \dot{x}_P &= \dot{x}_G - d\dot{\phi} \sin \phi \\ \dot{y}_Q &= \dot{y}_G - b\dot{\phi} \cos \phi, & \dot{y}_P &= \dot{y}_G + d\dot{\phi} \cos \phi\end{aligned}\tag{3.54}$$

Introducing the relations (3.54) into (3.53) yields:

$$\begin{aligned}\dot{x}_G \sin \phi - \dot{y}_G \cos \phi + b\dot{\phi} &= 0 \\ \dot{x}_G \sin(\phi + \psi) - \dot{y}_G \cos(\phi + \psi) - d\dot{\phi} \cos \psi &= 0\end{aligned}\tag{3.55}$$

Now, denoting by  $[\dot{x}_g, \dot{y}_g]$  the velocity of the center of gravity G in the local coordinate frame  $Gx_g y_g$  and applying the rotational transformation (2.17) {see. Example 2.1} we get:

$$\begin{bmatrix} \dot{x}_G \\ \dot{y}_G \end{bmatrix} = \begin{bmatrix} \cos \phi & -\sin \phi \\ \sin \phi & \cos \phi \end{bmatrix} \begin{bmatrix} \dot{x}_g \\ \dot{y}_g \end{bmatrix}\tag{3.56}$$

Introducing Eq.(3.56) into Eq.(3.55) yields:

$$\dot{y}_g = b\dot{\phi}, \quad \dot{\phi} = \frac{tg\psi}{D} \dot{x}_g\tag{3.57}$$

which, upon differentiation, give:

$$\ddot{y}_g = b\ddot{\phi}\tag{3.58a}$$

$$\ddot{\phi} = \frac{tg\psi}{D} \ddot{x}_g + \frac{1}{D \cos^2 \psi} \dot{x}_g \dot{\psi}\tag{3.58b}$$

From Eqs.(3.57) and (3.58a,b) we get:

$$\dot{y}_g = \frac{b}{D} (tg\psi) \dot{x}_g, \quad \ddot{y}_g = \frac{b}{D} (tg\psi) \ddot{x}_g + \frac{b}{D \cos^2 \psi} \dot{x}_g \dot{\psi}\tag{3.59}$$

Referring to Fig.3.5 we obtain the following Newton-Euler dynamic equations:

$$m(\ddot{x}_g - \dot{y}_g \dot{\phi}) = F_d - F_f \sin \psi\tag{3.60a}$$

$$m(\ddot{y}_g + \dot{x}_g \dot{\phi}) = F_r + F_f \cos \psi\tag{3.60b}$$

$$J\ddot{\phi} = dF_f \cos \psi - bF_r\tag{3.60c}$$

$$\dot{\psi} = -\frac{1}{T} \psi + \frac{K}{T} u_s\tag{3.60d}$$

where:

$m$  = mass of the WMR

$J$  = moment of inertia of the WMR about G

$F_d$  = driving force

$F_f, F_r$  = front and rear wheel lateral forces

$T$  = time constant of the steering system

$u_s$  = steering control input

$K$  = a constant coefficient (gain)

$F_d = (1/r) \tau_d$ , with  $r$  the rear wheel radius, and  $\tau_d$  the applied motor torque.<sup>6</sup>

We will now put the above dynamic equations into state space form, where the state vector is:

$$\mathbf{x} = [x_G, y_G, \phi, \dot{x}_g, \psi]^T \quad (3.61)$$

To this end, we solve Eq.(3.60c) for  $F_r$  and introduce it, together with Eq.(3.58a) into (3.60b) to get:

$$\begin{aligned} m(b\ddot{\phi} + \dot{x}_g\dot{\phi}) &= F_f \cos \psi + \frac{d}{b} F_f \cos \psi - \frac{J}{b} \ddot{\phi} \\ &= \frac{DF_f \cos \psi - J\ddot{\phi}}{b} \quad (D = b + d) \end{aligned}$$

whence:

$$F_f = \left( \frac{mb^2 + J}{D \cos \psi} \right) \ddot{\phi} + \left( \frac{mb\dot{x}_g}{D \cos \psi} \right) \dot{\phi} \quad (3.62)$$

Now, introducing Eqs.(3.57), (3.58b) and (3.62) into Eq.(3.60a) we get:

$$\ddot{x}_g = \frac{\dot{x}_g (mb^2 + J) \tan \psi}{a} \dot{\psi} + \frac{D^2 \cos^2 \psi}{a} F_d \quad (3.63a)$$

where:

$$a = (\cos^2 \psi) (mD^2 + (mb^2 + J) \tan^2 \psi) \quad (3.63b)$$

Finally, introducing Eq.(3.57) into Eq.(3.56) gives:

$$\begin{aligned} \dot{x}_G &= \{ \cos \phi - (b/D) (\tan \psi) \sin \phi \} \dot{x}_g \\ \dot{y}_G &= \{ \sin \phi + (b/D) (\tan \psi) \cos \phi \} \dot{x}_g \\ \dot{\phi} &= [(1/D) \tan \psi] \dot{x}_g \end{aligned} \quad (3.64)$$

$$\ddot{x}_g = (1/a) \left[ (mb^2 + J) (\tan \psi) \dot{\psi} \dot{x}_g \right] + (1/a) (D^2 \cos^2 \psi) F_d$$

$$\dot{\psi} = -(1/T) \psi + (K/T) u_s$$

with  $F_d = (1/r) \tau_d$ . The model (3.64) represents an affine system with two inputs  $(\tau_d, u_s)$ , a 5-dimensional state vector:

$$\mathbf{x} = [x_G, y_G, \phi, \dot{x}_g, \psi]^T \quad (3.65a)$$

a drift term:

$$\mathbf{g}_o(\mathbf{x}) = \begin{bmatrix} [\cos \phi - (b/D) (\tan \psi) \sin \phi] \dot{x}_g \\ [\sin \phi + (b/D) (\tan \psi) \cos \phi] \dot{x}_g \\ (1/D) (\tan \psi) \dot{x}_g \\ (1/a) [(mb^2 + J) (\tan \psi) \dot{\psi} \dot{x}_g] \\ -(1/T) \psi \end{bmatrix} \quad (3.65b)$$

and the two input fields:

---

<sup>6</sup> Here, the driving motor dynamics is not included. Derivation of DC motor dynamic models is provided in Example 5.1.

$$\mathbf{g}_1(\mathbf{x}) = \left[ 0, 0, 0, \frac{1}{ra} D^2 \cos^2 \psi, 0 \right]^T, \mathbf{g}_2(\mathbf{x}) = [0, 0, 0, 0, K / T]^T \quad (3.65c)$$

namely:

$$\dot{\mathbf{x}} = \mathbf{g}_0(\mathbf{x}) + \mathbf{g}_1(\mathbf{x})\tau_d + \mathbf{g}_2(\mathbf{x})u_s \quad (3.66)$$

### 3.5 Three-Wheel Omnidirectional Mobile Robot

Here, we will derive the dynamic model of a three –wheel omnidirectional robot using the Newton-Euler method [9]. This derivation is the same for any number of universal (orthogonal) omni-wheels.

Consider the WMR in the pose shown in Fig. 3.6 in which the three wheels are placed at angles  $30^\circ, 150^\circ, 270^\circ$ , respectively.

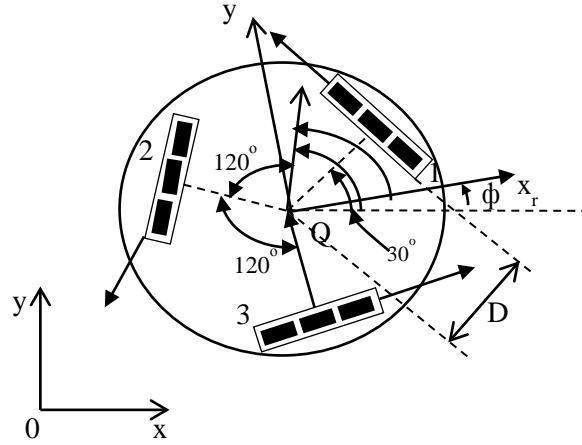


**Fig. 3.6 : Geometry of the three –wheel omnidirectional WMR.**

The rotation matrix of the robot's local coordinate frame  $Qx_r y_r$  with respect to the world coordinate frame  $Oxy$  is:

$$\mathbf{R}(\phi) = \begin{bmatrix} \cos \phi & -\sin \phi \\ \sin \phi & \cos \phi \end{bmatrix} \quad (3.67)$$

Let  $\mathbf{s}_Q = [x_Q \ y_Q]^T$  be the position vector of the center of gravity  $Q$ . Then:

$$\mathbf{M}\ddot{\mathbf{s}}_Q = \mathbf{F}_Q, \quad \mathbf{F}_Q = [F_{Qx} \ F_{Qy}]^T \quad (3.68)$$

where  $\mathbf{M} = \text{diag}(m, m)$ ,  $m$  is the robot's mass, and  $\mathbf{F}_Q$  is the force exerted at the center of gravity expressed in the world coordinate frame. Denoting by:

$$\mathbf{s}_r = [x_r \ y_r]^T, \quad \mathbf{F}_r = [F_{x_r} \ F_{y_r}]^T \quad (3.69)$$

the position vector of the center of gravity and the force vector expressed in the local (moving) coordinate frame, then Eq.(3.67) implies that:

$$\dot{\mathbf{s}}_Q = \mathbf{R}(\phi)\dot{\mathbf{s}}_r, \quad \mathbf{F}_Q = \mathbf{R}(\phi)\mathbf{F}_r \quad (3.70)$$

Thus, using (3.70) in (3.68) we get:

$$\mathbf{M}(\ddot{\mathbf{s}}_r + \mathbf{R}^T(\phi)\dot{\mathbf{R}}(\phi)\dot{\mathbf{s}}_r) = \mathbf{F}_r \quad (3.71)$$

Now, the dynamic equation of the rotation about the center of gravity  $Q$  is:



$$I_Q \ddot{\phi} = \tau_Q \quad (3.72)$$

where  $I_Q$  is the moment of inertia of the robot about Q, and  $\tau_Q$  is the applied torque at Q.

From the geometry of Fig.3.6 we obtain:

$$\begin{aligned} F_{xr} &= -\frac{1}{2}F_{d1} - \frac{1}{2}F_{d2} + F_{d3} \\ F_{yr} &= \frac{\sqrt{3}}{2}F_{d1} - \frac{\sqrt{3}}{2}F_{d2} \\ \tau_Q &= (F_{d1} + F_{d2} + F_{d3})D \end{aligned} \quad (3.73)$$

where D is the distance of the wheels from the rotation point Q, and  $F_{di}$  ( $i=1,2,3$ ) are the driving forces of the wheels.

The rotation of each wheel is described by the dynamic equation:

$$I_o \ddot{\theta}_i + \beta \dot{\theta}_i = K \tau_i - r F_{di} \quad (i=1,2,3) \quad (3.74)$$

where  $I_o$  is the common moment of inertia of the wheels,  $\theta_i$  is the angular position of wheel  $i$ ,  $\beta$  is the linear friction coefficient,  $r$  is the common radius of the wheels,  $\tau_i$  is the driving input torque of wheel  $i$ , and  $K$  is the driving torque gain.

Now, from the geometry of Fig.3.6 we see that the angles of the wheel velocities in the local coordinate frame are:

$$30^\circ + 90^\circ = 120^\circ, 120^\circ + 120^\circ = 240^\circ \text{ and } 240^\circ + 120^\circ = 360^\circ$$

Thus, we obtain the inverse kinematics equations from  $\dot{\mathbf{p}}_r = [\dot{x}_r, \dot{y}_r, \dot{\phi}]^T$  to

$$\dot{\mathbf{q}} = [\dot{\theta}_1, \dot{\theta}_2, \dot{\theta}_3]^T = [\omega_1, \omega_2, \omega_3]^T \text{ as:}$$

$$r\omega_1 = -\frac{1}{2}\dot{x}_r + \frac{\sqrt{3}}{2}\dot{y}_r + D\dot{\phi} \quad (3.75a)$$

$$r\omega_2 = -\frac{1}{2}\dot{x}_r - \frac{\sqrt{3}}{2}\dot{y}_r + D\dot{\phi} \quad (3.75b)$$

$$r\omega_3 = \dot{x}_r + D\dot{\phi} \quad (3.75c)$$

Using Eqs.(3.69) to (3.75c) we get after some algebraic manipulation:

$$\ddot{x}_r = a_1\dot{x}_r + a_2^*\dot{y}_r\dot{\phi} - b_1(\tau_1 + \tau_2 - 2\tau_3) \quad (3.76a)$$

$$\ddot{y}_r = a_1\dot{y}_r - a_2^*\dot{x}_r\dot{\phi} + \sqrt{3}b_1(\tau_1 - \tau_2) \quad (3.76b)$$

$$\ddot{\phi} = a_3\dot{\phi} + b_2(\tau_1 + \tau_2 + \tau_3) \quad (3.76c)$$

where:

$$a_1 = -3\beta(3I_o + 2mr^2), a_2^* = 2mr^2 / (3I_o + 2mr^2)$$

$$a_3 = -3\beta D^2 / (3I_o D^2 + I_Q r^2)$$

$$b_1 = Kr / (3I_o + 2mr^2), b_2 = Kr / (3I_o D^2 + I_Q r^2)$$

Finally, combining Eqs.(3.67), (3.68) and (3.76a-c) we get the following state –space dynamic model of the WMR's motion:

$$\dot{\mathbf{x}} = \mathbf{A}(\mathbf{x})\mathbf{x} + \mathbf{B}(\mathbf{x})\mathbf{u} \quad (3.77a)$$

$$\mathbf{y} = \mathbf{C}\mathbf{x} \quad (3.77b)$$

where:

$$\mathbf{x} = [x_Q, y_Q, \phi, \dot{x}_Q, \dot{y}_Q, \dot{\phi}]^T$$

$$\mathbf{y} = [\dot{x}_Q, \dot{y}_Q, \phi]^T$$

$$\mathbf{u} = [\tau_1, \tau_2, \tau_3]^T$$

$$\mathbf{A}(\mathbf{x}) = \begin{bmatrix} 0 & 0 & 0 & 1 & 0 & 0 \\ 0 & 0 & 0 & 0 & 1 & 0 \\ 0 & 0 & 0 & 0 & 0 & 1 \\ 0 & 0 & 0 & a_1 & -a_2\dot{\phi} & 0 \\ 0 & 0 & 0 & a_2\dot{\phi} & a_1 & 0 \\ 0 & 0 & 0 & 0 & 0 & a_3 \end{bmatrix}$$

$$\mathbf{B}(\mathbf{x}) = \begin{bmatrix} 0 & 0 & 0 \\ 0 & 0 & 0 \\ 0 & 0 & 0 \\ b_1\beta_1 & b_1\beta_2 & 2b_1\cos\phi \\ b_1\beta_3 & b_1\beta_4 & 2b_1\sin\phi \\ b_2 & b_2 & b_2 \end{bmatrix} = [\bar{\mathbf{b}}_1(\mathbf{x}) \quad \bar{\mathbf{b}}_2(\mathbf{x}) \quad \bar{\mathbf{b}}_3(\mathbf{x})]$$

$$\mathbf{C} = \begin{bmatrix} 0 & 0 & 0 & 1 & 0 & 0 \\ 0 & 0 & 0 & 0 & 1 & 0 \\ 0 & 0 & 1 & 0 & 0 & 0 \end{bmatrix}$$

$$a_2 = 1 - a_2^* = 3I_o / (3I_o + 2mr^2)$$

$$\beta_1 = -\sqrt{3}\sin\phi - \cos\phi, \beta_2 = \sqrt{3}\sin\phi - \cos\phi$$

$$\beta_3 = \sqrt{3}\cos\phi - \sin\phi, \beta_4 = -\sqrt{3}\cos\phi - \sin\phi$$

The azimuth of the robot in the world coordinate frame is denoted by  $\psi$ , where  $\psi = \phi + \theta$  ( $\theta$  denotes the angle between  $Qx_r y_r$  and  $F_r$ , i.e., the azimuth of the robot in the moving coordinate frame). Then:

$$\dot{x}_Q = v \cos\psi, \dot{y}_Q = v \sin\psi, v = \sqrt{\dot{x}_Q^2 + \dot{y}_Q^2}$$

Whence:

$$\psi = \tan^{-1}(\dot{y}_Q / \dot{x}_Q) \quad (3.78)$$

where the positive direction is the counterclockwise rotation direction. It is noted that the motions along  $x_Q$  and  $y_Q$  are coupled because the dynamic equations are derived in the world coordinate frame. But since the rotational angle is always equal to  $\phi = \psi - \theta$ , despite the fact that  $\theta$  may be changing arbitrarily, the WMR can realize a translational motion without changing the pose (i.e., the WMR is holonomic). The model (3.77a) can be written in a 3-input affine form with drift as follows:

$$\dot{\mathbf{x}} = \mathbf{g}_o(\mathbf{x}) + \sum_{i=1}^3 \mathbf{g}_i(\mathbf{x}) u_i \quad (3.79)$$

where:

$$\mathbf{g}_o(\mathbf{x}) = \mathbf{A}(\mathbf{x})\mathbf{x}, \quad \mathbf{g}_i(\mathbf{x}) = \bar{\mathbf{b}}_i(\mathbf{x}) \quad (i=1,2,3)$$

The dynamic model (3.77a) of a three-wheel omni-directional robot (with universal wheels) is one of the many different models available. Actually, many other equivalent models were derived in the literature.

### Example 3.2

Derive the dynamic equations of the 3-wheel omnidirectional robot using the unit directional vectors  $\boldsymbol{\varepsilon}_1, \boldsymbol{\varepsilon}_2, \boldsymbol{\varepsilon}_3$  of the wheel velocities.

### Solution

To simplify the derivation we select the pose of the WMR in which the wheel 1 orientation is perpendicular to the local coordinate axis  $Qx_r$  as shown in Fig.3.7 [8].

Thus the unit directional vectors  $\boldsymbol{\varepsilon}_1, \boldsymbol{\varepsilon}_2$  and  $\boldsymbol{\varepsilon}_3$  are:

$$\boldsymbol{\varepsilon}_1 = \begin{bmatrix} 0 \\ 1 \end{bmatrix}, \boldsymbol{\varepsilon}_2 = -\begin{bmatrix} \sqrt{3}/2 \\ 1/2 \end{bmatrix}, \boldsymbol{\varepsilon}_3 = \begin{bmatrix} \sqrt{3}/2 \\ -1/2 \end{bmatrix} \quad (3.80)$$

The rotational matrix of  $Qx_r y_r$  with respect to  $Oxy$  is given by (3.67).

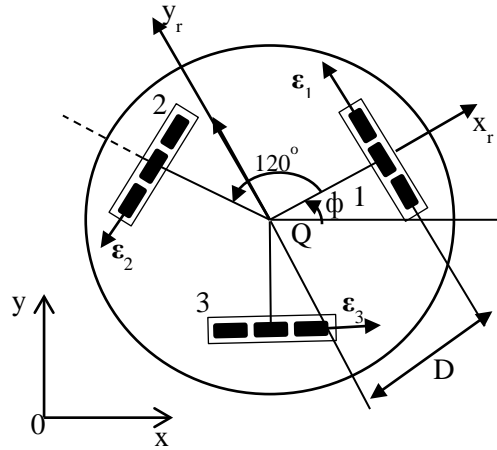


**Fig. 3.7 : The 3-wheel omnidirectional mobile robot ( $\boldsymbol{\varepsilon}_1$  perpendicular to  $Qx_r$ )**

Therefore, the driving velocities  $v_i$  ( $i=1,2,3$ ) of the wheels are:

$$\begin{aligned} v_1 &= r\dot{\theta}_1 = -\dot{x}_Q \sin \phi + \dot{y}_Q \cos \phi + D\dot{\phi} \\ v_2 &= r\dot{\theta}_2 = -\dot{x}_Q \sin(\pi/3 - \phi) - \dot{y}_Q \cos(\pi/3 - \phi) + D\dot{\phi} \\ v_3 &= r\dot{\theta}_3 = \dot{x}_Q \sin(\pi/3 + \phi) - \dot{y}_Q \cos(\pi/3 + \phi) + D\dot{\phi} \end{aligned}$$

or

$$\dot{\mathbf{q}} = \mathbf{J}^{-1}(\phi) \dot{\mathbf{p}}_Q \quad (3.81)$$

where:

$$\mathbf{J}^{-1}(\phi) = \frac{1}{r} \begin{bmatrix} -\sin \phi & \cos \phi & D \\ -\sin(\pi/3 - \phi) & -\cos(\pi/3 - \phi) & D \\ \sin(\pi/3 + \phi) & -\cos(\pi/3 + \phi) & D \end{bmatrix}$$

$$\dot{\mathbf{q}} = [\dot{\theta}_1, \dot{\theta}_2, \dot{\theta}_3]^T, \dot{\mathbf{p}}_Q = [\dot{x}_Q, \dot{y}_Q, \dot{\phi}]^T$$

This is the inverse kinematic model of the robot. Now, applying the Newton –Euler method to the robot we get:

$$m \begin{bmatrix} \ddot{x}_Q \\ \ddot{y}_Q \end{bmatrix} = \mathbf{s}_1(\phi) F_{d1} + \mathbf{s}_2(\phi) F_{d2} + \mathbf{s}_3(\phi) F_{d3} \quad (3.82a)$$

$$I_Q \ddot{\phi} = D(F_{d1} + F_{d2} + F_{d3}) \quad (3.82b)$$

where  $F_{di}$  ( $i=1,2,3$ ) is the magnitude of the driving force of the  $i$ th wheel,  $m$  is the robot mass,  $I_Q$  is the robot moment of inertia about  $Q$ , and:

$$\mathbf{s}_i(\phi) = \mathbf{R}(\phi) \mathbf{e}_i \quad (i=1,2,3) \quad (3.83)$$

are 2-dimensional vectors found using Eqs.(3.67) and (3.80). The driving forces  $F_{di}$  ( $i=1,2,3$ ) are given by the relation:

$$F_{di} = aV_i - \beta r \dot{\theta}_i \quad (i=1,2,3) \quad (3.84)$$

where  $V_i$  is the voltage applied to the motor of the  $i$ th wheel, ‘ $a$ ’ is the voltage-force constant, and  $\beta$  is the friction coefficient.

Combining (3.82a,b), (3.83) and (3.84) we obtain the model:

$$\mathbf{D} \ddot{\mathbf{p}}_Q + \mathbf{C}(\phi) \dot{\mathbf{p}}_Q = \mathbf{E} \mathbf{v} \quad (3.85a)$$

where:

$$\mathbf{D} = \begin{bmatrix} m & 0 & 0 \\ 0 & m & 0 \\ 0 & 0 & I_Q \end{bmatrix}, \mathbf{C}(\phi) = \left( \frac{\beta r}{a} \right) \mathbf{E}(\phi) \mathbf{J}^{-1}(\phi) \quad (3.85b)$$

$$\mathbf{E}(\phi) = a \begin{bmatrix} \mathbf{s}_1(\phi) & \mathbf{s}_2(\phi) & \mathbf{s}_3(\phi) \\ D & D & D \end{bmatrix}, \mathbf{v} = \begin{bmatrix} V_1 \\ V_2 \\ V_3 \end{bmatrix} \quad (3.85c)$$

The model (3.85a-c) has the standard form of the robot model described by Eqs.(3.11) and (3.13).

### Example 3.3

We are given a car-like robot where there are lateral slip forces and longitudinal friction forces on all wheels. It is desired to write down the Newton –Euler dynamic equations in the form (3.60a-d).

#### Solution

The free-body diagram of the robot is as shown in Fig.3.8.

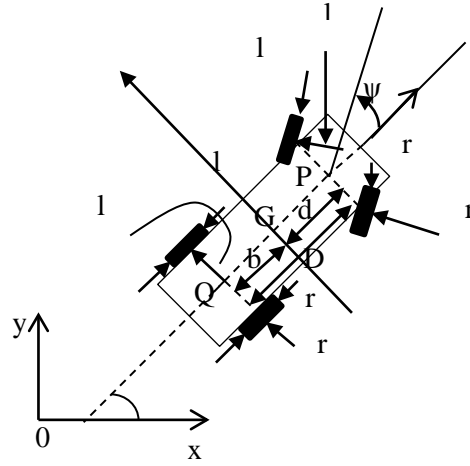


**Fig. 3.8 : Free-body diagram of the car-like WMR.**

We use the following definitions:

$$F_d = F_d^l + F_d^r \text{ (Total driving force)}$$

$$F_{x_g, r} = F_{x_g, r}^l + F_{x_g, r}^r \text{ (Rear total longitudinal friction)}$$

$$F_{x_g, f} = F_{x_g, f}^l + F_{x_g, f}^r \text{ (Front total longitudinal friction)}$$

$$F_{y_g, r} = F_{y_g, r}^l + F_{y_g, r}^r \text{ (Rear total lateral force)}$$

$$F_{y_g, f} = F_{y_g, f}^l + F_{y_g, f}^r \text{ (Front total lateral force)}$$

where the upper index r refers to the right wheel and the upper index l to the left wheel. Therefore, considering the bicycle model of the WMR we get the following Newton-Euler dynamic equations in the local coordinate frame:

$$m(\ddot{x}_g - \dot{y}_g \dot{\phi}) = F_d - F_{x_g, r} - F_{x_g, f} \cos \psi - F_{y_g, f} \sin \psi$$

$$m(\ddot{y}_g + \dot{x}_g \dot{\phi}) = F_{y_g, r} - F_{x_g, f} \sin \psi + F_{y_g, f} \cos \psi$$

$$J\ddot{\phi} = dF_{y_g, f} \cos \psi - bF_{y_g, r}$$

$$\dot{\psi} = -(1/T)\psi + (K/T)u_s$$

where all variables have the meaning presented in Section 3.4. From this point the development of the full model can be done as in Section 3.4.

### 3.6 Four Mecanum-Wheel Omnidirectional Robot

We consider the 4-wheel omnidirectional robot of Fig.3.9.a [3].

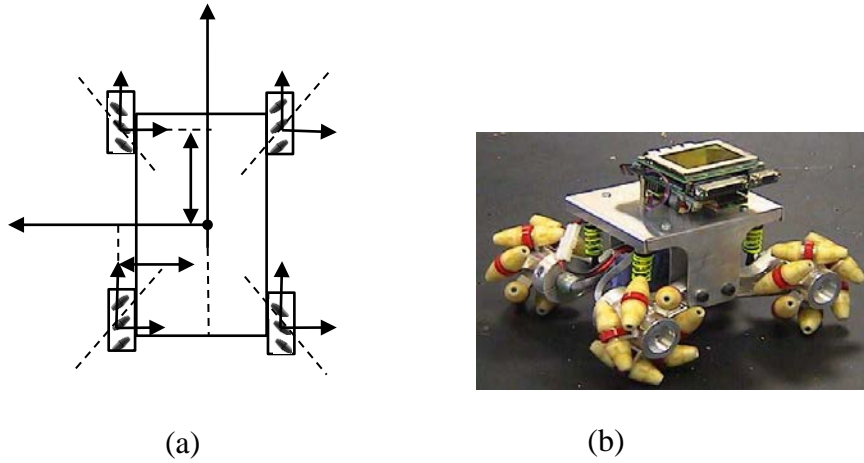


**Fig. 3.9 : (a) The 4-wheel mecanum WMR and the forces acting on it. (b) An experimental 4-wheel mecanum WMR prototype.**

[www.robotics.ee.uwa.edu.au/eyebot/doc/robots/omni.html](http://www.robotics.ee.uwa.edu.au/eyebot/doc/robots/omni.html)

The total forces  $F_x$  and  $F_y$  acting on the robot in the x and y directions are:

$$F_x = (F_{x1} + F_{x2} + F_{x3} + F_{x4}) \quad (3.86a)$$

$$F_y = (F_{y1} + F_{y2} + F_{y3} + F_{y4}) \quad (3.86b)$$

where  $F_{xi}, F_{yi}$  ( $i=1,2,3,4$ ) are the forces acting on the wheels along the x and y axes. In the absence of separate rotation motion, the direction of motion is defined by an angle  $\delta$  where:

$$\delta = \tan^{-1}(F_y / F_x) \quad (3.87)$$

The torque  $\tau$  that produces pure rotation is:

$$\tau = (F_{x1} - F_{x2} - F_{x3} + F_{x4})d_1 + (F_{y3} + F_{y4} - F_{y1} - F_{y2})d_2 \quad (3.88)$$

where positive rotation is in the counter-clock direction.

The Newton –Euler motion equations are:

$$m\ddot{x} = F_x - \beta_x \dot{x} \quad (3.89a)$$

$$m\ddot{y} = F_y - \beta_y \dot{y} \quad (3.89b)$$

$$I_Q \ddot{\phi} = \tau - \beta_z \dot{\phi} \quad (3.89c)$$

where  $\beta_x, \beta_y$  and  $\beta_z$  are the linear friction coefficients in the x,y, and  $\phi$  motion, and  $m, I_Q$  are the mass and moment of inertia of the robot. Equations (3.89a-c) show that the robot can achieve steady state velocities ( $\ddot{x}=0, \ddot{y}=0, \ddot{\phi}=0$ )  $\dot{x}_{ss}, \dot{y}_{ss}$  and  $\dot{\phi}_{ss}$  equal to:

$$\dot{x}_{ss} = \frac{F_x}{\beta_x}, \quad \dot{y}_{ss} = \frac{F_y}{\beta_y}, \quad \dot{\phi}_{ss} = \frac{\tau}{\beta_z} \quad (3.90)$$

#### Example 3.4

The problem is to calculate the wheel angular velocities which are required to achieve a desired translational and rotational motion (WMR velocities  $v$  and  $\dot{\phi}$ ) of the mecanum mobile robot of Fig.3.9a.

### Solution

A solution to this problem was provided by the relations Eqs.(2.84) and (2.85). Here we will provide an alternative method [3]. We draw the displacement and velocity vectors of a single wheel which are as shown in Fig. 3.10(a,b), where ‘ $a$ ’ is the roller angle ( $a = \pm 45^\circ$ ).

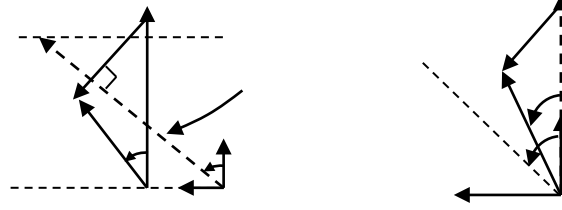


**Fig. 3.10 : (a) Displacement vectors of a wheel and roller, (b) velocity vectors ( $a$  is the rollers angle).**

The vector  $s_p$  represents the displacement due to the wheel rotation (in the positive direction),  $s_r$  represents the displacement vector due to rolling which is orthogonal to the roller axis, and  $s$  represents the total displacement vector. The dotted horizontal lines represent the discontinuities where the roller contact point transfers from one roller to the next. In Fig.3.10 the point A was selected in the middle of this discontinuity line to facilitate the calculation.

From Fig.3.10b we get:  $(\omega r) \cos a = v \cos(a - \gamma)$  because the components of  $\omega r$  and  $v = ds/dt$  along the roller axis are equal. Therefore:

$$\omega r = v \cos(a - \gamma) / \cos a \quad (3.91)$$

for  $a \neq \pi/2 + k\pi$  ( $k = 0, 1, 2, \dots$ ). If  $a = \pi/2 + k\pi$ , the rotation of the wheel does not produce translation motion of the rollers. Solving (3.91) for  $v$  we get:

$$v = \omega r \frac{\cos a}{\cos(a - \gamma)}, \quad a - \gamma \neq \frac{\pi}{2} + k\pi \quad (k = 0, 1, 2, \dots) \quad (3.92)$$

When  $a - \gamma = \pi/2$ , the rotational speed  $\omega$  of the wheel must be zero, but the wheel can have any value of translation velocity because of the motion of the other wheels.

We now calculate the wheel angular velocity  $\omega_i$  for a desired translational –motion velocity  $v$ . From Eq.(3.90) we see that the wheel velocity is proportional to the forces applied by each wheel, i.e.:

‘ $v$  proportional to  $(F_1 + F_2 + F_3 + F_4)$ ’, and because the WMR is a rigid body, all wheels should have the same translational speed, i.e.:

$$v_i = v \quad (i = 1, 2, 3, 4)$$

Therefore, from (3.92) we have:

$$\omega_i = \frac{v \cos(a_i - \gamma)}{r_i \cos a_i}, \quad a_i \neq \frac{\pi}{2} + k\pi \quad (k = 0, 1, 2, \dots) \quad (3.93)$$

Equation (3.93) gives the velocities  $\omega_i$  ( $i = 1, 2, 3, 4$ ) of the four wheels needed to get a desired translational velocity  $v$  of the robot.

Finally, we will calculate the wheel angular velocities required to get a desired rotational speed  $\dot{\phi}$ . Consider a robot with velocity  $v$ . Then, the instantaneous curvature radius (ICR) of its path is:

$$R = v / \dot{\phi} \text{ with } \varepsilon = \text{ctg}^{-1}(v_x / v_y) \quad (3.94)$$

These relations give the following world frame coordinates  $x_{ICR}, y_{ICR}$  of the ICR (see Fig.3.11):

$$x_{ICR} = -R \sin \varepsilon$$

$$y_{ICR} = R \cos \varepsilon$$

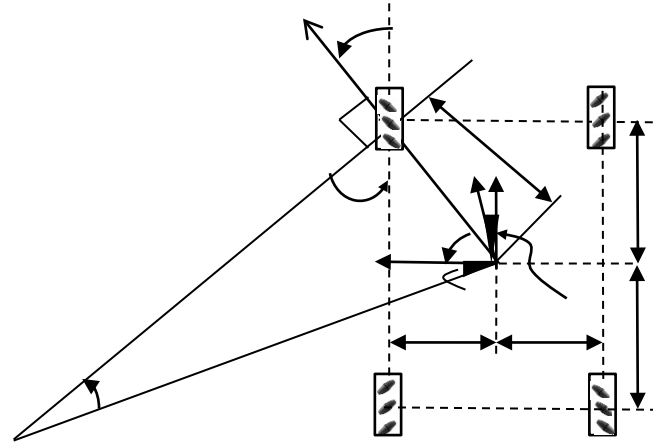


**Fig. 3.11 : Geometry of wheel  $i$  with reference to the coordinate frame  $Q_{x_i y_i}$ . Each wheel has its own total velocity  $v_i$  and angle  $\gamma_i$ .**

The geometry of each wheel is defined by its position  $(x_i, y_i)$  and the orientation  $a_i$  of its rollers. Let  $\Sigma_i$  be the contact point of wheel  $i$  then:

$$\eta_i = \text{tg}^{-1}(x_i / y_i), \quad l_i = \sqrt{x_i^2 + y_i^2} \quad (3.95)$$

where  $l_i$  is the same for all wheels due to the symmetricity of the wheels with respect to the point Q. The distance  $L_i$  of the ICR and the contact point  $\Sigma_i(x_i, y_i)$  is given by the triangle formula, as:

$$L_i = \sqrt{l_i^2 + R^2 - 2l_i R \cos(\eta_i + \varepsilon)} \quad (3.96)$$

The velocity  $v_i$  of the wheel should be perpendicular to the line  $L_i$ . Therefore, the angle  $\zeta_i$  of the line  $L_i$  with the x-axis is determined by the relation:

$$\text{tg} \zeta_i = (y_{ICR} - y_i) / (x_{ICR} - x_i) \quad (3.97)$$

whence:

$$\gamma_i = \pi / 2 + \zeta_i \quad (3.98)$$

because, in Fig.3.11,  $\zeta_i$  is actually negative ( $x_{ICR} - x_i < 0$ ). Now, in view of (3.94) we have:

$$|v_i| = L_i |\dot{\phi}| \quad (3.99)$$

Finally, using Eq.(3.99), equation Eq.(3.93) gives:



$$\omega_i = L_i \dot{\phi} \cos(a_i - \gamma_i) / r \cos a_i \quad (i = 1, 2, 3, 4) \quad (3.100)$$

for  $a_i \neq \pi/2 + k\pi$  ( $k = 0, 1, 2, \dots$ ), where  $r$  is the common radius of the wheels. Equation (3.100) gives the required rotational speeds of the wheels in terms of the position  $(x_{ICR}, y_{ICR})$  of ICR and the desired rotational speed  $\dot{\phi}$  of the robot. Actually, in view of Eqs.(3.94) and (3.96), Eq.(3.100) gives  $\omega_i$  in terms of the known (desired) values of  $v$ ,  $\dot{\phi}$ ,  $x_i$  and  $y_i$ .

### Example 3.5

It is desired to describe a way for identifying the dynamic parameters of a differential-drive WMR by converting its dynamic model to a linear form which uses the robot linear displacement in place of  $x_Q, y_Q$  and  $\phi$ .

The nonlinear dynamic model of this WMR is given by Eqs.(3.30a,b) and (3.31) which is written as:

$$\dot{v} = \gamma_1 u_1, \quad u_1 = \tau_r + \tau_l$$

$$\dot{\omega} = \gamma_2 u_2, \quad u_2 = \tau_r - \tau_l$$

$$\dot{x}_Q = v \cos \phi$$

$$\dot{y}_Q = v \sin \phi$$

$$\dot{\phi} = \omega$$

where  $\gamma_1 = 1/mr$  and  $\gamma_2 = 2a/Ir$  are the dynamic parameters to be identified. Using the robot's linear displacement:

$$l = x_Q \cos \phi + y_Q \sin \phi$$

in place of the components  $x_Q$  and  $y_Q$  (see. Fig.2.7) we get the linear model:

$$\dot{v} = \gamma_1 u_1, \quad \dot{\omega} = \gamma_2 u_2, \quad \dot{l} = v, \quad \dot{\phi} = \omega$$

which reduces to:

$$\ddot{l} = \gamma_1 u_1, \quad \ddot{\phi} = \gamma_2 u_2 \quad (3.101)$$

This is a linear model with two outputs  $l$  and  $\phi$ . The identification will be made rendering the model (3.101) to the standard linear regression model:

$$\mathbf{y} = \mathbf{M}(\mathbf{u})\boldsymbol{\xi} + \mathbf{e} \quad (3.102)$$

where:

$$\mathbf{y} = [y_1, y_2, \dots, y_m]^T \text{ (the vector of measurable signals)}$$

$$\boldsymbol{\xi} = [\xi_1, \xi_2, \dots, \xi_n]^T \text{ (the vector of unknown parameters)}$$

$$\mathbf{e} = [e_1, e_2, \dots, e_m]^T \text{ (the vector of measurement errors)}$$

$$\mathbf{M}(\mathbf{u}) = \begin{bmatrix} \mu_{11}(\mathbf{u}) & \dots & \mu_{1n}(\mathbf{u}) \\ \mu_{m1}(\mathbf{u}) & \dots & \mu_{mn}(\mathbf{u}) \end{bmatrix} \text{ (a } m \times n \text{ known matrix)}$$

The matrix  $\mathbf{M}(\mathbf{u})$  is known as ‘regressor matrix’. Under the assumption that  $\mathbf{e}$  is independent of  $\mathbf{M}(\mathbf{u})$ , and  $m > n$  the solution for  $\xi$  is given by <sup>7</sup>

$$\hat{\xi} = (\mathbf{M}^T(\mathbf{u})\mathbf{M}(\mathbf{u}))^{-1} \mathbf{M}^T(\mathbf{u})\mathbf{y} \quad (3.103)$$

To convert Eq.(3.101) into the regression form (3.102) we discretize it in time using the first order approximation:  $dx/dt \simeq (x_{k+1} - x_k)/T$ , where

$x_k = x(t)_{t=kT}$  ( $k = 0, 1, 2, \dots$ ), and  $T$  is the sampling period. Then, (3.101) becomes:

$$\begin{aligned} \Delta l_k &= \Delta l_{k-1} + \xi_1 u_{1,k} \\ \Delta \phi_k &= \Delta \phi_{k-1} + \xi_2 u_{2,k} \end{aligned} \quad (3.104)$$

where  $\xi_i = T\gamma_i$ , ( $i = 1, 2$ ). Clearly, the parameters  $\xi_1$  and  $\xi_2$  are identifiable, but the difficulty is that  $l$  cannot be measured. To overcome this difficulty we use a 2<sup>nd</sup>-order parametric representation of  $x_Q(t)$ ,  $y_Q(t)$  and  $\phi(t)$ , namely [15]:

$$x_Q(\mu) = a_2\mu^2 + a_1\mu + a_0, \quad y_Q(\mu) = b_2\mu^2 + b_1\mu + b_0$$

$$tg\phi(\mu) = f(\mu) = \frac{dy_Q/d\mu}{dx_Q/d\mu} = \frac{2b_2\mu + b_1}{2a_2\mu + a_1}$$

with boundary conditions:

$$x_Q(0) = x_Q^0 = a_0, \quad x_Q(1) = x_Q^1 = a_2 + a_1 + a_0$$

$$y_Q(0) = y_Q^0 = b_0, \quad y_Q(1) = y_Q^1 = b_2 + b_1 + b_0$$

$$f(0) = tg\phi(0) = b_1/a_1$$

$$f(1) = tg\phi(1) = (2b_2 + b_1)/(2a_2 + a_1)$$

From the above conditions, the parameters  $a_i$  and  $b_i$  ( $i = 0, 1, 2$ ) are computed as:

$$a_0 = x_Q^0, \quad a_1 = \frac{2(tg\phi(1))(x_Q^1 - x_Q^0) - y_Q^1 + y_Q^0}{tg\phi(1) - tg\phi(0)} \quad (3.105a)$$

$$b_0 = y_Q^0, \quad b_1 = a_1 tg\phi(0), \quad b_2 = y_Q^1 - y_Q^0 - a_1 \quad (3.105b)$$

The approximate length increment  $\Delta \hat{l}$  of  $\Delta l$  is given by:

$$|\Delta \hat{l}| = \int_0^1 \sqrt{\left(\frac{dx_Q}{d\mu}\right)^2 + \left(\frac{dy_Q}{d\mu}\right)^2} d\mu = \int_0^1 \sqrt{k_2\mu^2 + k_1\mu + k_0} d\mu \quad (3.106a)$$

where:

$$k_0 = a_1^2 + b_1^2, \quad k_1 = 4a_1a_2 + 4b_1b_2, \quad k_2 = 4a_2^2 + 4b_2^2 \quad (3.106b)$$

Equation (3.106a) is an integral equation, the close solution of which is available in integral tables. The sign of  $\Delta l$ , which determines whether the robot moved forward or backward, can be determined by the relation:

<sup>7</sup> Equation (3.103) can be found by minimizing the function  $J(\xi) = \mathbf{e}^T \mathbf{e} = (\mathbf{y} - \mathbf{M}\xi)^T (\mathbf{y} - \mathbf{M}\xi)$

with respect to  $\xi$ . An easy way to get Eq.(3.103) is by multiplying Eq.(3.102) by  $\mathbf{M}^T(\mathbf{u})$  and solving for  $\xi$ , under the assumption that  $\mathbf{M}^T(\mathbf{u})\mathbf{e} = 0$  ( $\mathbf{e}$  independent of  $\mathbf{M}(\mathbf{u})$ , and rank

$\mathbf{M}(\mathbf{u}) = \min(m, n) = n$ . Actually, Eq.(3.103) is  $\hat{\xi} = \mathbf{M}^\dagger \mathbf{y}$  where  $\mathbf{M}^\dagger$  is the generalized inverse of  $\mathbf{M}$  (see Eq.(2.8a)).

$$\Delta l = l_1 - l_0 = (x_Q^1 \cos \phi(0) + y_Q^1 \sin \phi(0)) - (x_Q^0 \cos \phi(0) + y_Q^0 \sin \phi(0))$$

where  $x_Q^1, y_Q^1$  is the current position and  $x_Q^0, y_Q^0$  is the past position of the robot. Several numerical experiments performed using the above WMR identification method gave very satisfactory results for both  $\Delta l$  and  $\Delta \phi$  [15].

### Example 3.6

Outline a method for applying the least squares identification model (3.102)-(3.103) to the general nonholonomic WMR model (3.19a-b)

#### Solution

The model (3.19a,b):

$$\bar{\mathbf{D}}(\mathbf{q}) \dot{\mathbf{v}} + \bar{\mathbf{C}}(\mathbf{q}, \dot{\mathbf{q}}) \mathbf{v} + \bar{\mathbf{g}}(\mathbf{q}) = \bar{\mathbf{E}} \boldsymbol{\tau}$$

is put in the form:

$$\dot{\mathbf{v}} = \mathbf{M}(\mathbf{v}, \boldsymbol{\tau}) \boldsymbol{\xi}$$

where  $\boldsymbol{\xi}$  is the vector of unknown parameters. The above model can be written in the form (3.102) by computing  $\mathbf{y}_k$  as:

$$\mathbf{y}_k = \mathbf{v}_k - \mathbf{v}_{k-1} = \left( \int_{(k-1)T}^{kT} [\mathbf{M}(\mathbf{v}, t), \boldsymbol{\tau}(t)] dt \right) \boldsymbol{\xi} \quad (3.107)$$

where  $\mathbf{v}_k = \mathbf{v}(t) \Big|_{t=kT}$  and  $T$  is the sampling period of the measurements.

Now, defining  $\bar{\mathbf{y}}_N$  and  $\bar{\mathbf{M}}_N$  as:

$$\bar{\mathbf{y}}_N = [\mathbf{y}_1, \mathbf{y}_2, \dots, \mathbf{y}_N]^T$$

$$\bar{\mathbf{M}}_N = \left[ \int_0^T \mathbf{M} dt, \int_T^{2T} \mathbf{M} dt, \dots, \int_{(N-1)T}^{NT} \mathbf{M} dt \right]^T$$

The model (3.107), after  $N$  measurements, becomes:

$$\bar{\mathbf{y}}_N = \bar{\mathbf{M}}_N \boldsymbol{\xi} \quad (3.108)$$

This method overcomes the noise problem posed by the calculation of the acceleration. The optimal estimate  $\hat{\boldsymbol{\xi}}$  of  $\boldsymbol{\xi}$  is given by Eq.(3.103):

$$\hat{\boldsymbol{\xi}} = (\bar{\mathbf{M}}_N^T \bar{\mathbf{M}}_N)^{-1} \bar{\mathbf{M}}_N^T \bar{\mathbf{y}}_N \quad (3.109)$$

The identification process can be simplified if it is splitted in two parts, namely: (i) identification when the robot is moving on a line without rotation, and (ii) identification when the robot has pure rotation movement. In the pure linear motion we keep the angle  $\phi$  constant (i.e.,  $\dot{\phi} = 0$ ), and in the pure rotation motion we have  $v_Q = 0$  (i.e.,  $\dot{x}_Q = 0$  and  $\dot{y}_Q = 0$ ).

### References

- [1] McKerrow P K. Introduction to Robotics. Addison. Reading, MA:Wesley; 1999.
- [2] Dudek G, Jenkin M. Computational Principles of Mobile Robotics. Cambridge :Cambridge University Press;2010.
- [3] De Villiers M, Bright G. Development of a control model for a four-wheel mecanum vehicle. Proceedings of 25<sup>th</sup> International Conference of CAD/CAM Robotics and Factories of the Future Conference Pretoria, South Africa, July, 2010.

- [4]Song J B, Byun K S. Design and control of a four-wheeled omnidirectional mobile robot with steerable omnidirectional wheels. *Journal of Robotic Systems* 2004; 21: 193-208.
- [5]Sidek S N. Dynamic Modeling and Control of Nonholonomic Wheeled Mobile Robot Subjected to Wheel Slip. Ph. D. Thesis, Vanderbilt University, Nashville , Tennessee, December 2008.
- [6]Williams II R L, Carter B E, Gallina P, Rosati G. Dynamic model with slip for wheeled omni-directional robots. *IEEE Transactions of Robotics and Automation*, 2002;18(3):285-93.
- [7]Stonier D, Se-Hyoung C, Sung –Lok C, Kuppuswamy N S, Jong-Hwan K. Nonlinear slip dynamics for an omniwheel mobile robot platform. *Proceedings of IEEE International Conference on Robotics and Automation*, Rome, Italy, 10-14 April, 2007,p.2367-72.
- [8] Kalmar-Nagy T , D’Andrea R, Ganguly P. Near-optimal dynamic trajectory generation and control of an omnidirectional vehicle. *Robotics and Autonomous Systems* 2007;46:47-64.
- [9]Watanabe K, Shiraishi Y, Tzafestas S G, Tang J, Fukuda T. Feedback control of an omnidirectional autonomous platform for mobile service robots. *Journal of Intelligent and Robotic Systems*1998;22: 315-330.
- [10]Handy A , Badreddin E. Dynamic modeling of a wheeled mobile robot for identification, navigation and control. *Proceedings of IMACS Conference on Modeling and Control of Technological Systems*. Lille, France, 1992,p.119-128.
- [11]Pin F G, Killough S M. A new family of omnidirectional and holonomic wheeled platforms for mobile robots. *IEEE Transactions on Robotics and Automation* 1994;10(4):480-9.
- [12]Rojas R.Omnidirectional control, Freie University Berlin, May 2005. <http://robocup.mi.fu-berlin.de/buch/omnidrive.pdf>
- [13]Connette C P, Pott A, Hagele M, Verl A. Control of a Pseudo – omnidirectional, non-holonomic , mobile robot based on an ICM representation in spherical coordinates. *Proceedings of 47<sup>th</sup> IEEE Conference on Decision and Control*, Canum, Mexico, December 9-11, 2008,p.4976-83.
- [14]Moore K L, Flann N S. A six-wheeled omnidirectional autonomous mobile robot. *IEEE Control Systems Magazine* 2000,20(6):53-66.
- [15]Cuerra P N, Alsina P J, Medeiros A A D , Araujo A. Linear modeling and identification of a mobile robot with differential drive. *Proceedings of ICINCO International Conference on Informatics in Control Automation and Robotics*, Setubal, Portugal, 2004,p.263-69.
- [16]Ivanjko E, Petrinic T, Petrovic I. Modeling of Mobile robot dynamics. *Proceedings of 7<sup>th</sup> EUROSIM Congress on Modeling and Simulation*, Prague 2010, September 6-9,p.479-86.
- [17]Moret E N. Dynamic modeling and control of a car-like robot. M. Sc. Thesis, Virginia Polytechnic Institute and State University. Blacksburg, Virginia, February 2003.

